DEVELOPMENT OF BED CONFIGURATIONS IN COARSE SANDS

by

Warren Russell Costello

B.Sc. (1968), M.Sc. (1970) McMaster University

SUBMITTED IN PARTIAL FULFILLMENT OF THE REQUIREMENTS FOR THE DEGREE OF DOCTOR OF PHILOSOPHY

at the

Massachusetts Institute of Technology

January, 1974

Signature of Author . . . . . .

Certified by . . . . . .
Thesis Supervisor

Accepted by . .
Chairman, Departmental Committee on Graduate Studies

ABSTRACT

Development of Bed Configurations in Coarse Sands

by

Warren Russell Costello

Submitted to the Department of Earth and Planetary Sciences
in partial fulfillment of the requirement for the
degree of Doctor of Philosophy

Flume experiments were conducted with five coarse sands of different sizes to investigate the development of bed configurations. For fixed depth and increasing velocity, the bed configurations are no movement, flat bed, ripples, bars, and dunes. For sand sizes coarser than about 0.70 mm, ripples are replaced by a flat bed. By introducing an irregularity on the sediment bed, ripples can be initiated in the no-movement and flat-bed phases.

Ripples develop because of the effect of turbulence on the bed in the reattachment zone. The resulting strong instantaneous shear stresses initiate a maximum in sediment transport, which generates a ripple. Bars, a newly defined bed configuration, form because of the merging of kinematic waves of bed height and sediment transport to form a kinematic shock wave. At higher velocities flow acceleration over the bars is strong enough to affect the bed downstream of reattachment so that a maximum in mean shear stress and sediment transport is established; this initiates dune development.

The sequence ripples↔bars↔dunes observed in the experiments matches that observed in rivers and in the ocean. Sand waves and transverse bars in natural environments are large-scale bars with similar mechanics and occupying the same stabiltiy field as the experimental bars reported here.

Thesis Supervisor: John B. Southard
Associate Professor of Geology

TABLE OF CONTENTS

LIST OF SYMBOLS

a	porosity of sediment
A	cross-sectional area of flow
A_1	bed wave amplitude
b	width of channel
c	slope of the sediment transport rate versus bed height curve
C_1	constant of discharge in equation 6, Chapter 4
C_2	empirical coefficient in sediment discharge equation
C_3	constant in equation 8, Chapter 4, $C_3 = C_1C_2$
d	depth of flow
D_g	geometric mean sieve size of bed load
f	Darcy-Weisbach friction factor, $f = 8\ (V_*/U)^2$
f_b	bed friction factor, $f_b = 8(V_{*_b}/U)^2$
F	Froude number, $F = U/(gd)^{1/2}$
g	acceleration due to gravity
g_s	sediment discharge per unit width
h	height of individual bed form or step
h_o	distance from water surface to some arbitrary datum
h_u	height of next individual bed form upstream
j	real fluid parameter (Kennedy, 1963), $j = \delta/d$
$K(x)$	autocorrelation function
ℓ	length of individual bed forms
L	length of sediment wave
q_s	local mean sediment transport rate

Q	mean flow discharge
P	wetted perimeter of channel
r	hydraulic radius, $r = A/P$
r_b	bed hydraulic radius, $r_b = rf_b/f$
R	flow Reynolds number, $R = 4Ur/\nu$
R_*	boundary Reynolds number, $R_* = V_* D_g/\nu$
S	energy slope (water surface slope)
t	time
T	water temperature
u	instantaneous streamwise flow velocity
U	mean flow velocity
U_o	mean velocity for threshold of particle motion
U_m	maximum velocity in a vertical section in flow
v	instantaneous spanwise flow velocity
V_*	shear velocity, $V_* = (grS)^{1/2}$
V_{*_b}	bed shear velocity, $V_{*_b} = (gr_bS)^{1/2}$
x	longitudinal coordinate along bed downstream
y	vertical coordinate, upward from bed
y^+	dimensionless distance above bed, $y^+ = y\ (\tau_o/\rho)^{1/2}/\nu$
α	attentuation factor in autocorrelation function
γ	specific weight of fluid, $\gamma = \rho g$
γ_s	specific weight of sediment, $\gamma_s = \rho_s g$
δ	distance local sediment transport lags behind local velocity
μ	dynamic fluid viscosity
ν	kinematic fluid viscosity

ρ density of fluid

ρ_s density of sediment

σ_g geometric standard deviation of sediment size

τ_o mean shear stress at bed

τ_* Shields parameter, $\tau_* = \tau_o / (\gamma_s - \gamma) D_g$

LIST OF FIGURES

LIST OF TABLES

ACKNOWLEDGMENTS

I wish to thank Professor John B. Southard for his guidance and support throughout this study. Without his valuable suggestions and criticisms this work would not have been completed. I also wish to thank Jon Boothroyd for the loan of his excellent field data on sand waves. My fellow students Wilford Gardner, Lawrence Boguchwal, Mary Jane Goettal and Robert Young have provided many hours of fruitful discussion and have helped to make life at M.I.T. more enjoyable.

Finally I offer my deepest appreciation to my wife, Susan, who was my typist, sand siever, draftswoman, and editor, for her patience and understanding.

This work was supported by the Office of Naval Research under contract N 00014-67-A-0204-0048.

1. INTRODUCTION

INTRODUCTORY NOTE

Sediment transported by water has an appreciable effect on the flow. High concentrations of suspended sediment alter the momentum exchange and hence the turbulence structure, while sediment transported along the bed alters flow depth and energy loss due to changes in channel geometry and roughness. In addition to the effect of transported sediment on the fundamental flow laws, knowledge of the capacity of a flow to transport sediment has economic relevance with respect to erosion, flood control, navigation, irrigation, pollution, and harbor maintenance.

In addition to these engineering applications, sediment transport is of primary interest to geologists who interpret modern and ancient sediments deposited by rivers, lakes, and the ocean. A ubiquitous characteristic of these sediments is cross-stratification, which seems to be largely the result of sediment being transported on the bed as migrating grain mounds. In the last two decades the study of these bed forms has increased greatly, first in an attempt to discern direction of transport in ancient environments, and, more recently, in an attempt to characterize the hydraulic setting in the ancient flow system.

However, up to the present time, the basic laws of

sediment transport have only been partially outlined. The result has been great uncertainty as to how well sediment transport can be predicted, even irrespective of what form the bed-load movement will assume. Without full knowledge of the mechanics of bed-form movement, engineers and geologists have had to resort to empirical classifications in attempts at prediction and interpretation. Out of this empirical approach has emerged the concept of a definite sequence of bed configurations; this concept has managed to put into some order a vast amount of empirical observation.

If the mechanics of development of different bed configurations can be accurately deduced, scientists will have an effective tool for prediction in modern sediment transport and for interpretation in ancient sedimentary deposits. Many theories have been put forward to explain this complex phenomenon. In the following section a brief historical summary outlines the main contributions.

HISTORICAL BACKGROUND

Flow-produced bed forms have been the subject of investigation by geologists and hydraulicians since the nineteenth century. It was Sorby who first interpreted cross-bedding as the result of ripple migration and used cross-laminated beds to infer paleoflow direction (1853, 1859). Deacon (1892) was one of the first to use ex-

periments to determine the current strengths which caused bed forms. Gilbert's (1914) early experiments provided the first clear descriptions of different bed configurations and the various stages of development and sequences of occurrence. Although there has been a great deal of empirical work since Gilbert's time, explicit recognition of a sequence of bed configurations awaited the comprehensive flume experiments of Simons and Richardson (1962, 1963). These investigators developed more explicitly than before the idea that different bed configurations succeed one another in a definite sequence as hydraulic conditions are changed. The ranges of hydraulic conditions for which each bed configuration develops were defined from extensive and systematic flume experiments, and the sequences of bed configurations were classified into two flow regimes. In the fine to medium sand range, the sand bed at first gives way to ripples with increased discharge. Further increases in discharge cause dunes, with a possible intermediate range of ripples on dunes. Ripples and dunes comprise the lower flow regime, which is hydraulically characterized by having Froude numbers less than unity (subcritical flow) and by having weak water-surface waves which are out of phase with the bed forms. With increased discharge the dunes are washed out, and a plane bed with grain motion ensues. For Froude numbers greater than about 0.8, antidunes are initiated under large

surface waves in phase with the bed forms. At still higher discharges a little-studied further stage called chutes and pools results and, together with antidunes, constitute the upper flow regime.

In coarser sands (greater than 0.60 mm) the lower flow regime is somewhat different (Guy et al., 1966; Williams, 1967). Ripples are not developed in the coarse sands: upon initiation of movement the sediment bed remains flat, and then at higher velocities dunes develop on the flat bed. At still higher velocities, and with the Froude number greater than about 0.8, the upper-flow-regime bed configurations develop.

Many investigators have sought to delineate the limiting hydraulic conditions for different bed configurations by constructing dimensionless graphs, partly in the hope that this would represent some improvement over the generalization of an upper and lower flow-regime sequence. Attempts at various dimensionless renderings of experimental data have been made by Albertson et al. (1958), Allen (1968), Blench (1969), Bogardi (1959), Bonnefille (1965), Chabert and Chauvin (1963), Garde and Albertson (1961), Garde and Ranga Raju (1963), Harms (1969), Larras (1963), Simons and Richardson (1963), and Southard (1971). Most of the proposed plots display considerable overlapping of stability fields, indicating that more understanding

of basic mechanics is needed before the flow-regime concept outlined above can be refined. All the proposed diagrams are two-dimensional except that of Southard (1971), which is three-dimensional. Southard's diagram was tested for only one set of data, that of Guy et al. (1966), but shows none of the scatter that the other diagrams do. In addition, Southard's diagram shows that it is more important to make the distinction between surface-independent bed configurations (ripples and dunes) and surface-dependent bed configurations (antidunes) than to use such terms as upper- and lower-flow-regime bed configurations.

Compared with the great number of efforts to obtain empirical relationships between the various bed forms, there have been few attempts at analytical treatment of bed-form genesis, in keeping with the complexity. One of the first attempts was that of Exner (1920), who, after deriving the sediment conservation equation, combined this equation with two very simple assumptions: fluid discharge is constant along the flow, and sediment discharge is a function of flow velocity. The results predict that a sinusoidal disturbance on the bed surface will lengthen and steepen at the downstream end until a slipface forms and the bed disturbance takes on the characteristic shape of a bed form.

The next analytical treatments of bed-form generation

were a series of stability analyses by Kennedy (1963), Reynolds (1965), Engelund and Hansen (1966), Gradowczyk (1968), Hayashi (1970), and Smith (1970). Reynolds (1965) used the same assumptions as Exner (1920) and combined them with the momentum equation for steady, one-dimensional shallow flow. A perturbation is introduced into the linearized equations, and the perturbation grows provided that there is a phase lag between erosion and mean velocity. However, the phase lag needed to obtain a growing bed form moving downstream is unrealistically large.

A different analytical approach was attempted by Kennedy (1963). Kennedy used a potential-flow model for a stability analysis. His assumptions are an irrotational, incompressible flow with an initial sinusoidal perturbation. To make the perturbation other than neutrally stable, Kennedy introduced the concept of a lag or response time, which Reynolds (1965) was to adopt in a similar potential-flow analysis. Kennedy's result for the prediction of antidunes in the upper flow regime is very good, but the prediction of lower-flow-regime bed configurations is poor and does not differentiate between ripples and dunes. Potential-flow analyses have always proved valuable in wave problems; this is physically very similar to the case of antidunes, in which bed waves and surface waves are strongly coupled, but in

the case of subcritical flow there is little or no such dynamic coupling. Also, the critical concept of lag distance, which is necessary to produce a growing bed form, has not been demonstrated to be applicable. Similar analytical approaches have been attempted by Engelund and Hansen (1966) and Hayashi (1970), but these have added little to Kennedy's and Reynolds' results.

Gradowczyk's (1968) linear stability analysis utilizes the shallow-water momentum equation similar to that of Reynolds (1965). For strongly coupled bed and surface waves, and again using the concept of a lag distance or phase lag, Gradowczyk recovered most of the results of Reynolds and Kennedy, though more rigorously. Gradowczyk further noted that the growing sediment wave predicted by his theory is a kinematic wave in the sense of Lighthill and Whitham (1955).

Smith (1970) attempted a more sophisticated stability analysis utilizing the full momentum equations with an assumption of constant eddy viscosity and using an empirical sediment-discharge relationship. Like the others described above, Smith's analysis produced a growing condition for finite perturbations. Having shown a perturbation to be growing, Smith hypothesized that flow separation over the bed perturbation would cause a maximum in shear stress to occur at some distance downstream, dependent upon the height of the slipface and the co-

efficient of friction. No distinction between ripples and dunes is inherent in this model.

Bagnold (1956) presented a very different analytical approach to the generation of bed forms. He introduced the concept of a dynamic coefficient of friction, defined as the ratio of tangential to normal stresses in a flowing granular mass. When the dimensionless shear stress, otherwise described as the Shields function, exceeds 0.4, the bed surface grains are put into suspension. Grains can be moved on the bed at values of dimensionless stress lower than 0.4, but this gives rise to a deficit in resistance which causes the bed to deform in such a way as to create form drag. Therefore the bed surface alters to a rippled pattern as primary and then secondary ripples form. Bagnold did not include dunes in his analysis, but suggested that they form due to local slope changes on the sediment bed surface.

Pratt (1971), in an experimental study of bed configurations compared his findings to Bagnold's hypotheses and concluded that the primary ripples proposed by Bagnold were ripples and the secondary ripples were dunes. Pratt's data do not clearly substantiate any other of Bagnold's hypotheses about the angle of the bed-form back slope or the value of applied shear stress at which all bed forms disappear. Furthermore, the legitimacy of Bagnold's basic concept of dividing the

stress into two distinct parts, that due to fluid stress and that due to grain collisions, is not proven.

Recently research on bed-form development has turned to the observational approach in the hope of better understanding the mechanics of the bed forms. Raudkivi (1963), studying ripple development from an initially flat sediment bed, found that chance piling up of grains occurs when the threshold conditions of sediment transport are exceeded. The flow separates over these pilings, and a core of intense turbulent eddies acts on the sediment bed and entrains additional sediment where the flow reattaches. Further downstream the turbulent fluctuating components of velocity are smaller in magnitude and the additional entrained sediment cannot be maintained, so that the sediment is deposited, leading to formation of a new mound and renewed flow separation. Raudkivi made it clear that the process was one of progressive ripple growth downstream from a disturbance rather than amplification of a bed disturbance of a given wavelength. This progressive ripple formation is completely at variance with the predictions of spontaneous bed deformation by Bagnold's theory.

Southard and Dingler (1971) described in detail the development of ripples from mounds. Furthermore they pointed out that there is a range of bed shear stresses for which a flat bed in uniform flow will not

develop ripples spontaneously from flow-developed obstructions but which maintain a metastable state until a large enough perturbation is applied to the bed.

Recently Williams and Kemp (1971) investigated ripple propagation in more detail with a view to determining how the flow constructs the piling up of grains and how these very small obstructions trigger ripple development. They found that random high-velocity streaks invade the viscous sublayer and interact with the bed, locally increasing the velocity by up to 30%. The surface of the bed then becomes streaky due to these erosive velocity filaments. When these streaks overlap or cross, they construct an obstacle capable of causing flow separation and ripple development. This process of bed-surface streaking and resulting ripple development was shown to occur more easily and quickly in finer than in medium sands.

Another approach that has been attempted to try to understand the mechanics of bed configurations is that of examining the statistical properties of bed profiles. Investigations by Nordin and Algert (1966), Ashida and Tanaka (1967), and Squarer (1970) have tried to relate bed-profile spectra to bed-form geometry. Statistical models such as the Markov process have been suggested but not proven. The stochastic analysis of bed forms should well describe the randomness of the surface of

the bed forms once established, but it should tell very little about the reasons for initial generation of bed forms.

Some conclusions can now be drawn as to the present state of knowledge about bed configurations. The empirical approach has successfully delineated the sequence of bed configurations that occur in flumes and only partly delineated the sequence in natural environments, but has not yet been able to apply more definite hydraulic limits to their stability fields. The analytical theories have successfully predicted and described the upper-flow-regime antidunes but have had poor success at predicting the more commonly occurring lower-flow-regime ripples and dunes. The linear stability analyses of Kennedy, Reynolds, and Gradowczyk all predict an instability representative of bed-form development provided that a phase lag between sediment transport and local velocity and shear stress is included. Smith's stability analysis, numerically solved for low Reynolds numbers, also predicts that the perturbations will be unstable for wavelengths less than a critical wavelength defined by the inertial phase lag of the sediment transport. However, there is no theoretical or experimental evidence to confirm the existence of a lag distance. Furthermore, none of these stability analyses can predict the occurrence of two very different lower-flow-regime bed forms, ripples and dunes.

Bagnold's model of stress instability predicts the spontaneous development of ripples, whereas observations prove the mode of generation of ripples to be one of gradual growth dependent upon mechanics of flow separation.

The approach that describes physical mechanisms of bed form generation has shown good success in constructing a viable model of ripple generation. However, the dune bed forms have not as yet been investigated. Since analytical models cannot describe the origin of dunes, the experimental approach appears to be the most likely mode of investigation.

PURPOSE AND OUTLINE

In the following chapters, an experimental study into the mechanics of lower-flow-regime bed configurations is outlined. The study is focused on the range of medium to coarse sands, to fill in a gap that exists in this region in experimental observation (Southard and Boguchwal, 1973). Of more importance, this range of grain sizes is a region in which dune formation can be observed without the obstruction of ripples. Also, it is within this region that ripples disappear with increasing grain size, so that the study of this size range should give important insights into ripple mechanics. Therefore, it is in this range of medium to coarse grain

sizes that fundamentally important processes are largely unobscured, and it is these processes which are the target of this study.

Chapter 2 is a description of the experimental system and procedure. Chapter 3 presents the results of the experiments and a discussion of the most significant new observational data. In Chapter 4, the observations have been incorporated into coherent models with a theoretical basis. An attempt is made in Chapter 5 to test the proposed models of lower-flow-regime bed-form mechanics with all the relevant field data available. In Chapter 6 the new conclusions of this research are presented.

2. EXPERIMENTAL APPARATUS AND PROCEDURE

APPARATUS

The experiments described in this chapter were performed in two recirculating flumes. Runs in series E were made in a flume 5.5 m long, and were preliminary runs to observe the general characteristics of bed configurations in coarse sand. Runs for series A,B,C, and D were made in a flume 11.5 m long, and concentrated on the detailed mechanics and geometry of bed configurations in medium to coarse sands. Descriptions of the flumes and their apparatus are given in the following sections.

5.5 m Flume

The 5.5 m flume is a tilting, recirculating flume with a rectangular cross section 17 cm wide and 34 cm deep (Fig. 2.1). A connected pair of I beams support the transparent acrylic channel as well as the return pipe and centrifugal pump. The flume is supported at the upstream end by a pivot support and at the downstream end by a coupled pair of screw jacks. The jacking system allows a range of slope from -0.001 to +0.015.

Discharge is measured with an orifice meter connected to a water-mercury differential manometer. The orifice meter was built to standard geometry, with D_1 = 5.08 cm,

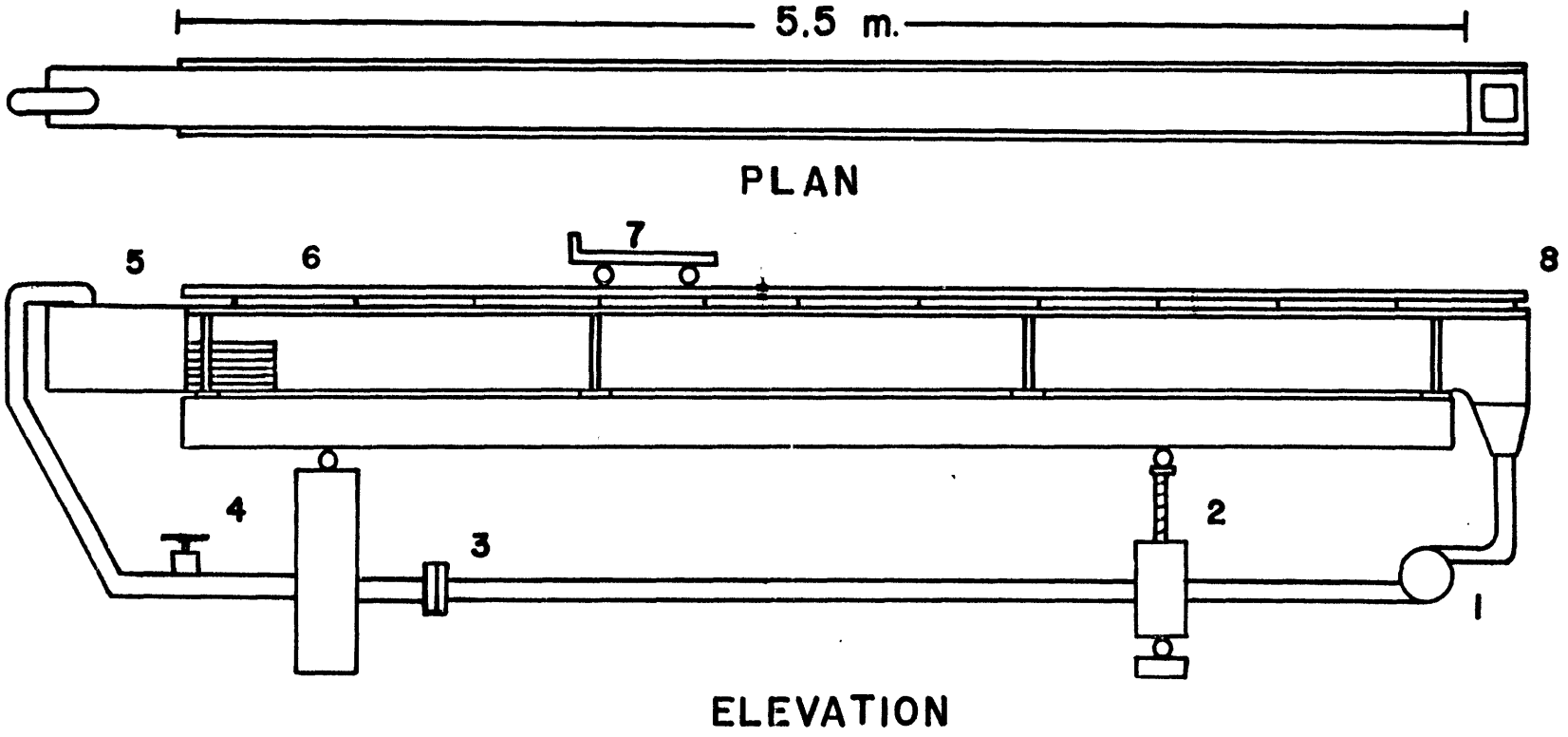

Fig. 2.1. Schematic diagram of 5.5 m flume.

D_2 = 3.56 cm. Discharge is controlled by gate valves in the return pipe near the upstream end of the flume, and by varying the diameter of the sheaves on the pump and motor.

At the entrance section of the flume, the flow passed through a grid of 0.95 cm diameter plastic straws, which helped make the velocity more uniform at the entrance. A piece of plywood 60 cm long was floated on the water surface just downstream of the grid to prevent surface waves from being introduced into the channel. Also, a planar false bottom 96.5 cm long and 3.8 cm high was placed on the channel bottom downstream of the grid to prevent erosion due to the high shear stress in the developing boundary layer and residual nonuniformities generated at the inlet.

A pair of one-inch steel rods mounted above the channel sidewalls served as rails for an instrument carriage. These rails were carefully aligned with a still water surface at zero slope prior to the study. The carriage supported a rack-and-pinion point gage which could be read to within 0.05 mm. The point gage could traverse the length and width of the flume. The instrument carriage could also carry a Pitot tube as well as a bed-leveling device.

11.5 m Flume

The 11.5 m flume, shown schematically in Fig. 2.2, is 91.5 cm wide and 56 cm deep. The channel is constructed of transparent acrylic plastic and is supported on a steel truss. The truss has a pivot support near the downstream end and a pair of synchronized power-driven screw jacks near the upstream end capable of lifting the flume through a slope of -0.006 to +0.02. The channel is connected to a fixed tailbox by a flexible rubber collar.

A vertical propeller pump driven by a 20 hp motor leads from the tailbox to the return pipes. Valves between the pump and the return pipe allow any or all of the flow to be returned directly to the tailbox, and thus bypass the flume. Another discharge control is the pump speed, which can be varied in steps by means of various pulley combinations. Two gate valves in the return pipe can also control flume discharge. Return flow is through 6-inch galvanized steel pipes which split into a series of 14 2-inch rubber hoses after passing through splitter cones. The 2-inch hoses have valves for fine adjustments to the discharge.

Venturi meters (D_1 = 15.6 cm, D_2 = 10.2 cm) in the return pipes near the upstream end of the flume are connected to water-mercury manometers which can be read to the nearest 0.00125 cm. Upstream of the meters

Fig. 2.2. Schematic diagram of 11.5 m flume.

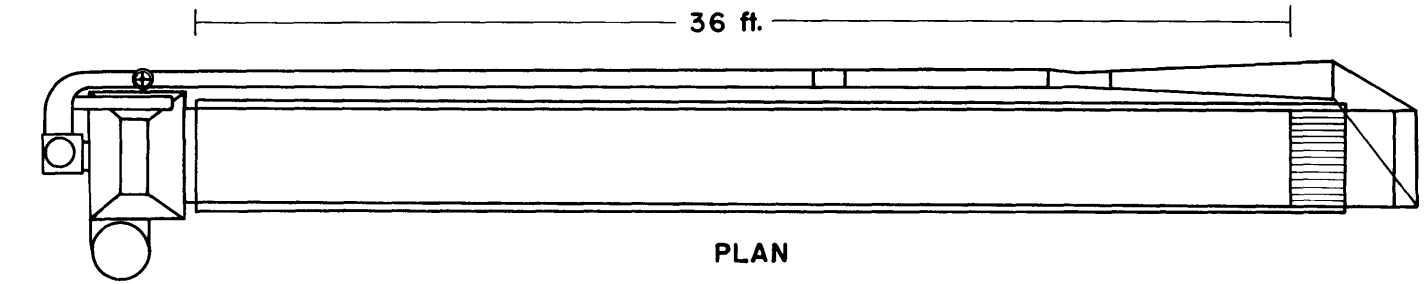

PLAN

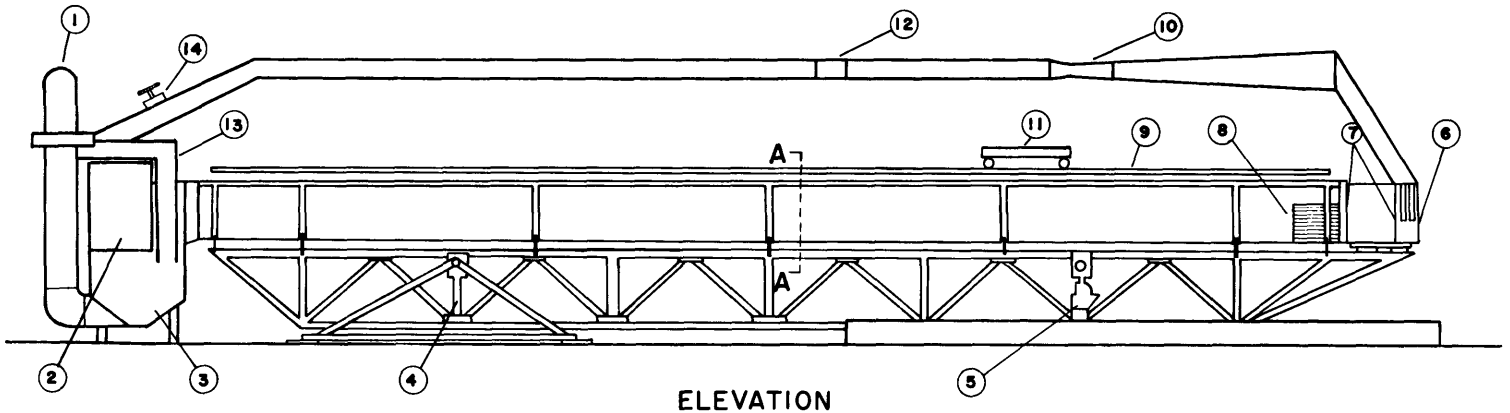

ELEVATION

LEGEND

1. PUMP
2. SETTLING BARREL
3. TAILBOX
4. PIVOT SUPPORT
5. JACKING SUPPORT
6. INLET SECTION
7. BAFFLES
8. STRAWS
9. CARRIAGE RAILS
10. VENTURI METER
11. INSTRUMENT CARRIAGE
12. TRANSPARENT PIPE
13. FLUME BYPASS
14. GATE VALVE

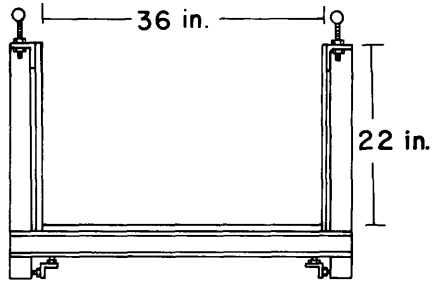

SECTION A-A

is a 30-cm section of clear plastic pipe for visual inspection of the return flow. From observation of the return pipes and the headbox, it was apparent that sediment was not being stored in the return system. All sediment entering the tailbox was returned directly to the upstream end of the flume.

At the channel inlet are two baffles constructed of acrylic sheet with a hexagonal array of one-inch holes. Just downstream is a grid of thick-walled plastic straws about one centimeter in diameter and 45 cm long. These baffles serve to straighten the flow, reduce the scale of the turbulence, and make the velocity uniform across the channel width. The grid of tubes causes the flow to back up slightly, resulting in small surface waves downstream of the grid; a plywood sheet, 70 cm long and as wide as the channel, was in contact with the water surface downstream of the straws to suppress those surface waves. A wooden false bottom 3.8 cm high and as wide as the channel extended 1 m downstream from the channel entrance to prevent scour by the developing boundary layer. The sand bed in the flume tapered onto the false bottom.

The tailbox formed a large reservoir to prevent any drawdown or backing up of the water during pumping. Water was pumped by an auxiliary system from near the surface of the tailbox into a settling and overflow

barrel, from which sediment-free water was pumped separately to flush the bearings of the main pump. The overflow water was passed through a fiberglass filter to remove any algae or fines from the water and to maintain good water clarity throughout the experiments. A copper cooling coil carrying a controlled flow of cold tap water was immersed in the settling barrel to maintain a constant water temperature (to within $\pm$1°C) not greater than room temperature during the run. During the entire set of experiments, there was a 5°C seasonal variation in room temperature.

Two 3.8 cm steel rods mounted on the upper flanges of the channel supports served as rails for an instrument carriage. The rails were aligned with the still water surface prior to the experiments and were rechecked at intervals between experiments. The steel instrument carriage served to hold the point gage and Pitot tube, which could be positioned laterally across the channel.

A bed-leveling device, consisting of a wooden board beveled to a knife edge and reinforced by angle steel, could be clamped to the instrument carriage. The bed leveler could be carefully adjusted to any depth and could produce a flat bed with less than one grain diameter relief.

Sediment Discharge Measurement

Sediment discharge was measured at the downstream end of the large flume using the technique described by Rathbun and Guy (1967). A wire-mesh tray was installed which could catch all the size grades of the sediment. The trap, 91.5 cm wide, 20 cm long, and 15.4 cm deep, was constructed of plastic struts and copper screening. The design of the trap allowed it to fit onto the end of the flume channel in the tailbox so that it was level with the flume bottom. The mesh at the sides and back of the trap was high enough to catch all grains moving as bed load and to hold a large sediment sample (0.03 m^3 approximately), but low enough to let the sediment-free water pass over it without backwater effects. Since the trap was situated in the tailbox, it could be emplaced and removed during an experiment without disturbing the bed configurations.

Velocity Profile Measurement

Local velocities in the flow were measured with a Prandtl-Pitot tube connected to an air-water differential inclined manometer that could be read to the nearest 0.00125 cm. The Pitot tube has a 0.95 cm O.D. and a 0.32 cm I.D.

SANDS

Source

The sands used in experiments A,B,C,D were different size fractions of a composite sand. The two components of the sand were Type 0 Blasting Sand supplied by the Holliston Sand Company (Holliston, Mass.) and washed sand supplied by The F.V. Lawrence Co. (Falmouth, Mass.). Both sands were predominantly medium to coarse sands and had been washed and partially sieved to remove finer sand and clay.

The blasting sand was a subangular quartz sand with a high percentage of metamorphic rock fragments. The washed sand was a subrounded glacial outwash sand having more than 90% quartz. The composite sand averaged 80% quartz and 20% metamorphic rock fragments.

The different size fractions were separated using large sieves with mesh sizes of 0.869, 0.787, 0.681, 0.630, 0.581, and 0.530 mm. The sands were washed after sieving and then placed in the flume to form a bed eight to ten cm thick.

Series E sand was obtained from glacial outwash deposits near Wellfleet, Mass. It is a subrounded quartz-rich sand (90%) with minor amounts of quartzite and gneiss. The sand was sieved using 1.40 and 1.00 mm sieves.

Sediment Analysis

A sieve analysis was made for each sediment to obtain mean size and standard deviation. The size fractions were separated with a set of $\sqrt[4]{2}$ mesh sieves shaken on a Tyler Rotap shaker. The samples were sieved for 10 to 15 minutes, and the sediment retained on each screen was weighed on an analytical balance. The size distributions were then plotted on logarithmic probability paper as almost straight lines (Fig. 2.3). The geometric mean size and standard deviation were then calculated from the size-distribution plot.

The specific gravities of the sediments were measured using a pycnometer. This instrument allows comparison of the weight of dry sediment and the weight of water displaced by the sediment.

Roundness and shape of the sand grains were determined visually from photomicrographs of the sediments (Fig. 2.4). The mean size, standard deviation, specific gravity, and shape of each sediment sample are shown in Table 2.1.

EXPERIMENTAL PROCEDURE

Brooks (1958) demonstrated that, in open-channel flows transporting sediment, velocity and sediment discharge are not uniquely determined by bed shear stress or by combinations of depth and slope or hydraulic radius and slope, as had previously been assumed. If velocity

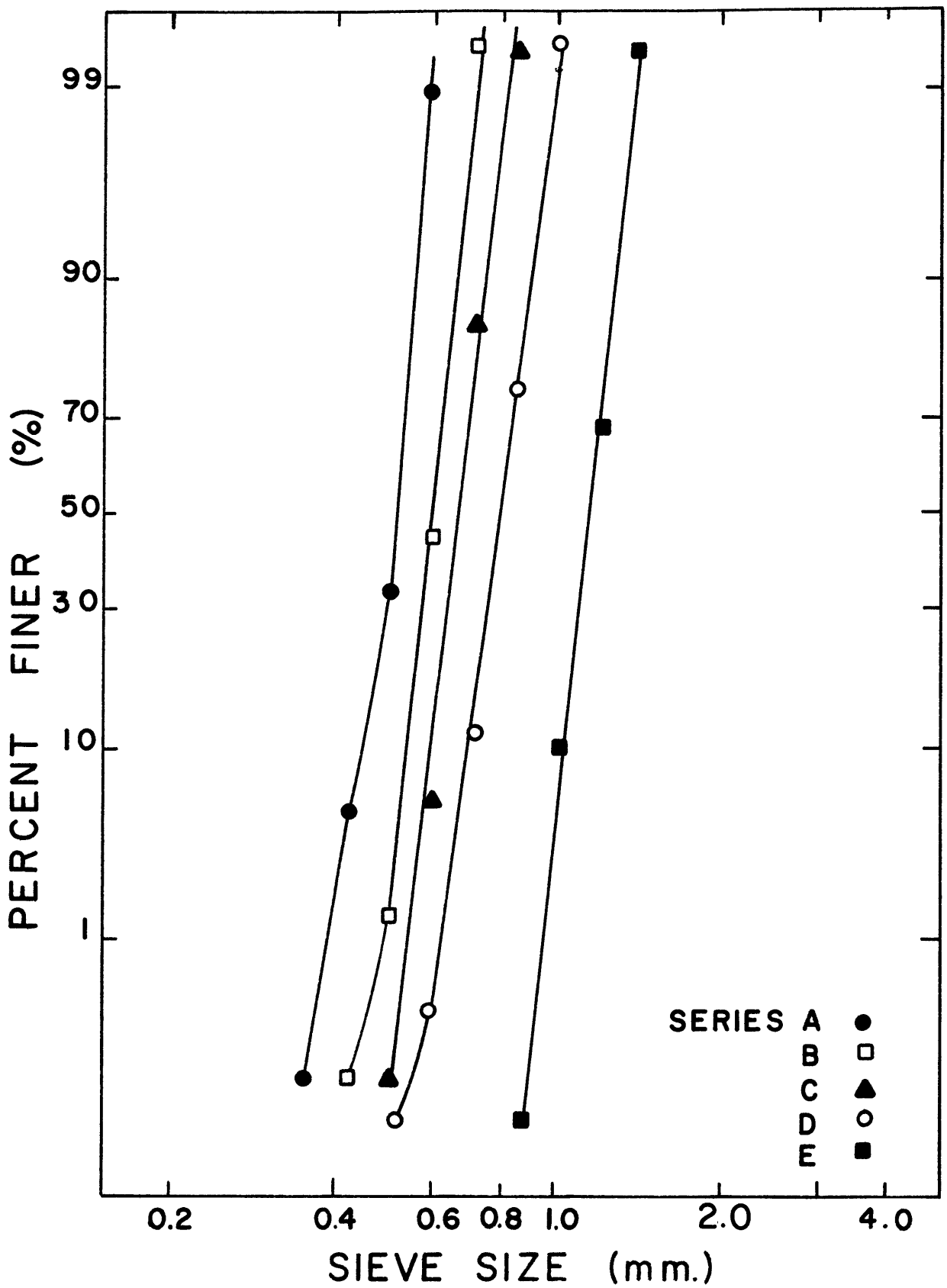

Fig.2.3. Distribution of grain sizes of the sands used in series A-E.

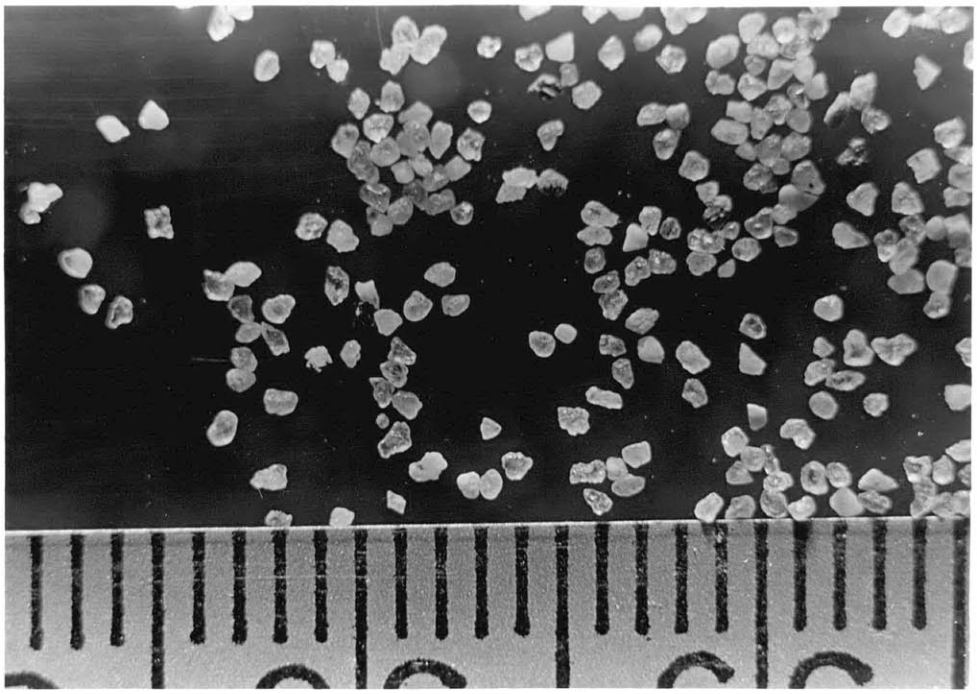

Fig. 2.4a. Photograph of sample of 0.51 mm sand (series A)

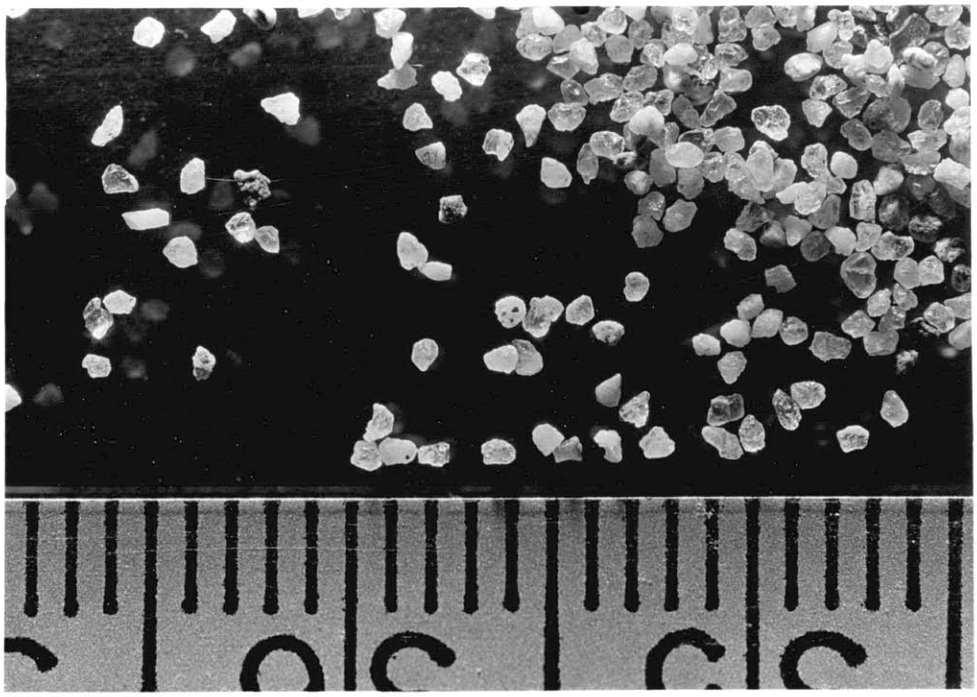

Fig. 2.4b. Photograph of sample of 0.60 mm sand (series B)

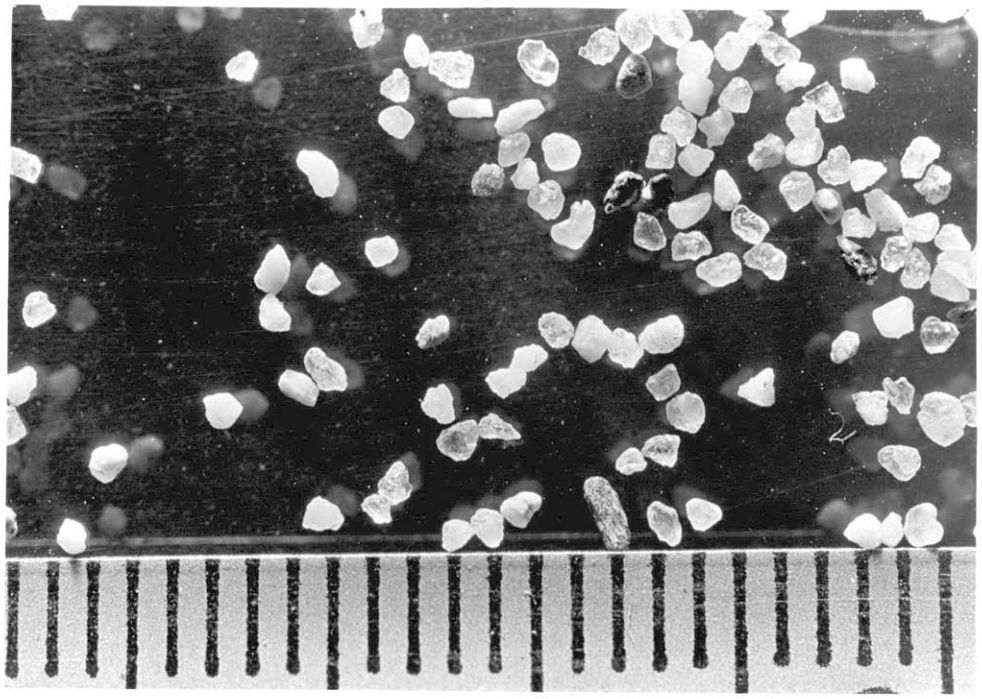

Fig. 2.4c. Photograph of sample of 0.66 mm sand (series C)

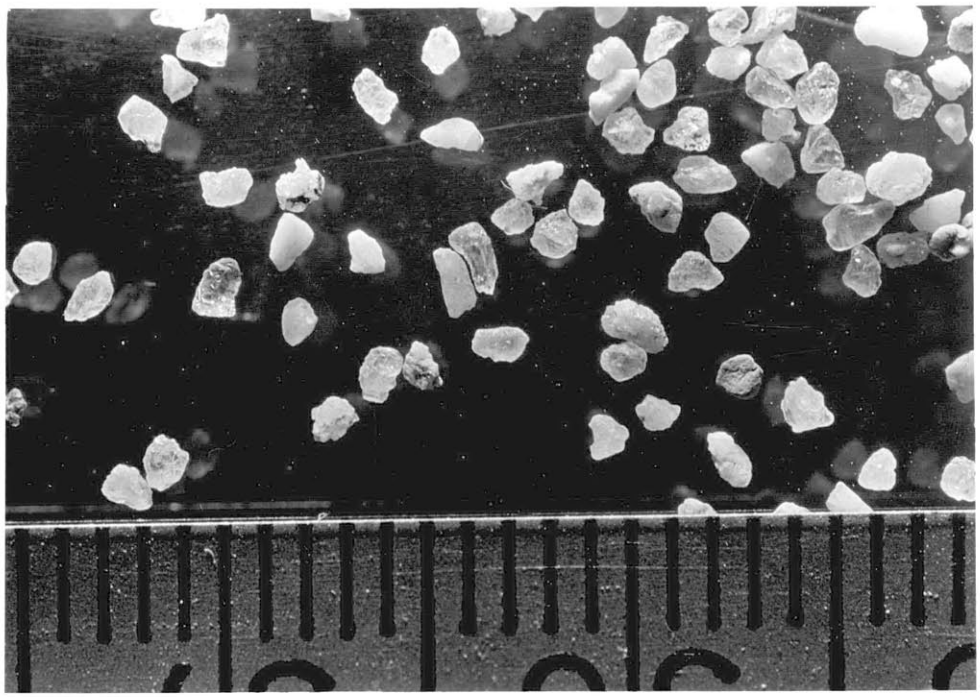

Fig. 2.4d. Photograph of sample of 0.80 mm sand (series D)

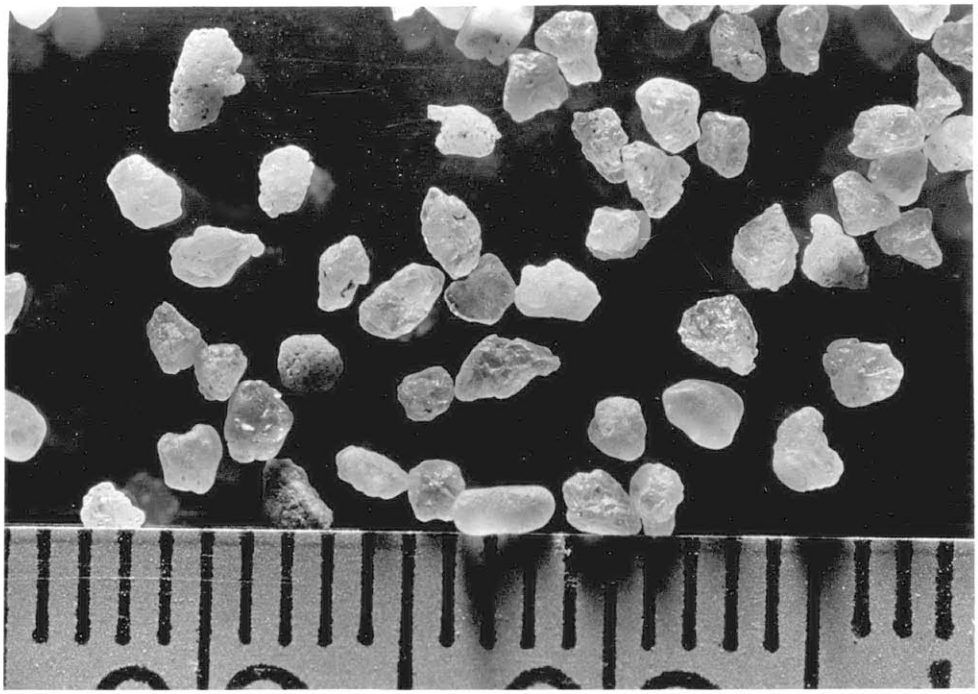

Fig. 2.4e. Photograph of sample of 1.14 mm sand (series E)

TABLE 2.1 Physical Characteristics of Sands

Series	D_g Geometric Mean Size (mm)	σ_g Geometric Standard Deviation	ρ_s Mean Density (gm/cm^3)	Shape
A	0.51	1.08	2.65	subangular
B	0.60	1.09	2.65	subangular
C	0.66	1.05	2.65	subangular
D	0.79	1.08	2.66	subangular
E	1.14	1.10	2.65	subangular

and depth are experimentally set, bed shear stress and slope are single-valued and vary in an orderly fashion. Following this concept, depth and discharge were preset in these experiments, and slope and bed shear stress were allowed to assume their equilibrium values.

The experiments were all carried out at a constant depth, for two reasons. First, the effects of the small range of depths possible in laboratory flumes is not appreciable, except for very shallow depths, and is well recorded for coarse sands (Williams, 1970). Second, by holding the depth constant and by changing only one variable, the velocity, trends in the data could be more easily recognized and correlated.

In order to compare the effect of closely spaced grain sizes, the sediment was extensively sieved to provide well sorted and very uniform sands. Mean grain size was carefully controlled and sorting was eliminated as a variable.

Close control of the experimental variables such as water temperature, sediment sorting, and mean flow depth, and the systematic variation of mean flow velocity and sediment size makes the experimental design far different from natural streams. However, it was hoped that the experimental simplicity would help in recognition of trends in the fundamentally important variables which are usually masked by the variation of quantities with

only second-order importance.

For each series of experiments the sand bed was first carefully leveled. At the channel entrance, the sand bed was tapered upward downstream from the false bottom floor to the desired level of the sand bed over a 70 cm length. Any disturbances in this region were leveled by hand.

The slope of the flume bottom was preset to an approximate value obtained from published results of Guy et al. (1966) and Williams (1970), who conducted experiments over the same range of velocity and depth with finer and coarser sands. The flume was filled to the desired depth with water heated to approximately the desired temperature, and the pump was then started. The discharge was slowly increased to the experimental value.

For runs in series A,B,C, and D, the water-surface slope was determined by measuring water-surface elevations with the point gage at 10 cm intervals along the centerline of the flume. A straight line was fitted to the data by eye. For the runs with a flat bed, the bed-surface slope was easily measured, as was the depth, by direct measurement along the flume walls. In runs with large variations in bed elevation caused by migration of bed forms, the flow was stopped slowly and carefully after the water-surface profile had been measured. A bed-

surface profile along the flume centerline was then measured with a point gage at 10 cm intervals. The slopes of the best-fit straight lines through the profiles of water surface and bed surface were then compared to determine if uniform flow was being maintained. If the two slopes were not parallel, the slope of the flume was adjusted to approximate uniform flow in the channel. The sand bed would adjust its slope by erosion and deposition to produce a uniform flow if left to itself. However, this adjustment depends on the movement of a large quantity of sand and so takes a long time. Therefore, adjustments to the flume slope produced uniform flow much more quickly and reduced the time needed for the bed to reach equilibrium.

This procedure of checking water-surface slope and adjusting the flume slope for maintenance of uniform flow was carried out many times in the first 6 to 12 hours of the experiment. Adjustments to the flume slope were usually small, depending on the accuracy of the approximate preset slope, and each successive adjustment became smaller until the water-surface slope became stable.

From the monitoring of the water surface and bed surface, the flow depth was checked and any loss of water due to evaporation was replenished. During an experimental run the water level varied less than ± 3 mm. In two runs the sand bed was noticed to increase in height at

the upstream end of the flume. This was assumed to indicate that the flume slope was too small. When the slope was increased slightly, the sand became redistributed downstream, and a new wedge did not form at the upstream end of the flume.

The experiments lasted from 24 to 120 hours, with the majority lasting about 48 hours. Sufficient time was allowed for bed forms to develop fully, migrate through the flume, be caught at the tailbox, and reform at the upstream end to develop again. However, in most of the runs with a rippled bed, development of the ripples was so slow in the coarse sand as to preclude establishment of true equilibrium without probably several hundred hours of running time. In these cases the run was terminated after a definite trend of development was established and the run was noted as not having reached full equilibrium.

When equilibrium had been established, the bed-load discharge was measured with the mesh trap. The measurement periods varied from 1/2 hour up to 12 hours, depending on the sediment transport rate. Approximate amounts of sand were gradually introduced into the upstream end of the flume to compensate for the sand captured by the bed load trap. The centerline velocity profile was also measured at this time using a Prandtl-Pitot tube.

Finally, the water-surface profile was measured at

the centerline in 3 cm intervals using the point gage. Then the discharge was slowly decreased and the pump was stopped. With sufficient care only a small water wave developed in the channel, and the wave did not disturb the sediment bed as it passed down the channel.

The bed-surface profile was measured with the point gage along the centerline at 1 cm intervals over a long uniform-flow reach well away from the inlet. Least-square straight lines were fitted to the bed-surface and water-surface profiles, and from these the mean flow depth and energy slope were calculated.

The bed-load samples were dried and weighed to obtain the bed-load discharge, and then the samples were sieved to check the size distribution.

3. PRESENTATION AND DISCUSSION OF EXPERIMENTAL RESULTS

BASIC DATA

General

In this section changes in bed configurations are compared to changes in mean flow variables. The second set of experiments, which include series A,B,C, and D, was designed to investigate in detail the different bed configurations formed, for Froude numbers less than one, in sands intermediate in size between 0.49 mm and 0.80 mm. The hydraulic data from series A,B,C, and D are presented in Tables 3.1 and 3.2, and the data from series E are presented in Table 3.3.

The data in Table 3.2 have been corrected for sidewall effects using the technique devised by Johnson (1942) and modified by Vanoni and Brooks (1957). An outline of the sidewall correction method is presented in Appendix A along with definitions of bed friction factor, bed hydraulic radius, and bed shear velocity.

Reproducibility and Equilibrium

Table 3.4 shows the results of two pairs of closely comparable runs. In the pair of experiments C1-C2, which produced a flat-bed configuration, the slope, bed friction factor, and sediment discharge are all in excellent agreement for similar values of velocity,

TABLE 3.1 Summary of Data 11.5 Meter Flume

Run No.	Q Discharge (m^3/sec)	U Velocity (cm/sec)	d Depth (cm)	S Friction Slope	T Water Temp. (°C)	g_s Sediment Discharge (gm/cm sec x10^{-3})	Bed State
A-1*	0.0342	22.80	16.40	0.00017	31.0	0	Ripple/No Move
A-2	0.0390	28.80	14.80	0.00047	31.0	0.04	Ripple/Flat
A-3	0.0425	31.05	14.95	0.00056	31.0	0.78	Ripple
A-4	0.0444	31.80	15.25	0.00054	31.0	2.09	Ripple
A-5	0.0484	34.60	15.30	0.00061	30.0	3.59	Bar
A-6	0.0464	34.40	14.75	0.00059	31.0	1.40	Bar
A-7	0.0560	40.40	15.15	0.00068	30.0	5.34	Bar
A-8	0.0601	44.60	14.70	0.00077	30.0	8.49	Bar
A-9	0.0667	47.50	15.30	0.00102	29.0	-	Dune
B-1*	0.0390	27.40	15.55	0.00025	30.0	0	Ripple/No Move
B-2*	0.0419	28.20	16.25	0.00034	31.0	0.05	Ripple/Flat
B-3	0.0464	32.00	15.85	0.00037	31.0	0.24	Flat
B-4	0.0505	34.50	16.00	0.00040	31.0	3.46	Flat
B-5	0.0539	36.90	15.95	0.00042	31.0	3.11	Bar
B-6	0.0599	43.00	15.20	0.00054	31.0	18.20	Bar
B-7	0.0653	48.55	14.70	0.00076	31.0	48.82	Dune
B-8	0.0667	50.30	14.50	0.00090	31.0	46.27	Dune

* Bed State Not At Equilibrium

TABLE 3.1 Summary of Data 11.5 Meter Flume

Run No.	Q Discharge (m^3/sec)	U Velocity (cm/sec)	d Depth (cm)	S Friction Slope	T Water Temp. (°C)	g_s Sediment Discharge (gm/cm sec x10^{-3})	Bed State
C-1	0.0503	34.80	15.80	0.00037	28.0	2.97	Flat
C-2	0.0530	35.40	16.35	0.00039	29.0	2.99	Flat
C-3	0.0563	40.30	15.25	0.00045	28.0	6.74	Bar
C-4	0.0583	41.50	15.35	0.00049	28.0	38.98	Bar
C-5*	0.0441	32.00	15.05	0.00027	29.0	0.15	Ripple/Flat
C-6	0.0469	32.50	15.80	0.00029	29.0	0.42	Flat
C-7*	0.0402	29.90	14.70	0.00010	29.0	0	Ripple/No Move.
C-8	0.0603	45.10	14.60	0.00069	29.0	23.68	Bar
C-9	0.0644	50.10	14.05	0.00101	29.0	65.57	Dune
D-1	0.0503	35.70	15.40	0.00022	27.0	0.41	Flat
D-2	0.0526	36.00	16.10	0.00034	27.0	1.21	Flat
D-3	0.0563	38.65	15.90	0.00046	27.0	2.88	Flat
D-4	0.0599	43.05	15.20	0.00050	27.0	8.01	Bar
D-5	0.0603	44.80	14.70	0.00051	27.0	16.87	Bar
D-6	0.0583	41.10	15.50	0.00048	27.0	3.42	Bar
D-7	0.0627	49.00	14.00	0.00077	28.0	69.95	Dune
D-8	0.0665	46.60	15.60	0.00061	28.0	65.03	Dune
D-9	0.0422	30.30	15.20	-	28.0	0	No Move.

* Bed State Not At Equilibrium

TABLE 3.2 Summary of Data 11.5 Meter Flume

Run No.	V_* Shear Velocity (cm/sec)	f Friction Factor	F Froude No.	r_b Bed Hydraulic Radius (cm)	f_b Bed Friction Factor	V_{*b} Bed Shear Velocity (cm/sec)	D_g Load Mean Size (mm)
A-1*	1.42	0.031	0.18	13.81	0.035	1.52	-
A-2	2.27	0.050	0.24	13.37	0.060	2.48	0.51
A-3	2.49	0.051	0.26	13.55	0.061	2.73	0.52
A-4	2.46	0.049	0.26	13.77	0.059	2.70	0.51
A-5	2.62	0.046	0.28	13.74	0.055	2.87	0.50
A-6	2.54	0.044	0.29	13.23	0.052	2.77	0.51
A-7	2.75	0.037	0.33	13.36	0.043	2.98	0.51
A-8	2.90	0.034	0.37	12.90	0.039	3.12	0.50
A-9	3.88	0.041	0.39	12.75	0.045	3.57	-
B-1*	1.69	0.030	0.22	13.19	0.034	1.80	-
B-2*	2.00	0.040	0.22	14.35	0.048	2.19	0.59
B-3	2.07	0.033	0.26	13.66	0.038	2.23	0.58
B-4	2.16	0.031	0.28	13.67	0.036	2.31	0.58
B-5	2.21	0.029	0.30	13.53	0.033	2.36	0.59
B-6	2.46	0.026	0.35	12.81	0.029	2.60	0.58
B-7	2.88	0.028	0.40	12.61	0.032	3.06	0.58
B-8	3.12	0.031	0.42	12.64	0.036	3.34	0.58

* Bed State Not At Equilibrium

TABLE 3.2 Summary of Data 11.5 Meter Flume

Run No.	V_* Shear Velocity (cm/sec)	f Friction Factor	F Froude No.	r_b Bed Hydraulic Radius (cm)	f_b Bed Friction Factor	V_{*b} Bed Shear Velocity (cm/sec)	D_g Load Mean Size (mm)
C-1	2.06	0.028	0.28	13.31	0.032	2.19	0.67
C-2	2.14	0.029	0.28	13.80	0.033	2.28	0.66
C-3	2.24	0.025	0.33	12.71	0.028	2.37	0.64
C-4	2.35	0.026	0.34	12.40	0.029	2.48	0.65
C-5*	1.73	0.023	0.26	12.29	0.025	1.80	0.68
C-6	1.81	0.025	0.26	13.04	0.028	1.91	0.65
C-7*	1.05	0.010	0.25	9.34	0.008	0.96	-
C-8	2.73	0.029	0.38	12.59	0.033	2.91	0.64
C-9	3.26	0.034	0.43	12.40	0.039	3.51	0.65
D-1	1.57	0.015	0.29	11.37	0.015	1.56	0.82
D-2	1.98	0.024	0.29	13.15	0.027	2.08	0.82
D-3	2.31	0.029	0.31	13.47	0.033	2.47	0.84
D-4	2.36	0.024	0.35	12.60	0.027	2.48	0.80
D-5	2.35	0.022	0.37	12.08	0.024	2.45	0.80
D-6	2.34	0.026	0.33	12.96	0.029	2.47	0.79
D-7	2.85	0.027	0.42	11.99	0.030	3.01	0.79
D-8	2.64	0.026	0.28	13.10	0.029	2.80	0.79
D-9	-	-	0.25	-	-	-	-

* Bed State Not At Equilibrium

TABLE 3.3 Summary of Data 5.5 Meter Flume

Run No.	U Velocity (cm/sec)	d Depth (cm)	S Slope	T Temp. (°C)	Bed State
E-1	35.0	5.0	0.00266	30.0	Flat
E-2	36.0	5.6	0.00213	30.0	Flat
E-3	40.6	5.4	0.00334	30.0	Flat
E-4	47.0	4.9	0.00286	30.0	Dune
E-5	48.0	5.1	0.00460	30.0	Dune
E-6	57.0	5.0	0.00346	32.0	Dune
E-7	38.0	5.8	0.00247	31.0	Flat
E-8	42.0	5.8	0.00180	31.0	Bar
E-9	48.0	5.2	0.00433	32.0	Dune
E-10	45.0	5.7	-	30.0	Bar
E-11	45.0	2.8	-	31.0	Flat
E-12	46.0	5.4	0.00293	32.0	Bar
E-13	41.0	5.8	0.00120	25.0	Flat
E-14	31.0	5.8	-	25.0	No Move.
E-15	33.0	5.8	-	25.0	Flat
E-16	42.0	5.8	0.00273	30.0	Bar
E-17	31.0	7.5	0.00094	30.0	No Move.
E-18	33.0	7.4	0.00067	30.0	No Move.
E-19	42.0	6.8	0.00113	30.0	Flat
E-20	30.0	10.0	0.00060	34.0	No Move.
E-21	36.0	8.4	0.00180	33.0	Flat
E-22	33.6	10.2	0.00235	30.0	Flat
E-23	33.2	4.9	0.00160	30.0	Flat
E-24	37.7	5.0	0.00133	30.0	Flat

TABLE 3.4 Reproducibility of Experimental Runs

Run No.	A.5	A.6	C.1	C.2
Q, Discharge (m^3/sec)	0.0484	0.0464	0.0503	0.0530
d, Depth (cm)	15.3	14.8	15.8	16.3
U, Mean Velocity (cm/sec)	34.6	34.4	34.8	35.4
S, Friction Slope	0.00061	0.00059	0.00037	0.00039
T, Temperature (°C)	30.0	31.0	28.0	29.0
f, Friction Factor	0.055	0.052	0.032	0.033
g_s, Sediment Discharge (gm/cm sec x10^{-3})	3.51	1.40	2.97	2.99
Bed State	Bar	Bar	Flat	Flat

depth, and temperature. For the experimental pair A5-A6, the slope and bed friction factor are again in good agreement, but the sediment discharge is at variance. These experiments produced a bar bed configuration. This variance of sediment transport rate does not necessarily imply a lack of reproducibility between these experiments or a poor sediment-discharge measurement. Rathbun and Guy (1967) made many measurements of bedload discharge in experiments in which ripples developed. The measurements displayed up to one hundred percent variance for long sampling times and large sample sizes. To obtain a stable average sediment-transport rate in experiments with bed-form development, a very long sampling time would be necessary, and this massive sample would introduce irregularities in sediment resupply to the upstream end of the flume. It is concluded that for experimentally feasible sampling times there will be an inherent fluctuation in sediment transport rate as shown in A5-A6. The reproducibility of these experiments is therefore judged to be good.

BED CONFIGURATIONS

Terminology

Southard (1971) has introduced convenient terms to describe the various aspects of any kind of bed configuration. These new terms are defined below and will

be used in this study.

A bed form is an individual structural element such as a ripple or dune.

A bed configuration is an individual or specific geometrical representation of the sand bed, such as a flat bed, a ripple-covered bed, or a bed with a complex assemblage of different bed forms. The term bed configuration is used to describe the geometry of the entire bed, whereas the term bed form is used to describe an individual geometrical element of a bed configuration.

A bed state is the average or totality of all particular bed configurations that can be formed by a given set of average flow conditions. For example, during a given run the bed configuration is different for every different time, but the bed state remains the same (i.e., the ripple bed state).

A bed phase is the aggregate of all bed states that involve a particular kind of bed configuration or a particular characteristic assemblage of bed configurations. For example, a series of flume runs for different depths, velocities, and grain sizes could all be characterized as involving the dune bed state. The totality of such dune bed states would constitute the dune bed phase, and the range of mean flow conditions (mean velocity, mean depth, grain size) within

which the dune phase exists would constitute the dune-phase stability field.

This definition of bed phase closely approximates that independently proposed by Pratt (1971) to divide hydraulically defined regions of similar bed-form development.

Terminology for specific bed configurations was discussed and defined by a Task Force of the Committee on Sedimentation of the American Society of Civil Engineers (1966). The purpose of these definitions was to provide an unambiguous term for every kind of alluvial bed configuration. However, no attempt was made to provide terminology to characterize hierarchical succession of bed configurations, since at that time there was no consensus as to the hydraulic criteria that accurately define the occurrence of each bed configuration. In the literature the terms bed form and bed configuration have been used interchangeably and have included the meanings of the terms bed form, bed configuration and bed state as defined here.

The bed configurations described in this chapter include flat bed with no movement, flat bed with grain movement, ripples, and dunes. One additional bed configuration, bars, will be introduced, and the detailed basis of distinguishing this bed configuration will be presented in the following sections of this chapter. Costello and Southard (1971) observed the bar bed form

in 1.14 mm sand and compared it to the bancs (bars) described by Chabert and Chauvin (1963) in 0.96 mm sand. Pratt (1971) reported identical bed configurations in 0.49 mm sand and has called them "intermediate flattened dunes." Bars have lengths and heights comparable to dunes but do not have the regularity of spacing that dunes display; also bars are largely two-dimensional, with straight crests and very little scour downstream of the slipface, whereas dunes are more three-dimensional, with scour pockets downstream of the slipface.

In the following sections of this chapter, distinctions between different bed configurations will be made by observing the effects of each bed configuration on the flow and by observing the actions and geometries of the bed configurations with changes in flow conditions. If the bed configuration is undergoing a transition rather than simply varying its form, the mean flow characteristics (such as energy slope or friction factor) and the sand bed geometries (spacing or height of bed forms) should show recognizable changes in trends, as should observations of kinematics of bed forms.

Observations

This section describes the observed differences in kinematics of bed configurations with increasing mean flow velocity. The descriptions are only brief and quali-

tative and are designed to define the bed phases. More detailed observations will follow in a later section of this chapter.

At velocities too low to cause grain movement, a leveled sand bed remains unchanged. Closeup observations of the sand bed revealed that sand grains sitting exposed above the bed level, or sand grains entrained by turbulence at the inlet, roll a short way down the bed until they fill a vacant hole on the bed surface. Sand grains well packed into the bed surface are not moved or reoriented. In the finer sands, series A,B, and C, ripples can develop on a bed with no grain movement: if a small surface irregularity (2-3 grain diameters high) is present on the sand bed or one is introduced onto the bed, a train of ripples is observed to grow very slowly downstream from the disturbance (Fig. 3.1). The ripple train propagates downstream and later the upstream part of the ripple train spreads across the width of the flume.

At higher velocities, grains can be set in motion on the flat bed. Exposed grains, located above the average bed level, are the first to be move. More deeply imbedded grains are initially flipped over to produce an imbricated bed. Motion occurs in bursts which erode patches of motionless grains and roll them downstream until the grains find a protected shelter or vacant hole in the bed surface or until they reach

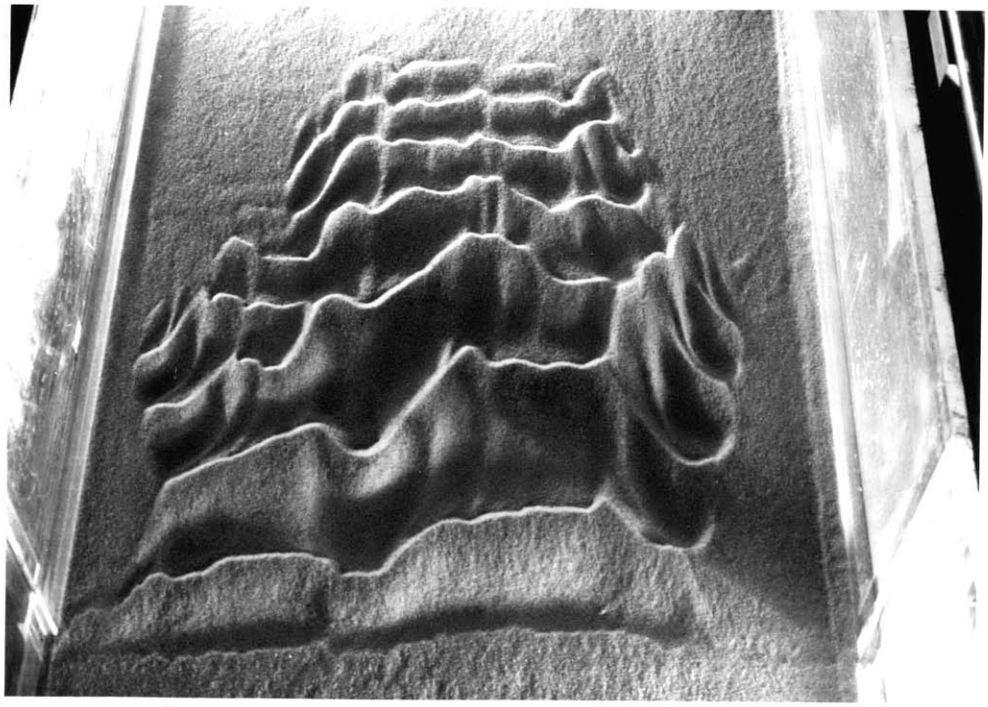

Fig. 3.1. Development of a ripple train from a line disturbance on a flat bed with no grain motion (Run C-7, D_g = 0.66 mm , flow from bottom to top).

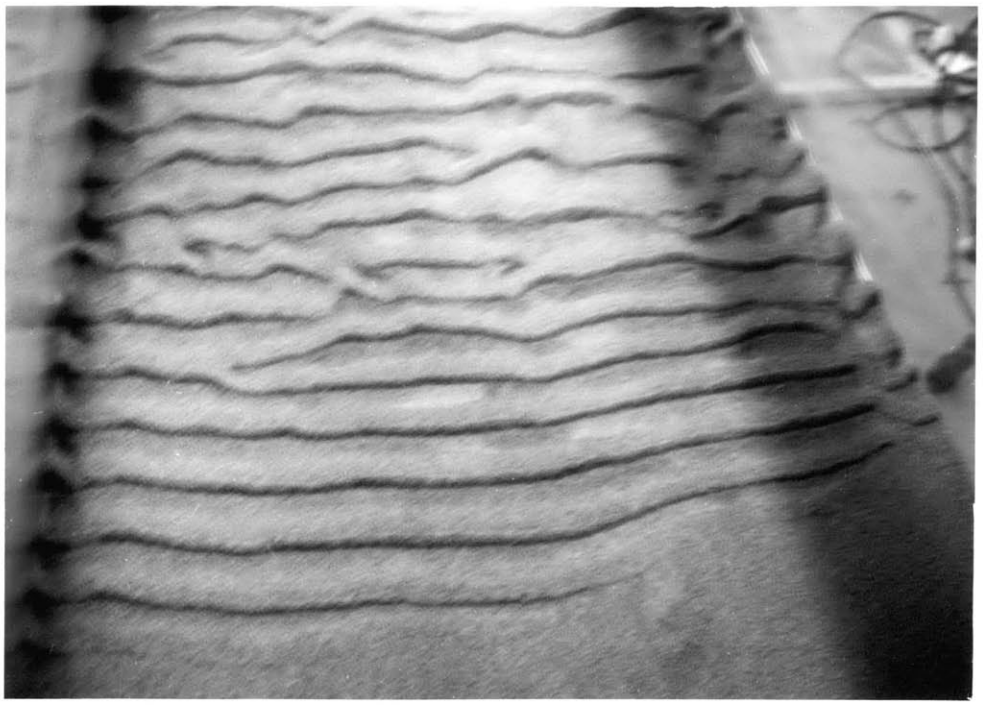

Fig. 3.2. Newly formed ripples in the flat bed (metastable ripple) phase (Run B-2, D_g=0.60 mm , flow from top to bottom).

an area of the bed which is free of bursts of motion. The rate at which sediment is entrained is approximately the same as that at which grains are redeposited in sheltered positions. The patchy erosion creates a hummocky bed topography but does not cause a general restructuring of the bed.

For sands B and C, ripples do not develop spontaneously in this lowest range of velocities for which grains are moved, but obstacles placed on the bed give rise to ripple development. Ripples develop in a train, spreading out across the flume channel and migrating downstream (Fig. 3.2). At slightly higher velocities, these same disturbances are slowly effaced, and ripples do not develop down the length of the flume. For the finest sand, series A, initiation of movement causes an erosional hummocky topography to develop, and ripples develop spontaneously in this terrain at all velocities for which grains are moved (Fig. 3.3). Rates of ripple development are faster than in the coarser sands: ripples quickly grow in trains from several point sources and interfere with one another to give a complex geometry.

With a further increase in velocity, grain motion becomes general on a flat bed. Small areas of higher transport rates or higher bed elevation appear in the general grain motion. These "waves" grow and quickly dissipate. When one wave overtakes a larger and slower

Fig. 3.3. Upstream view of a rippled bed surface (Run A-3, D_g= 0.51 mm , flow from top to bottom).

Fig. 3.4. Migration of small sediment waves on a flat bed (Run C-3, D_g= 0.66 mm , flow from top to bottom).

one, they merge to produce a bar with a small slipface 2 to 3 grain diameters high (Fig. 3.4). The larger bar then grows or dissipates as it migrates downstream. If the velocity is sufficiently high, small bars merge with one another to produce higher slipfaces, up to 5-6 mm high. The spacing between slipfaces can be either regular or irregular, and the rate of advance varies inversely with height. At higher velocities, the waves continue to grow until they become straight-crested bars extending across the width of the flume. The low and long bars (Fig. 3.5) became more dunelike in appearance as flow velocity is increased.

A further increase in velocity causes the dunelike bars to take on the full characteristics of dunes. Dunes are higher and shorter than bars, and quasi-periodic in spacing. Dunes are also more three-dimensional, with crests not extending across the width of the flume and with scour pits downstream of the slipfaces (Fig. 3.6). In plan view the crestlines are more sinuous. Ripples still form on the backs of dunes, but they are much lower. Sediment transport on the dune backs is strong, in sheet-like flow. Some sediment is thrown into suspension at the dune crest rather than avalanching down the slipface.

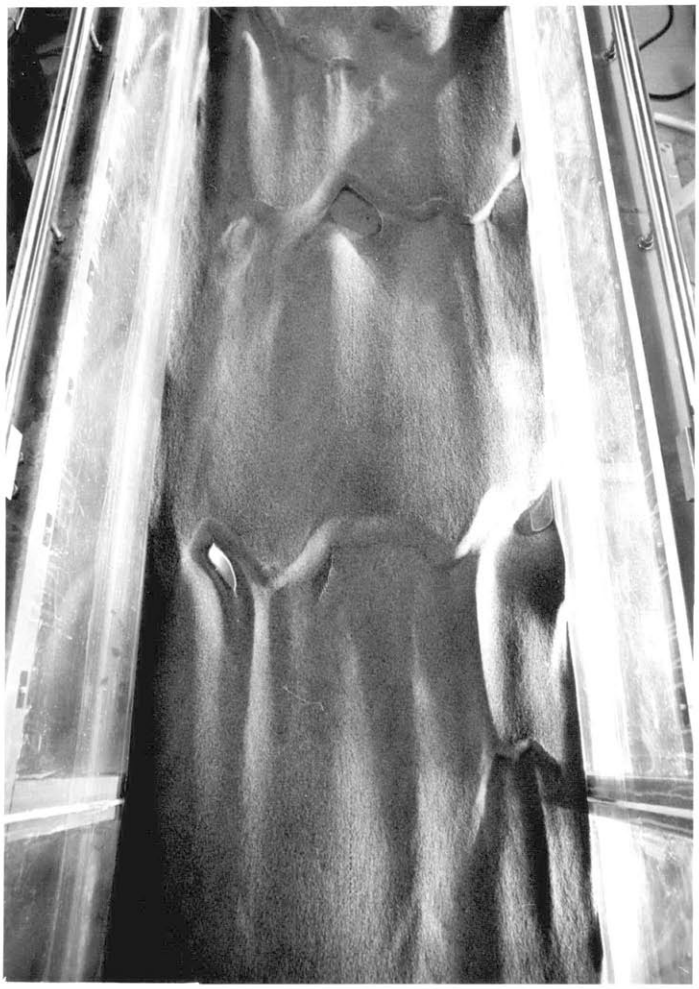

Fig. 3.5. Large, fully developed bars stretching across the width of the flume (Run B-5, D_g = 0.60 mm , flow from top to bottom).

Fig. 3.6. View upstream of fully developed dunes with three-dimensional geometry and ripples on the stoss slopes (Run B-7, D_g = 0.60 mm, flow from top to bottom).

Hydraulic Data

The bed configuration molded in response to a given depth and velocity of flow will exert a controlling effect on the energy loss within a flow, and hence on the energy slope and friction factor. Changes in both slope and bed friction factor with changes in mean velocity and grain size are shown in Fig. 3.7.

It is clear that although series B,C, and D show similar trends and magnitudes in bed friction factor and energy slope, series A attains higher values for both quantities. This distinct departure is the result of a fundamental difference in bed-form development between series A and the other sands. It is in series A that ripples are most rapidly developed, as well as being formed over the largest range of velocities.

Besides forming a distinct bed phase, ripples are well developed as secondary features on the upstream slopes of bars and dunes in series A runs. This additional roughness in the bar and dune bed states accounts for the higher values of bed friction factor and energy slope for these bed states in series A relative to the values in the other series.

Taking into account these larger friction factors and energy slopes in series A, the trends for all four sands are very similar, as shown in Fig. 3.7. In series C, the ripples were only partially developed,

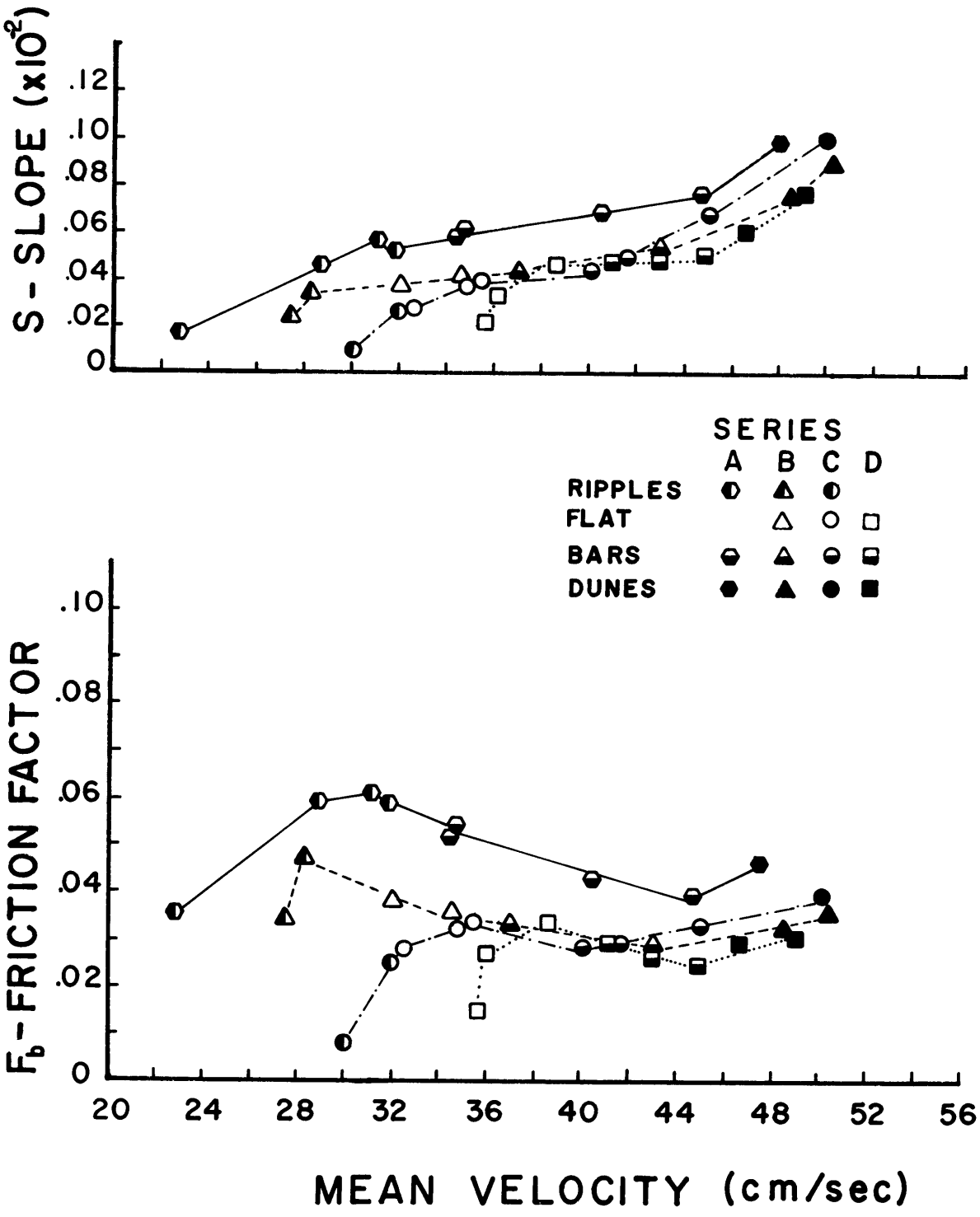

Fig. 3.7 . Variation of energy slope and bed friction with changes in mean velocity.

while those in series B were better developed, and those in series A were fully developed. With the trend to better development of ripples, the bed friction factor increases to its highest value, which is a feature well documented for fine sands (Vanoni and Brooks, 1957).

With change to a flat bed, the bed friction factor decreases to a range of 0.03 to 0.04. In series C and D, in which ripples are poorly developed or absent, the bed friction factor increases to the same range of values. An increase in velocity causes a further reduction in bed friction below those values characteristic of ripples and flat bed. In series C, the bed friction factor starts to increase once more, but this trend is not shown in the other series. This range of decreasing bed friction is characteristic of runs in which bars develop. It is also apparent that in series A, in which the bars are covered with ripples, change in bed state still causes a marked decline in bed friction factor.

The range of velocities for which dunes are developed shows a trend of increasing bed friction factor. This trend is in sharp contrast to the previous trend of decreasing bed friction factor characteristic of bars, and underlines the hydraulic differences between the two superficially similar bed phases.

Different trends in the energy slope with increases

in velocity can also characterize the development of different bed states (Pratt, 1971). The rate of increase of energy slope with increasing velocity is slightly higher for the onset of ripples than for flat bed, but the trends are similar (Fig. 3.7). Bar development is characterized by a lower rate of increase in energy slope for all sands except series C. The onset of dunes is mirrored by a sharp increase in energy slope.

A plot of sediment discharge versus mean velocity is presented in Fig. 3.8, and it is apparent that the data display considerable scatter. As would be expected, larger quantities of finer sand than coarser sand are transported for a given velocity. It can be concluded that, as velocity increases, sediment discharge also increases, though at a decreasing rate. No trends are established by the different bed phases.

Transitions between different bed phases result in definite changes in the flow. Each phase is represented by a different trend in the bed friction factor and, to a lesser but still recognizable degree, in the energy slope. The friction factor is definitely related to the form of the bed roughness and therefore should be a good indicator of transitions between bed phases. Sediment discharge, because of the fluctuations noted above, will indicate only gross trends in bed phases.

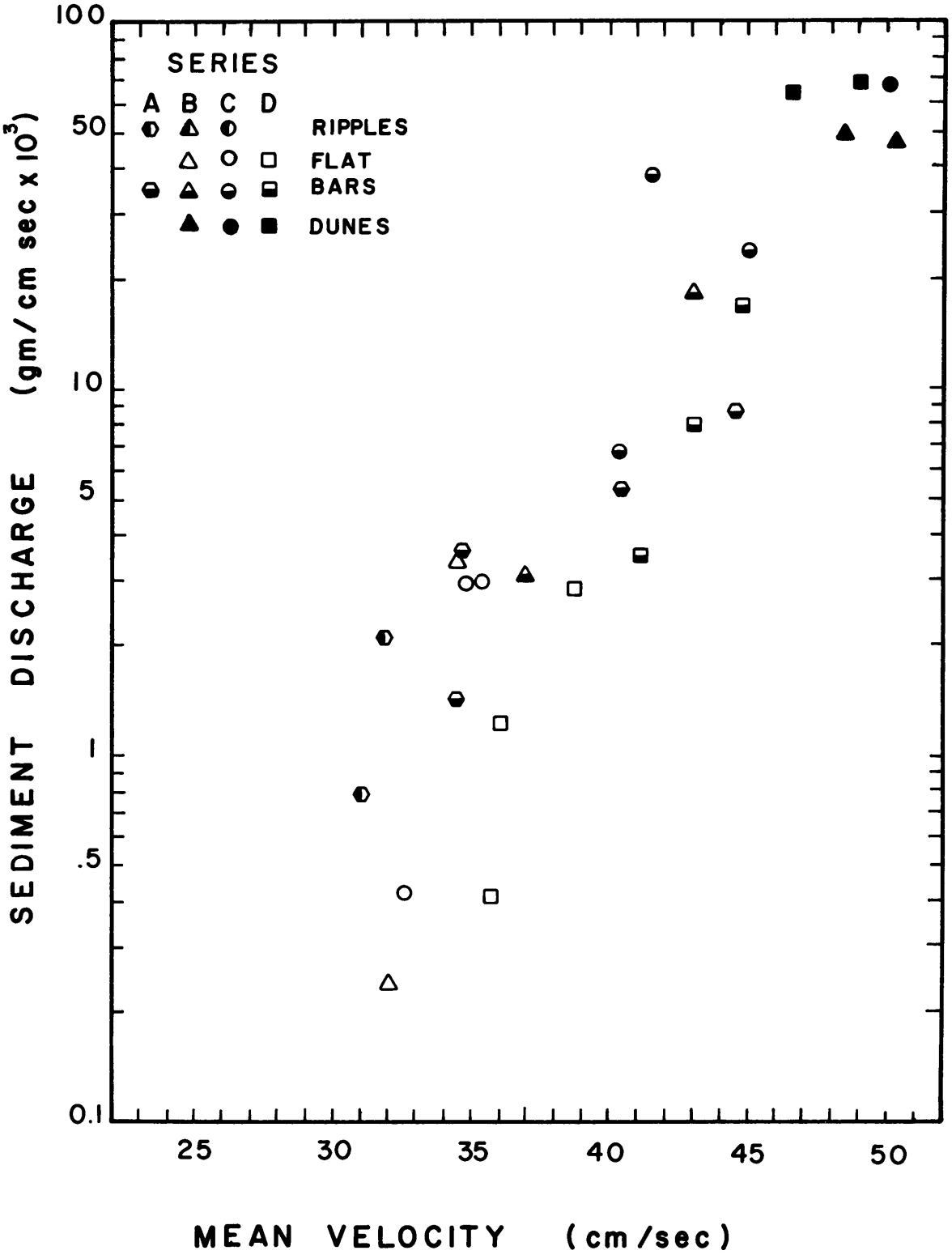

Fig. 3.8 . Variation of sediment transport rate with changes in mean velocity.

Geometrical Properties of Bed Forms

Figs. 3.9 and 3.10 show histograms of bed-form length and height for series A,B,C, and D. The dimensions described are for the major bed forms only, not for minor bed forms. For example, for a run with ripples on the backs of bars or dunes, only the bar or dune dimensions have been analyzed, since they typify the bed state. Bed-form length is defined as the horizontal distance between the crests of adjacent bed forms. Bed-form height is the vertical distance from the crest of the bed form to the lowest point in the trough downstream of the slipface.

Comparison of the lengths of the three kinds of bed forms indicates that these bed forms represent three different populations. The distribution of ripple lengths is clearly unimodal, with a very strong and clearly defined mode at 10 to 15 cm. Lengths of bars show a much greater range of values, with a weak mode at 50 to 60 cm. Lengths of dunes overlap those of bars but do not show as great a spread of values. The mode for dunes is at 50 to 75 cm. The modes of the three populations are not greatly different for different sand sizes.

Bed-form heights (Fig. 3.10) also represent three distinct populations in a frequency distribution. Ripples display a wide but strong mode at 0.6 to 1.5 cm. Bars again show a wide range in values, with a weak mode at

Fig. 3.9. Histograms of ripple, bar, and dune lengths.

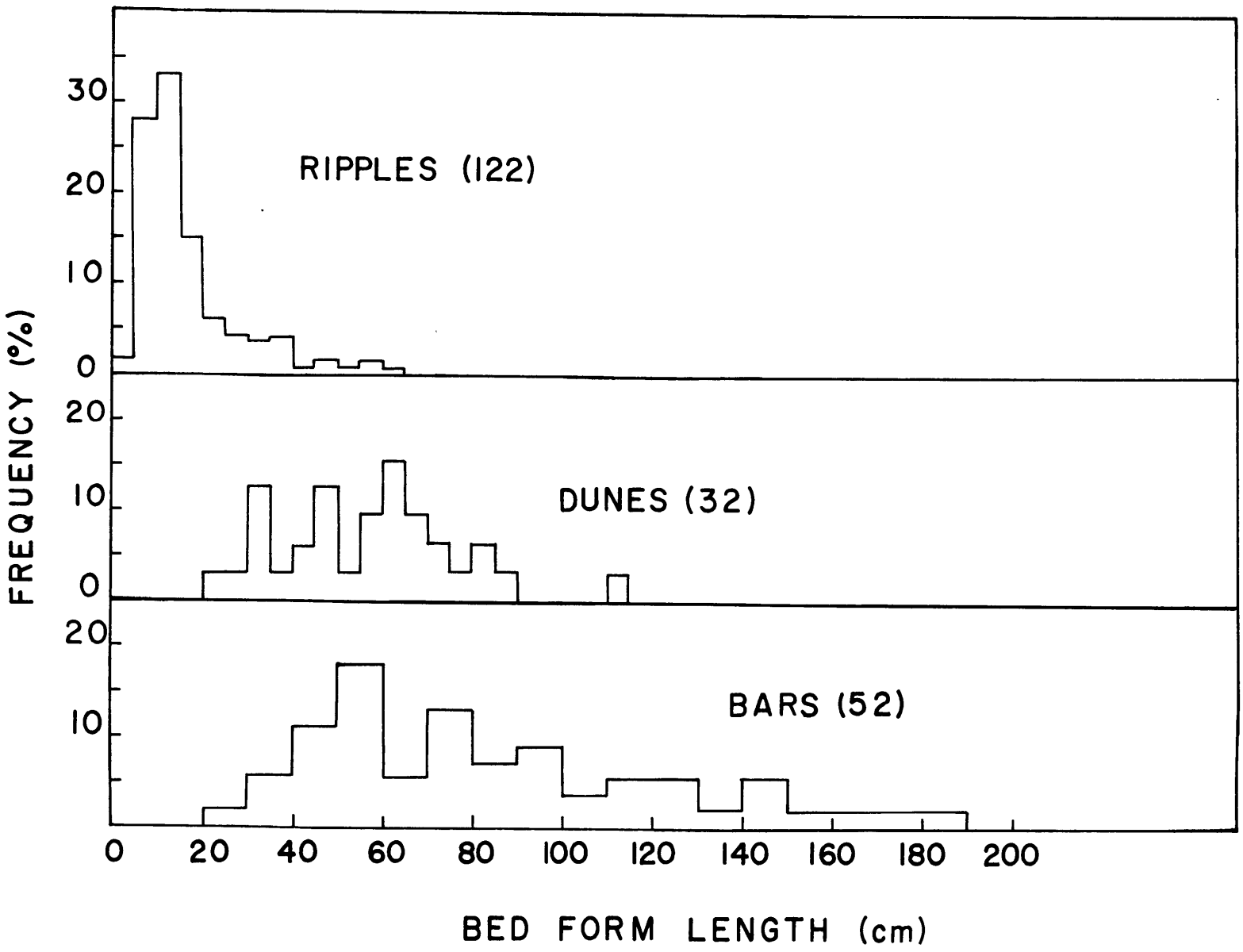

Fig. 3.9. Histograms of ripple, bar, and dune lengths.

Fig. 3.10. Histograms of ripple, bar, and dune heights.

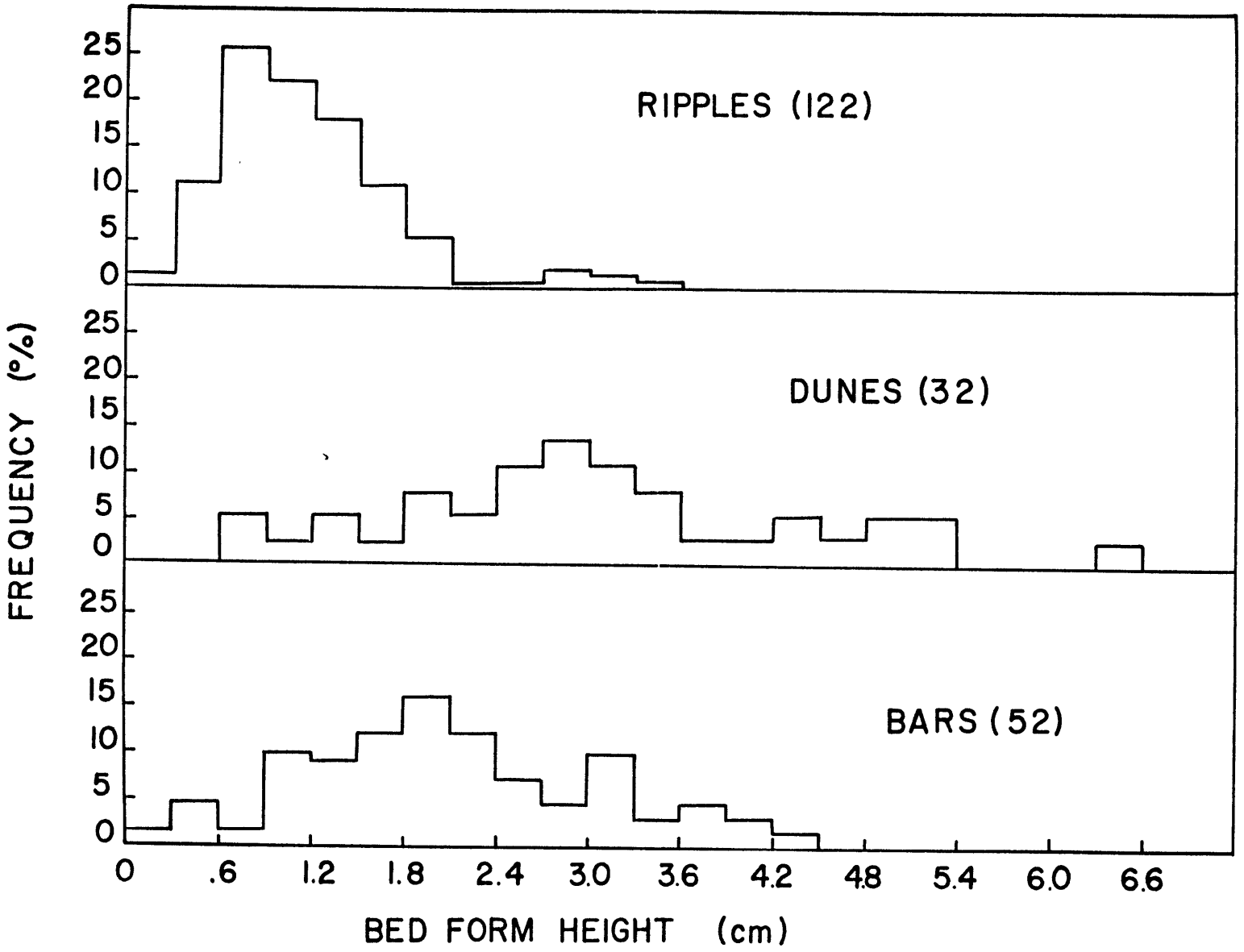
RIPPLES (122)
DUNES (32)
BARS (52)
FREQUENCY (%)
25
20
15
10
5
0
0
.6
1.2
1.8
2.4
3.0
3.6
4.2
4.8
5.4
6.0
6.6
BED FORM HEIGHT (cm)

1.80 to 2.10 cm. Dunes have the largest heights, with a mode at 2.40 to 3.60 cm. Again no strong variation in heights is apparent for changes in grain size.

The bed-form dimensions characterize the differences in the three bed configurations. Ripples are short and low, and do not show great variations in either height or length. Bars are long and low and display a great variation, almost a random variation, in length. Dunes are high and long, showing most variation in height, and having more regular spacing. This description is reinforced by a plot of frequency distribution of length/height ratio (Fig. 3.11). Ripples show a unimodal distribution. Bars show a randomness derived from the length distribution. Dunes show more variation than ripples but much less than bars. Also, dunes have a mode in ℓ/h values intermediate between the mode for ripples and that for bars.

Thus, different characteristic bed phases are identifiable on the basis of observations of kinematics and geometrical properties of bed configurations, and also changes in the mean flow (energy slope and friction factor). These bed phases are no movement, flat bed, ripples, dunes and the newly described bars. In the following sections, the regions of occurrence of the bed phases are defined in more detail.

Fig. 3.11. Histograms of length/ height ratios for ripples, bars ,and dunes.

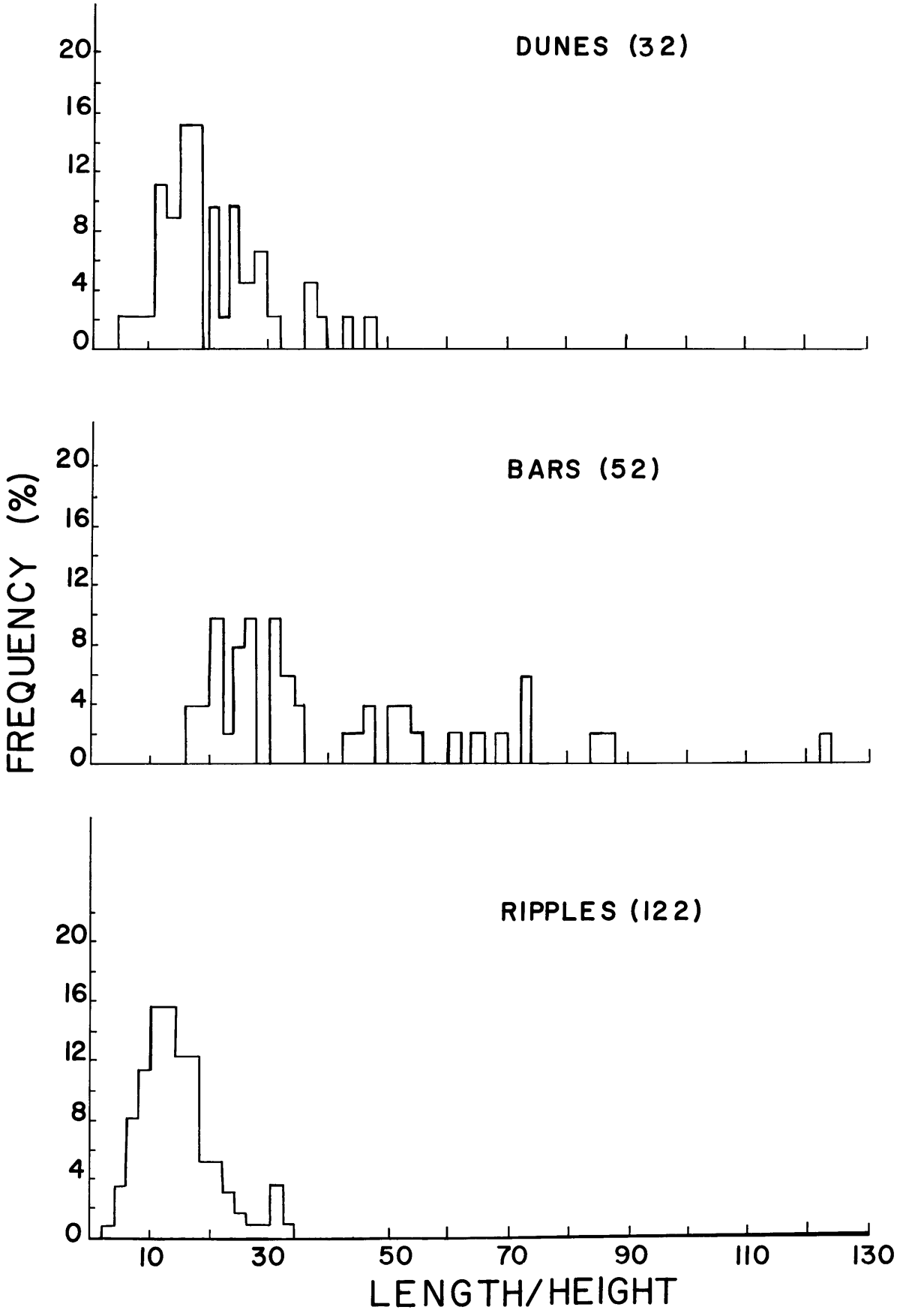

Fig. 3.11. Histograms of length/height ratios for ripples, bars, and dunes.

BED PHASES

1.14 mm Sand

Southard (1971) has proposed a three-dimensional diagram, with dimensionless measures of mean flow depth, mean flow velocity, and sediment size, to distinguish different bed phases. For study and comparison of experiments on quartz sand in water over a small range in temperature, the diagram involves axes of mean depth, mean velocity, and sediment size, since the other relevant variables (ρ, ρ_s, μ, and g) remain constant.

Bed states produced in series E sand are plotted on a depth-velocity diagram in Fig. 3.12. Along with the data on the 1.14 mm sand are included data by Williams (1967, 1970) for 1.35 mm sand. For each combination of velocity and depth there should be one and only one bed state (Brooks, 1958). The correctness of this hypothesis is represented by the absence of overlap of bed states. Plots for U.S. Geological Survey flume data on sands of sizes 0.19 mm, 0.28 mm, 0.45 mm, and 0.93 mm by Southard (1971, Fig. 2) clearly display the lack of overlap.

In Fig. 3.12, regions of similar bed states represent different bed phases. Bed-phase stability fields are areas in the depth-velocity plane for which a combination of depth and velocity will produce one definite type of bed state. For this sediment size there are phase

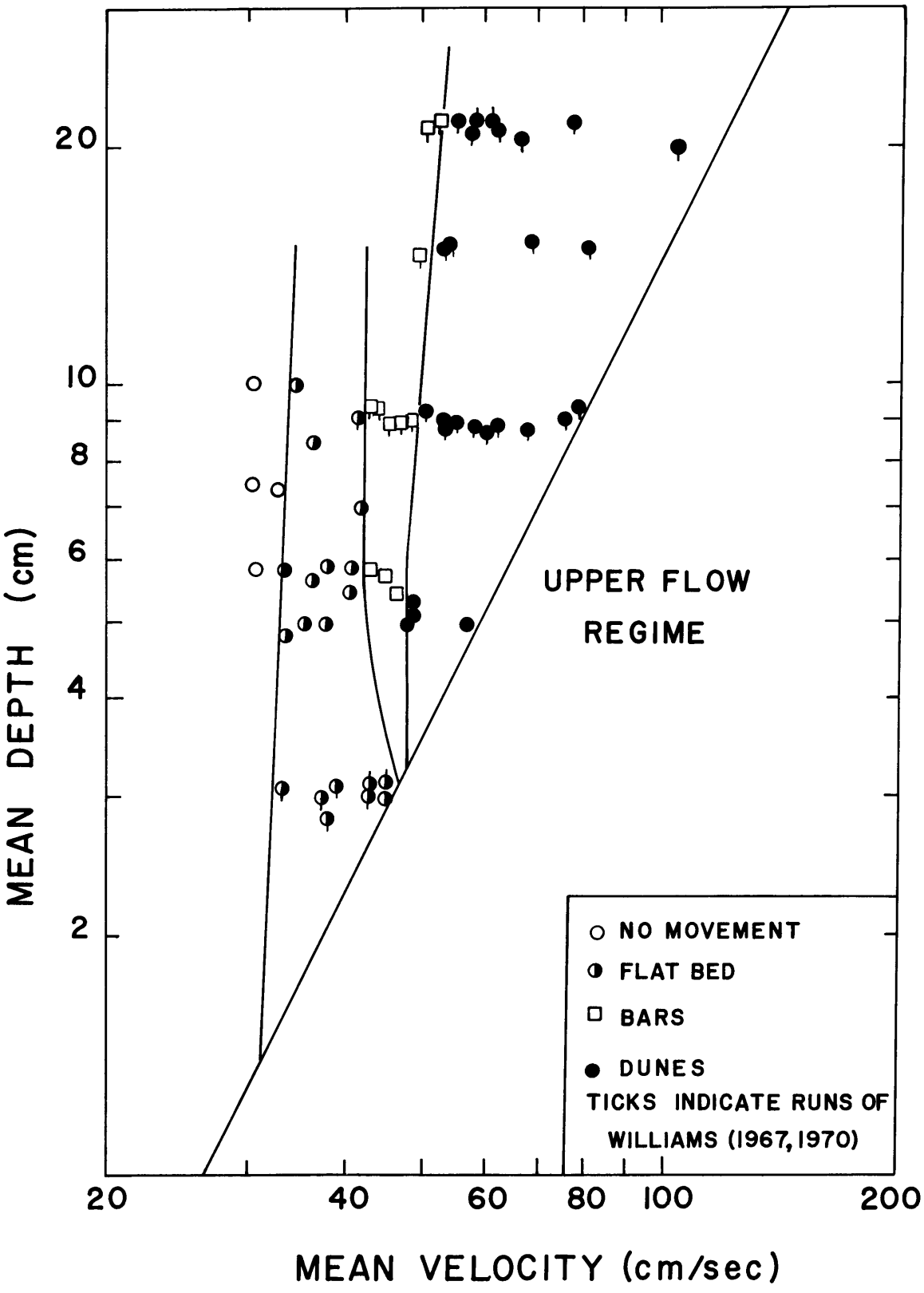

Fig. 3.12. Depth-velocity diagram for 1.14 mm sand.

stability fields for no sediment movement, flat bed with sediment movement, bars, and dunes in the lower flow regime (Froude number less than about one).

0.51 mm - 0.80 mm Sands

Depth-velocity diagrams (Southard, 1971) show that changes in bed phases occur largely with changes in velocity. Sands A,B,C, and D are plotted in a grain size versus velocity plane for a depth of 15.4 cm (Fig. 3.13). Again there is only one bed state for a given combination of depth, velocity, and grain size, and regions of identical bed states define various bed phases in the size-velocity plane. For series D there are the same four bed phases as for series E. However, with a further decrease in grain size the number of bed phases increases and the phases interfinger and pinch out.

Also plotted in Fig. 3.13 are data from Pratt (1971), who defined the bed phases with different criteria in a much larger flume. The agreement between sand A (0.51 mm) and Pratt's 0.49 mm sand is excellent. Pratt did not differentiate different ripple phases, as was done for series A-E. The no movement (metastable ripple) phase could be recognized in his data and is identified. The flat bed (metastable ripple) phase could not be differentiated. Also included in Fig. 3.13 is the lower-flow-regime bed-form sequence of Simons and Richardson

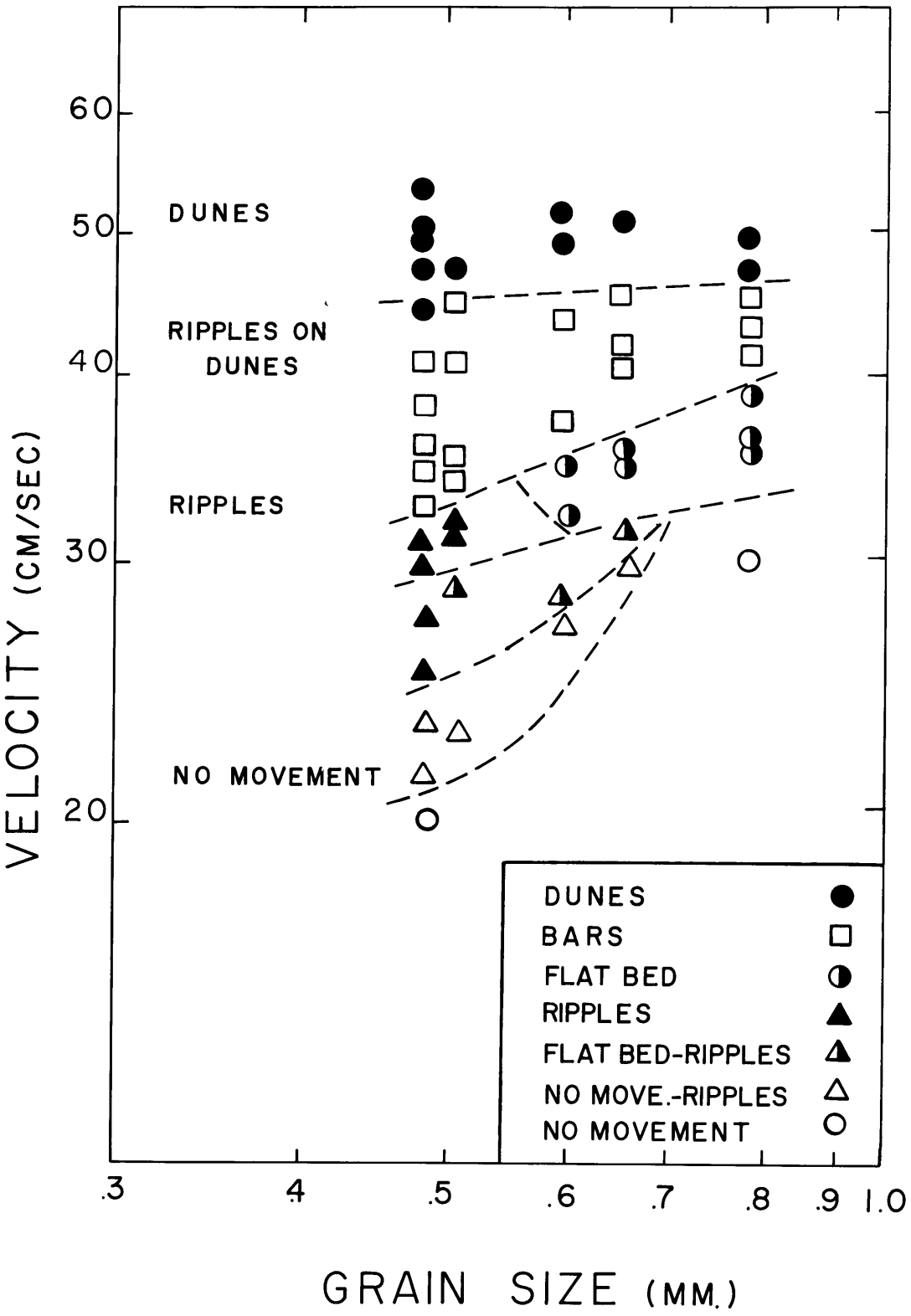

Fig. 3.13. Depth-velocity diagram for sands in series A-D.

(1962, 1963), for sands with sizes 0.19 mm to 0.45 mm.

Discussion of Phase Relations

The no movement phase is best described for series E runs. Table 3.5 and Fig. 3.14 give data for this phase, plotted on a Shields diagram. Initiation of motion agrees well with the Shields criterion. As shown in Fig. 3.13 transition from the no-movement phase to the flat-bed phase is at higher velocities with an increase in grain size. Any artificial disturbance placed on the bed within the limits of this phase stability field would not cause propagation of ripples.

The no movement (metastable ripple) phase for sands finer than 0.70 mm is a complex phase, capable of having two stable bed states. If the sand bed is smooth and is left free from any irregularities, then the bed will remain flat and sediment will not move. If an artificial disturbance of sufficient height is placed on the bed, then the disturbance will propagate a train of stable ripples downstream. Since the stable flat bed can be perturbed to initiate ripples, the ripples are considered to be a metastable phase. The initial bed geometry, whether smooth or irregular, determines which bed state will dominate.

Rathbun and Guy (1967) observed this same phenomenon in 0.30 mm sand, as have Southard and Boguchwal (1973)

TABLE 3.5 Data on Initiation of Movement

Run No.	U Velocity (cm/sec)	d Depth (cm)	S Slope	R_* Boundary R_e	τ_* Shields' Stress	Bed State
E-17	31.0	7.5	0.00094	12.4	0.035	No Move
E-18	33.0	7.4	0.00067	10.4	0.025	No Move
E-20	30.0	10.0	0.00060	11.1	0.030	No Move
E-21	36.0	8.4	0.00180	57.9	0.076	Flat

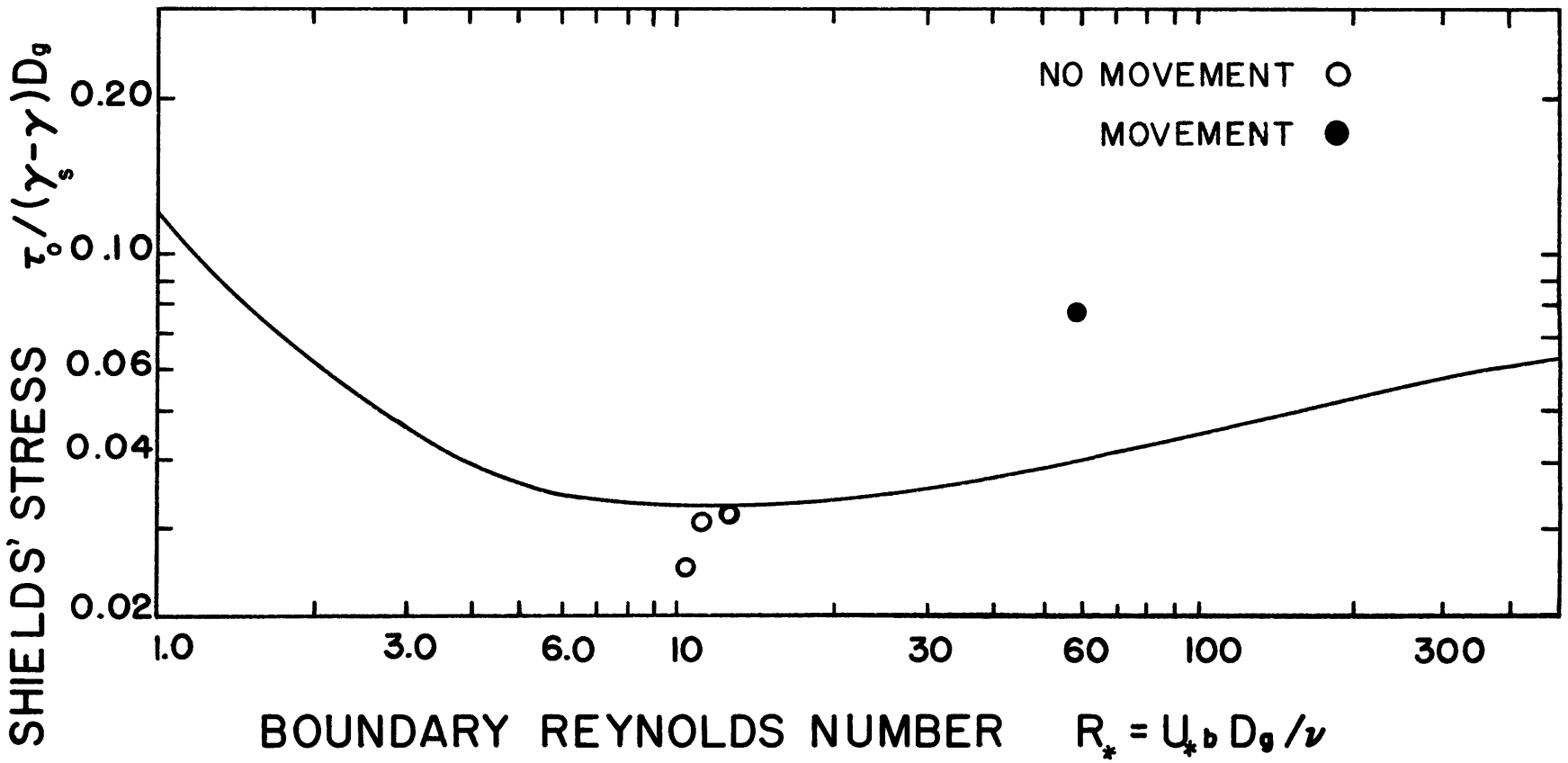

Fig. 3.14. Comparison of grain motion with Shields' criterion.

in sands with mean sizes of 0.49, 0.56, and 0.65 mm. Rathbun and Guy (1967) further demonstrated that ripples produced in this phase continue to migrate at velocities lower than those at which they are generated. The exact lower limit of velocity for this phase must in some way be determined by the interaction between the mean velocity and the size of the bed irregularity. For lower velocities, higher bed irregularities would be needed to start ripple propagation. The stability field of this phase parallels the boundary for initiation of motion at finer sizes, and pinches out at a size of about 0.70 mm.

With increased velocity in sands coarser than 0.70 mm, the no-movement phase gives way to the flat-bed phase. This phase is best developed in coarser sands and dies out with decreasing sand size around 0.55 mm. Grains on the bed move in bursts, eroding the bed surface. The bursts of motion are few and widely scattered at low velocities, but increase in magnitude and frequency with increasing velocity. The bursts of motion create relief of one to two grain diameters on the bed surface, giving it a rough, eroded texture. Grain motion under these flow conditions has been described in detail by Vanoni (1964), Sutherland (1967), and Williams and Kemp (1971). The topography has a streaky lineation which is not parallel but rather crosses at low angles (Fig. 3.15). Where the lineations cross, a bed irregularity is pre-

Fig. 3.15. Erosive lineations on a hummocky bed surface (Run C-6, D_g = 0.66 mm , flow from left to right).

sented to the flow, but flow separation does not cause ripple generation. Any obstacles imposed on the bed likewise fail to start ripple generation.

The flat bed (metastable ripple) phase is developed in sands finer than 0.70 mm and at flow velocities intermediate between those characteristic of the no-movement and flat-bed phases. If the sand bed is initially flat the sediment starts to move in bursts, resulting in the typical hummocky topography one to two grain diameters high. The bed will remain flat even left indefinitely, provided that no artificial disturbance is allowed to develop at the upstream end of the channel. Flat beds in this phase have been maintained for up to 65 hours with no ripple development. It is conceivable that if the bed had been left for a longer time it might have become rippled, but there was no tendency for this to happen. If the bed starts with a small disturbance on its surface, two to three grain diameters high, then ripples propagate from that disturbance in a widening train. As ripples develop, energy slope and friction factor increase in response to the increased roughness of the bed. This same metastability between flat bed and ripples has previously been reported by Southard (1970) for 0.19 mm sand and by Williams and Kemp (1972) for 0.14 mm and 0.45 mm sand.

With increase in velocity, the flat bed (metastable

ripple) phase passes into the flat-bed phase (for sands coarser than 0.60 mm) or the ripple phase (for sands finer than 0.60 mm). In the flat-bed phase, pre-existing ripples do not continue to propagate more ripples downstream. Flat bed stretches slowly spread down the flume, overtaking ripples from upstream. For sands finer than 0.60 mm,ripples develop from the crossing points in the streaky flat-bed texture. The flow has become strong enough that flow separation over flow-constructed features can cause propagation of ripples (Williams and Kemp, 1972). A flat sediment bed cannot persist within this phase stability field. At the phase boundary, the bed changes so slowly that the bed state has characteristics of two phases: flat bed sections and rippled patches. The ripple phase dies out for sand sizes greater than 0.60 mm, whereas the metastable ripple phases can exist for sand sizes up to 0.70 mm diameter. Like the metastable-ripple phases, the ripple phase reverts to the flat-bed phase with increasing grain size or velocity.

Thus, the onset of ripples is caused by local effects in the flow, such as the construction or imposition of some irregularity on the bed surface and flow separation over it. Since ripples can be excited by bed conditions, their onset can be below, near, or above the onset of sediment motion as predicted by Shields.

The transition from patchy random grain motion to

general grain motion over the entire bed surface is observed to coincide with the transition from the flat-bed phase to the bar phase with increasing velocity.

Small waves of sediment randomly distributed over the bed surface grow, dissipate, and merge with one another. When waves coalesce they form low bars with slipfaces about 5-10 mm high. These small bars migrate down the flume and undergo growth and dissipation as they move. Small waves are continually merging with the bars, and some faster moving bars overtake slower ones. In general the bigger bars show less randomness in spacing and a lower frequency of merging and dying out than the smaller waves from which the bars grew. In Fig. 3.16 the paths of some bars are represented in space and time. The pathlines are not straight and so indicate that the bar celerity changes as the bar grows or dissipates. There are some instances of bars merging. Also noticeable in Fig. 3.16 is the variation in bar spacings. With increasing velocity the dune phase stability field is approached, and the bars become more regular in spacing and more dunelike in geometry. The boundary between the two bed phases is gradational.

In series B,C,D, and E the bars develop as very small waves on a flat bed. In series A, the bars develop from a rippled bed in a complex manner. First ripples start to coalesce by one ripple overtaking another.

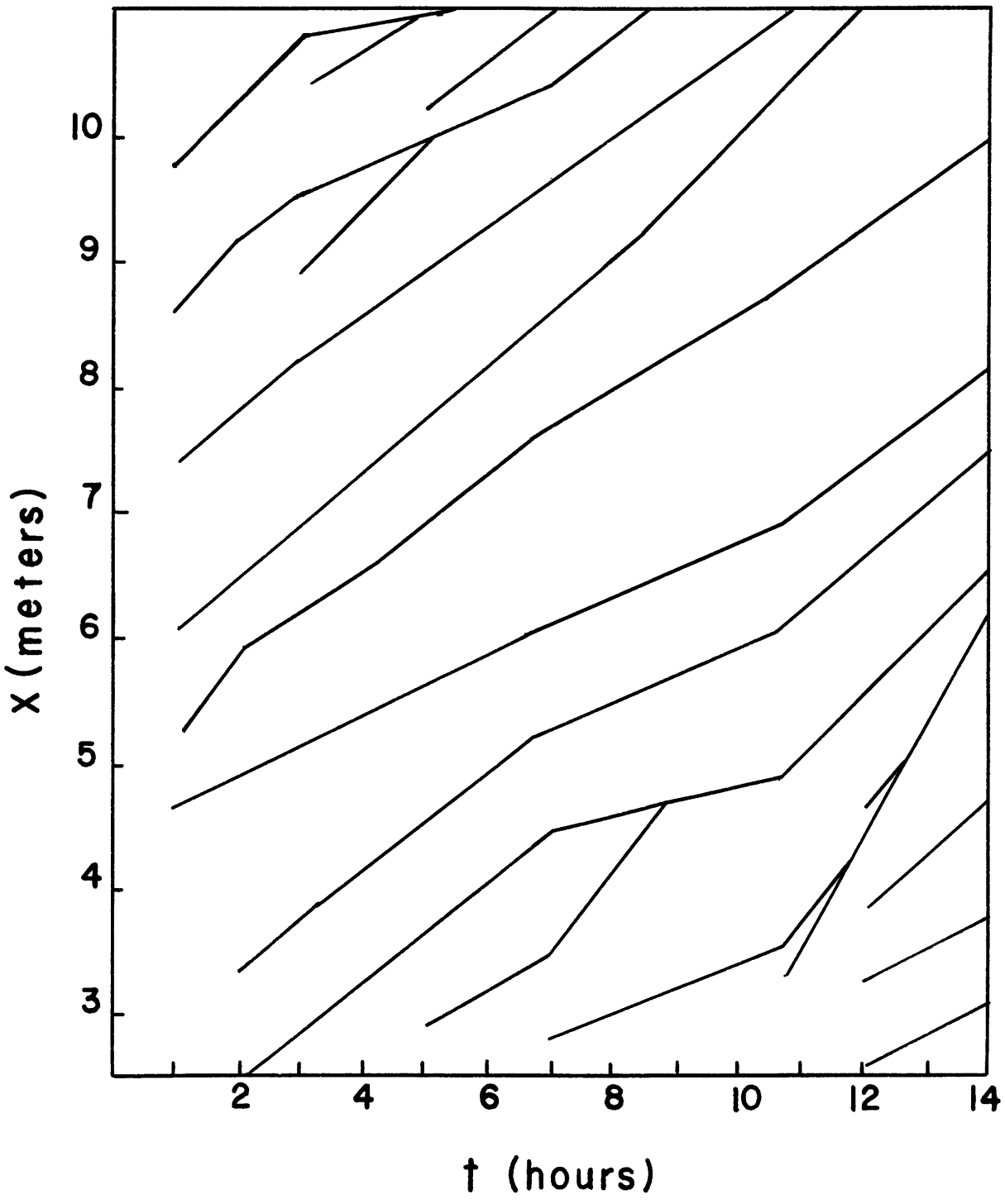

Fig. 3.16. Pathlines of bars in space and time.
(Run C-3, D_g= 0.66 mm)

This produces short patches of flat-bed topography with large downstream slipfaces. Gradually the flat-bed sections grow until they become recognizable as the backs of bars. Once the bars form, small ripples are generated on their backs. Ripples form just downstream of a bar slipface and migrate in trains or individually up the backs of the bars. Such ripples are well developed in series A and become much lower and poorly defined in the coarser sands. Pratt (1971) observed these diminished-ripple forms in his experiments and refers to them as "rollers". These seem not to be a separate bed form but rather a weaker development of ripples.

Development of ripples locally on bar backs in sands coarser than 1 mm has not been previously recognized. It highlights the theory that ripples are a local phenomenon resulting from flow separation. Ripples on the backs of bars develop in sands much coarser than those for which the ripple phase exists, and at larger mean-flow velocities than for the ripple phase. Bar slipfaces provide strong flow acceleration when the flow separates.

Since bars undergo a transition to dunes with increased velocity, it might be hypothesized that bars are the initial stage of dune development and would eventually change to dunes if the flume were a great deal longer. Such a hypothesis would suggest that bars are not a

separate bed phase. Observation of bars developing in series A-D runs indicates that when bars first form in the upstream end of the flume they indeed grow in size as they migrate downstream. However, in the downstream half of the flume, bars do not grow in height or spacing but display constant geometry (in the mean), suggesting that they are not undergoing transient growth as they migrate but are equilibrium bed configurations. Also in Fig. 3.1, bars and dunes display markedly different trends in bed friction factor and energy slope; this would not be the case if bars are an initial stage of dunes. Bars have been recognized in a longer flume (25 meters) by Pratt (1971) and have been produced, but not recognized as a separate bed phase, in the 65-meter flume at Colorado State University (Guy et al., 1966, Figs. 62 and 63). It is concluded that bars are a separate, equilibrium bed configuration and are not just an initial stage in the development of dunes.

In Fig. 3.13, Simons' and Richardson's (1962) regime classification for fine to medium sands is seen to incorporate the bar phase partly into ripples and partly into ripples on dunes. The lower boundary of the bar phase is masked by ripples in the medium sand in series A. However, in the coarser sands the boundary between the flat-bed and bar phases is well defined. The lower boundary is situated at higher velocities in coarser sands,

suggesting that the bar field may pinch out in coarser sediment. The upper boundary of the bar phase is gradational but also displays a slight trend to be positioned at higher velocities in coarser sands for a fixed depth.

Dunes are easily distinguishable in that they are longer and higher than ripples. The distinction between bars and dunes is not so apparent, because their lengths and heights are of the same order of magnitude. However, the reverse trends in bed friction factor, and the increase in energy slope for dunes to that for bars (Fig. 3.1) clearly depicts the hydraulic differences between bars and dunes. Geometrically, dunes are somewhat higher than bars and have a greater regularity of spacing. In addition, dunes are more three-dimensional than bars, and dunes have scour pits downstream of their slipfaces whereas bars do not.

As dunes develop from a flat bed, bars always form first. The bars then start to interact and become larger and more regularly spaced. The bar slipfaces cause a strong flow separation, and it appears that the dunes need this process in order to form.

In coarse sands the dune phase is initiated at slightly higher velocities (Fig. 3.13) but does not show the strong dependence on velocity that the initiation of motion does. It seems likely that in sands coarser than two or three millimeters the bar phase will cease

to exist and the dune phase field will continuously shrink in its range of velocities.

There were no apparent geometric differences between dune bed forms with changes in grain size such as occurs in finer sediments. Perhaps the range of sizes was too small to show any effect. The only noticeable difference was in the ripples on the dune backs; they became progressively smaller from series A to E.

In summary, the various observed bed phases display complex relationships with one another with changes in mean velocity, mean depth, and grain size. Phases do not overlap but occupy distinct stability fields, indicating that velocity, depth, and grain size are indeed the important variables controlling bed phases. In the next chapter the mechanics of ripples, bars, and dunes will be investigated and hypotheses about their origins will be formulated and tested in light of the observed phase interrelationships.

4. MECHANICS OF BED FORMS

Mechanics of development of ripples, bars, and dunes are investigated in this chapter. Existing theories are examined in the light of the previously described observations of each bed phase, particularly the differences in geometry and behavior between different phases. For bars and dunes, discrepancies between theory and observation, or lack of theoretical treatment altogether, lead to formulation of new hypotheses. These new hypotheses are tested with the observed characteristics of the different bed phases.

RIPPLES

Ripples have been the most extensively studied bed configuration. This is partially the result of their early recognition. It was much later that dunes were regarded as separate bed configurations (Simmons and Richardson, 1962), while bars have heretofore not been explicitly defined as a separate form. However, extensive studies have failed to provide an analytical theory to describe ripples. As Yalin (1973, p. 209) comments, "the considerations of J.F. Kennedy are confined to dunes and antidunes only; ripples could not have been included, for the length of ripples is independent of depth." Existing theory on ripple formation is based on qualitative

descriptions of their kinematics, which are outlined below.

Inglis-Raudkivi Model

The earliest and most successful theory on the development of ripples was proposed initially by Inglis (1949) and later by Menard (1950). Inglis proposed that, during initial grain motion on a flat bed, small mounds of grains are randomly constructed on the bed surface by the turbulent flow. These sediment mounds cause flow separation and erosion of grains downstream of the separation eddy. The eroded sediment is transported for a short distance downstream of the separation eddy and then deposited to form a new mound. The mound becomes a new ripple, and the process continues downstream. Inglis did not elaborate on the reasons for the formation of a mound or the process of continued ripple formation.

From an experimental study of ripple generation, Raudkivi (1963) amplified Inglis's hypothesis. Raudkivi observed that ripples develop from a point source on the bed and spread laterally downstream from this initial disturbance. The initial disturbance is due to a piling up of sediment grains caused by intermittent transport at flow velocities slightly greater than the threshold of movement. The piling up of sediment is caused by three factors: an overtaking of slow particles by faster ones, intermittent eddy action, and nonuniformity

of sediment sizes.

Flow over the piles of grains is visualized as qualitatively the same as flow separation over a negative step. As the flow separates, there is intense mixing along the separation surface, and turbulent eddies are generated. At the point of reattachment, this core of turbulent eddies interacts with and scours the bed surface, causing sediment to be entrained. Sediment entrained by the turbulence in the region of reattachment is deposited a short distance downstream, where the turbulence intensity is diminished. A new ripple forms where the sediment is deposited as a mound.

Flow Separation over a Negative Step

Flow separation plays a very important role in the models of Inglis and Raudkivi, and so some of the qualitative aspects of flow separation are reviewed here. Flow separation is characteristic of flows with a strong adverse (positive) pressure gradient. The adverse pressure gradient (usually developed in an expanding flow downstream of an obstacle to the flow) retards the motion of the fluid near the boundary. Fluid adjacent to the wall region may stop or reverse in direction, and the flow away from the wall is deflected up and over the reverse flow. This reversal of flow and deflection is termed flow separation. Where the fluid near the boundary

once again moves downstream, the flow is said to be reattached. A line joining the point of separation to the point of reattachment is called the separation streamline (Fig. 4.1). (Actually, in turbulent flow the streamlines represent averages of fluid motions and so are really time-averaged streamlines.)

The reverse-flow region can itself be subdivided into regions. Abbot and Kline (1962) divided reverse flow downstream of a negative step into three regions. The first region, immediately adjacent to the step, is that containing a small three-dimensional eddy. The second region contains the large two-dimensional reverse-flow eddy commonly observed in flows separated over a step. The last region, farthest downstream of the step, is the range in which the reattachment point oscillates back and forth in response to the eddy motion.

In Fig. 4.2, overall length ℓ of the separated region observed by several investigators is plotted against step height h and flow depth d. The reattachment point is between 4 to 8 step heights downstream. Where h is a small fraction of d (less than 20%), ℓ/h is between 4 and 6. For larger h/d, ℓ/h is between 6 and 8. Values of ℓ/h of about 6 are the mean.

After the flow separates, a free-shear layer develops along the streamline separating the main flow and back flow. This is a region of steep velocity gradients

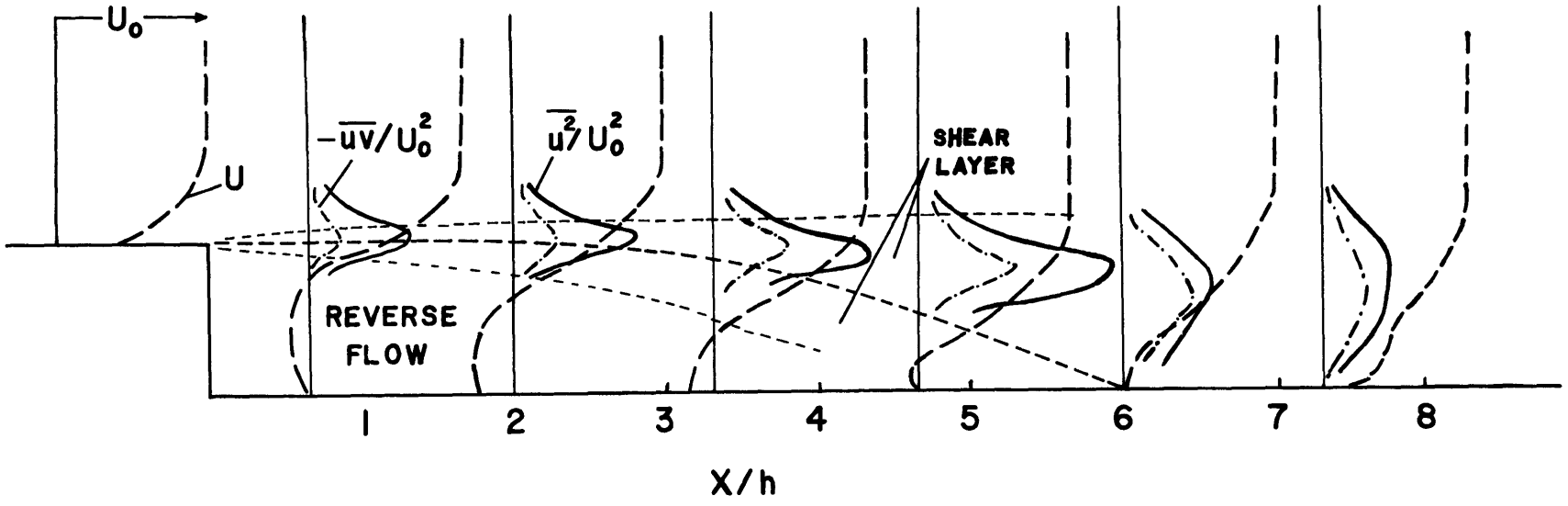

Fig. 4.1. Velocity and turbulence measurements downstream of a negative step (after Tani, 1957; Mueller and Robertson,1962).

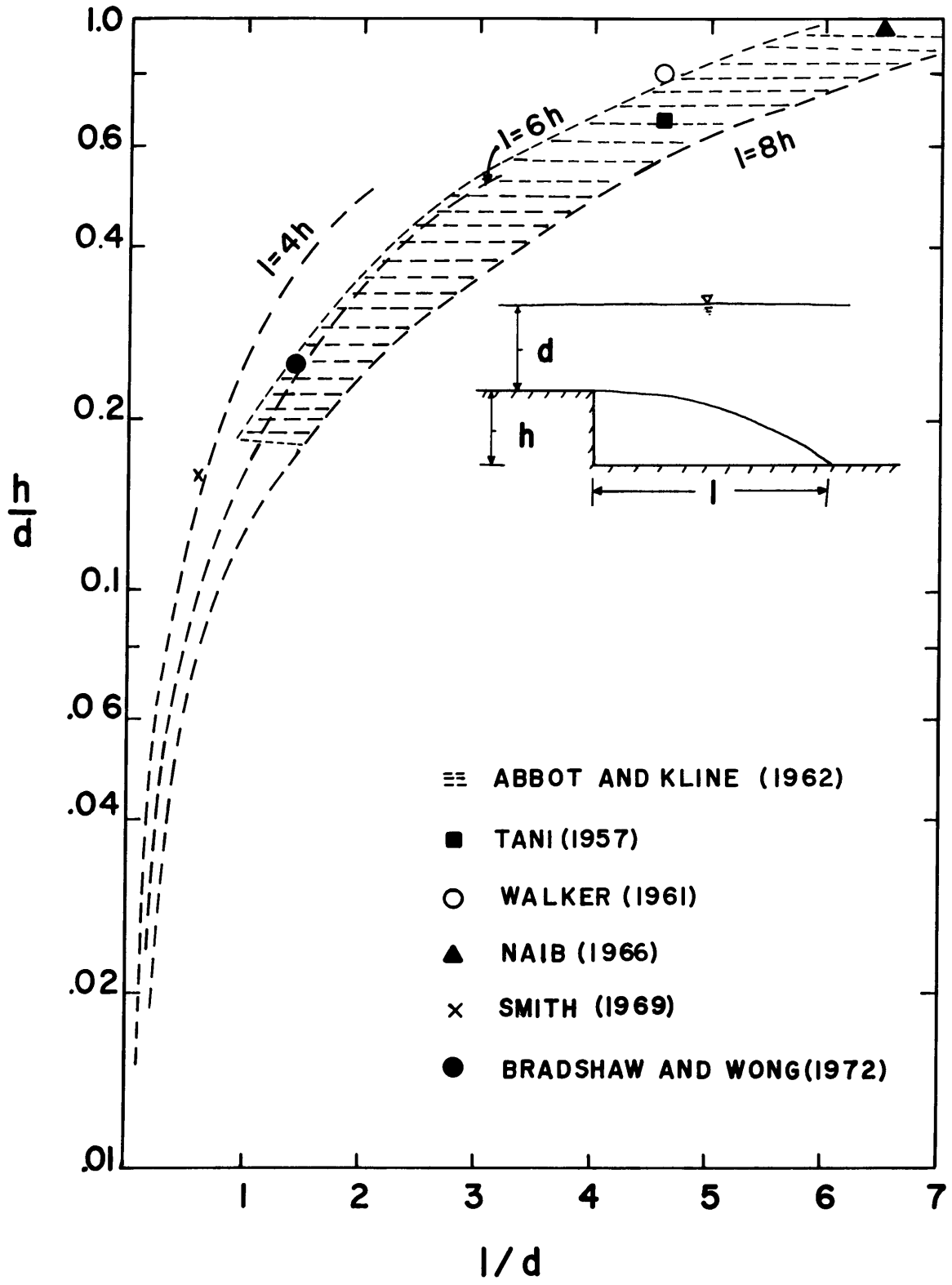

Fig.4.2. Length of reverse flow region downstream of a negative step.

(Fig. 4.1), where there is strong turbulent shear. Tani (1957), Walker (1961), and Mueller and Robertson (1962) measured the turbulent shear stress and turbulence intensities in this region and found that the turbulent shear increased several-fold over that in a normal turbulent boundary layer. The free-shear layer develops after separation and spreads out downstream. The maximum values of turbulent shear stress and turbulence intensities also increase downstream toward reattachment. The distributions of high values of $-\overline{uv}/U^2$ and $\overline{u^2}/U^2$ spread out laterally downstream, matching the increase in eddy sizes generated by the growing free shear layer. In the vicinity of reattachment, the free shear layer, with its increased turbulence intensity and large eddies, comes in contact with the boundary and must therefore exert very large instantaneous forces on the bed.

Development of Initial Bed Disturbance

Inglis (1949) and Raudkivi (1963) suggested that the initial disturbance on the bed which causes flow separation is the piling up of very small mounds of sediment grains owing to the action of random eddies in turbulent flow. The action of eddies close to the wall region in turbulent flows has recently received a great deal of attention in relation to the mechanisms of turbulence production in boundary layers.

Kline et al. (1967) observed that the viscous sublayer is a region of three-dimensional motion close to the boundary ($0 \leq y^+ \leq 10$, where $y^+ = y(\tau_o/\rho)^{1/2}/\nu$). In this region there are alternating streaks of high- and low-velocity fluid which are randomly created and destroyed. The low-velocity streaks are ejected outward from the boundary into the buffer region ($8 \leq y^+ \leq 12$), where they oscillate and break up. The high-velocity fluid streaks then sweep down onto the boundary, instantaneously increasing the local velocity by up to 30%. The spacing of the streaks and the ejection frequency is a function of the mean-flow Reynolds number.

Corino and Brodkey (1969), using microscopic techniques to observe the wall region in turbulent flow, examined the bursts of movement and the ejection sequence described by Kline et al. (1967). They confirmed the qualitative picture and also described the transfer of kinetic energy to the outer boundary layer by the ejected low-momentum fluid. Kim et al. (1971) and Grass (1971) also described the same sequence of events using hydrogen-bubble techniques, whereas Willmarth and Lu (1972) and Wallace, Eckelmann, and Brodkey (1972) made hot-wire anemometer measurements of the turbulence and verified the earlier qualitative hypotheses.

Grass (1971), studying the high- and low-velocity streaks over a rough boundary reported the same low-

velocity fluid ejection from the wall region and interaction of high-velocity fluid with the rough bed. The areas between roughness elements of the rough boundary act as reservoirs of low-momentum fluid in the same manner as the viscous sublayer does for smooth boundaries. A characteristic width of the order of 2 to 3 mm is observed for the erosion streaks on the bed.

Williams and Kemp (1971) studied the very-small-scale detail of a deforming bed surface and compared their observations with those of Kline et al. (1967). Williams and Kemp observed a random, streaky motion of sediment which results in an erosive, streaky topography. The high-velocity fluid streaks interacting with the bed surface force the bed particles to move laterally to form low ridges, one or two grain diameters high, to either side of the longitudinal scoured area. Streaks of fluid appear to have a characteristic width, and this is imposed on the bed surface. The erosive furrows develop at small angles to one another, occasionally forming a low barrier a few grain diameters in height transverse to the flow. Williams and Kemp noticed that grains rolling along the bed are stopped at these ridges, and the flow separates over the ridges for part of the time. The backflow of the separation eddy arrests further rolling grains until a low mound is formed. This grows to have a size sufficient to cause full-time

flow separation with strength sufficient to start erosion of grains at the reattachment point downstream. Ripples then form as already outlined.

Ripple Model

The theory of ripple development proposed by Inglis (1949) and Raudkivi (1963) and refined by Williams and Kemp (1971) best describes the observations of ripples in this study.

The initiation of particle motion on a flat bed is characterized by random bursts or gusts of motion. The bursts are narrow and directed longitudinally downstream as well as laterally. The bursts of motion are random in space and time and result in a streaky bed topography (Fig. 3.15) with low ridges one to two grain diameters high intersecting at small angles. The streaky pattern was observed in series A-D. The pattern of sediment motion and the nature of the resulting bed topography are identical to that described by Williams and Kemp (1971).

Ripples developed spontaneously from the streaky bed topography only with the smallest-diameter sand, series A. The reason for spontaneous development of ripples versus no ripple development given this bed topography seems to be related to the rate at which grain particle weight increases with particle size.

Particle weight increases as the third power of particle radius, whereas particle cross-sectional area available for drag increases only as the second power of particle radius. Therefore, for small increases in particle size there must be a compensating large increase in applied shear stress in order to continue transporting particles. This means that in the case of flow separation over a grain mound on the bed, there must be a large increase in the instantaneous shear stresses at reattachment with small increases in grain size. If this additional instantaneous shear stress is not supplied, sand grains are not eroded at the reattachment point and so cannot be deposited some distance downstream to initiate a new ripple.

Instantaneous shear stress at reattachment results from the interaction of large eddies from the core of the free shear layer (Fig. 4.1) with the bed (Raudkivi, 1963; Williams and Kemp, 1971). In order to increase this instantaneous shear stress, the intensity of the turbulence has to be increased. To do this the size of the flow-separation obstacle can be increased to cause strong flow acceleration or the mean flow velocity can be increased. Both of these actions would support development of a stronger shear layer and so a larger turbulence level.

However, the sizes of the roughness elements on a streaky bed are the same order of magnitude, one or two

grain diameters, for all sand sizes. This appears to be the limiting height that the erosive eddy bursts can construct. The absolute heights of the bed topography will vary linearly with the grain size, and the increase in height with changes in grain size will be so small as to have a negligible effect on the flow acceleration.

Increases in mean flow velocity will have only a partial effect on the instantaneous shear stress on the bed since the shear stress is governed by the turbulence intensity developed by the shear layer. Turbulence intensity in the shear layer is a function of the step geometry and the reverse flow velocity downstream of the step as well as the mean flow velocity. Large increases in mean flow velocity are needed to produce significant increases in turbulence and the instantaneous shear stress. However, as the mean velocity is increased it will have a primary effect on the mean sediment transport rate. Therefore, substantial increases in flow velocity which are needed to increase the turbulence intensity can result in general, flat-bed sediment transport which will destroy the streaky bed topography necessary to initiate flow separation.

The only other means of increasing the instantaneous shear stress at reattachment is to artificially increase the size of the flow-separation obstacle by placing or constructing a large irregularity on the bed. A sand

grain much larger than the mean sand size or a foreign object represent such bed irregularities, and they are often present in natural flows. Such imposed and flow constructed bed irregularities can initiate stronger flow separation with more intense turbulence at reattachment.

Southard and Dingler (1971) developed a hypothesis for ripple development like the one just described. They visualized ripple development as being governed by flow separation and eddy impingement downstream of bed irregularity. They suggested that ripple development is governed by a relationship between the minimum height of bed irregularity that is necessary to initiate ripples on a flat bed and the maximum height of bed irregularity that the flow can construct on a flat bed. When the flow cannot construct a bed irregularity of sufficient height to initiate ripples, one would have to be imposed for ripple development.

The hypothetical cases outlined above are in fact what are seen to occur in series B,C,and D. In series B and C, at velocities which spontaneously initiate ripples in series A (ripple phase), ripples can form only from imposed flow-separation bed irregularities. Ripples in series B and C formed in this way belong to the flat bed (metastable ripple) phase. For the same velocities in series D, only a flat bed exists even for imposed separation obstacles. Velocity can be increased, but

this results in uniform sediment transport on the bed surface and the obliteration of the hummocky topography. Therefore, as grain size is increased, ripples will be initiated in different ways, resulting in several ripple phases.

Besides this variation in ripple development with changes in grain size, ripples can develop in different ways with increases in velocity. First the no movement (metastable ripple) phase is initiated, followed by the flat bed (metastable ripple) phase, and finally the ripple phase. The transitions between these phases can be explained in light of the Inglis-Raudkivi theory.

In the no movement (metastable ripple) phase, an artificially imposed mound (one not constructed by uniform flow) causes flow separation and reattachment (Fig. 4.3). At the reattachment point turbulent eddies generated along the flow-separation shear layer interact with the bed and produce large instantaneous shear forces on the bed. The time-average shear stress at the reattachment point is zero but is nonzero and increasing downstream. Instantaneous shear stresses are high enough to initiate particle movement in the reattachment region and so a small average sediment transport rate is established (q_s'). The turbulence energy and intensity decrease rapidly downstream of the reattachment point (Raudkivi, 1963; Tani, 1957; Mueller and Robertson; 1962), and the small

Fig. 4.3. Idealized model of ripple development.

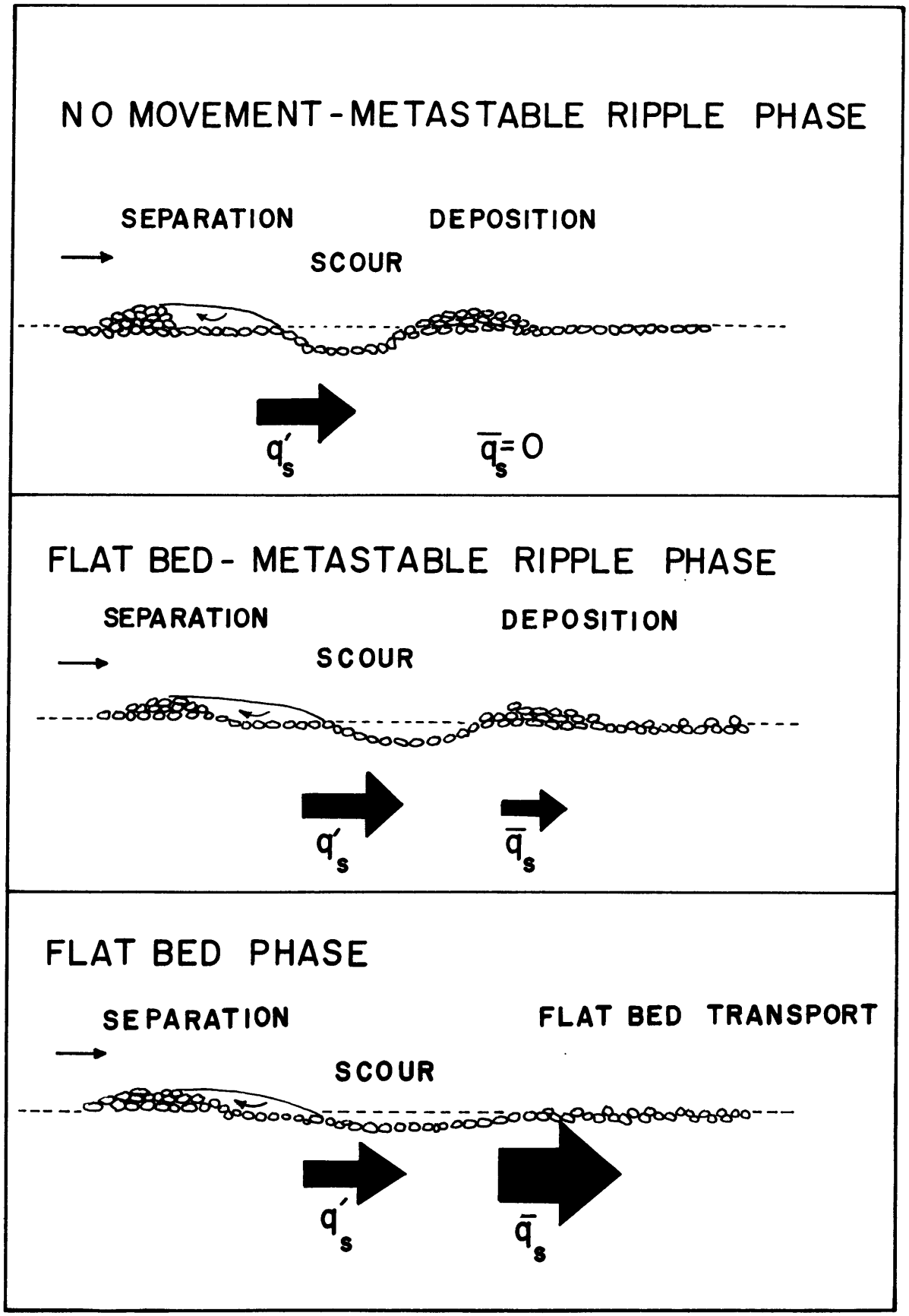

Fig. 4.3. Idealized model of ripple development.

amount of entrained sediment settles out as it passes downstream since the mean sediment transport rate $\overline{q_s}$ is zero (average τ_o less than critical Shields τ_o). Deposition of the sediment forms a new mound which becomes a ripple.

This process of ripple development is described in detail by Southard and Dingler (1971). Furthermore, Southard and Dingler and later Williams and Kemp (1972) developed the hypothesis that the propagation versus nonpropagation of ripples downstream of an artificially imposed mound is in some way the result of the interrelation between mound height and bed shear stress.

In the flat bed (metastable ripple) phase and the ripple phase (Fig. 4.3), the same sequence occurs in setting some grains in motion at the reattachment point. However, downstream the mean sediment transport rate is nonzero, though small. If the entrained sediment transport rate is greater than the mean flat-bed sediment transport rate ($q_s' > \overline{q_s}$), then the mass of grains representing the difference constitutes a maximum in sediment discharge and will initiate a new mound, which will continue the ripple process.

At higher velocities the mean flat-bed transport rate increases. When it becomes equal to or greater than q_s' (there is no maximum in q_s), no new mound can form (Fig. 4.3), and ripples will cease propagating. This

closely describes the transition from ripples to flat bed, which is characterized foremost by the inability of a ripple train to continue propagating downstream, so that the flat bed slowly becomes established from upstream. It is to be expected that $\overline{q_s}$ becomes greater than q_s', since $\overline{q_s}$ is approximately a function of the mean flow velocity, which is increasing, whereas q_s' is a result of turbulent eddy interaction and is not as quickly increased with increases in velocity without large changes in the flow-separation configuration as well.

From the previous sections it is clear that the process of ripple development undergoes gradational changes with increases in grain size and velocity. These gradational changes are not viewed as a breaking down of the primary ripple-forming processes (separation and reattachment), but rather an overwhelming of the effects on the local sediment transport rate q_s' by the mean flow.

That the ripple process is still active at higher velocities and coarser grain sizes is shown by observations of small, low ripples on the upstream slopes of bars and dunes in runs from series D and E (Fig. 3.8). In these runs the major bed forms are much larger than ripples, causing very strong flow acceleration prior to separation and therefore increasing the turbulence generated

in the shear layer. The resulting increase in the needed instantaneous shear stress at reattachment can produce a small maximum in sediment transport on the upstream slope of the bar or dune. Sediment can be entrained at reattachment which cannot be maintained by the flow farther downstream on the bar or dune; this leads to the formation of a ripple.

If flow separation and reattachment are the most important factors in ripple development, there should be a strong correlation between ripple spacing and height of the upstream ripple crest. Furthermore, ripples that have just formed should best display this possible correlation, since ripples become highly modified and three-dimensional with time, because of inherent randomness in turbulent flow and nonlinearities in sediment transport.

In Fig. 4.4 the ratio of ripple length to crest height of the same ripple, ℓ/h and also the ratio of ripple length to crest height of the ripple upstream, ℓ/h_u, are plotted against frequency of occurrence, for newly developed ripples. The ratio ℓ/h has a strong mode at 10 to 15; ℓ/h_u has an even stronger and better defined mode at 10 to 12. Ripple lengths are thus well correlated with upstream ripple crest heights, suggesting that they are dependent on flow separation and reattachment. From the previous discussion it

Fig. 4.4. Histograms of ripple length/ ripple height and ripple length/ upstream ripple height.

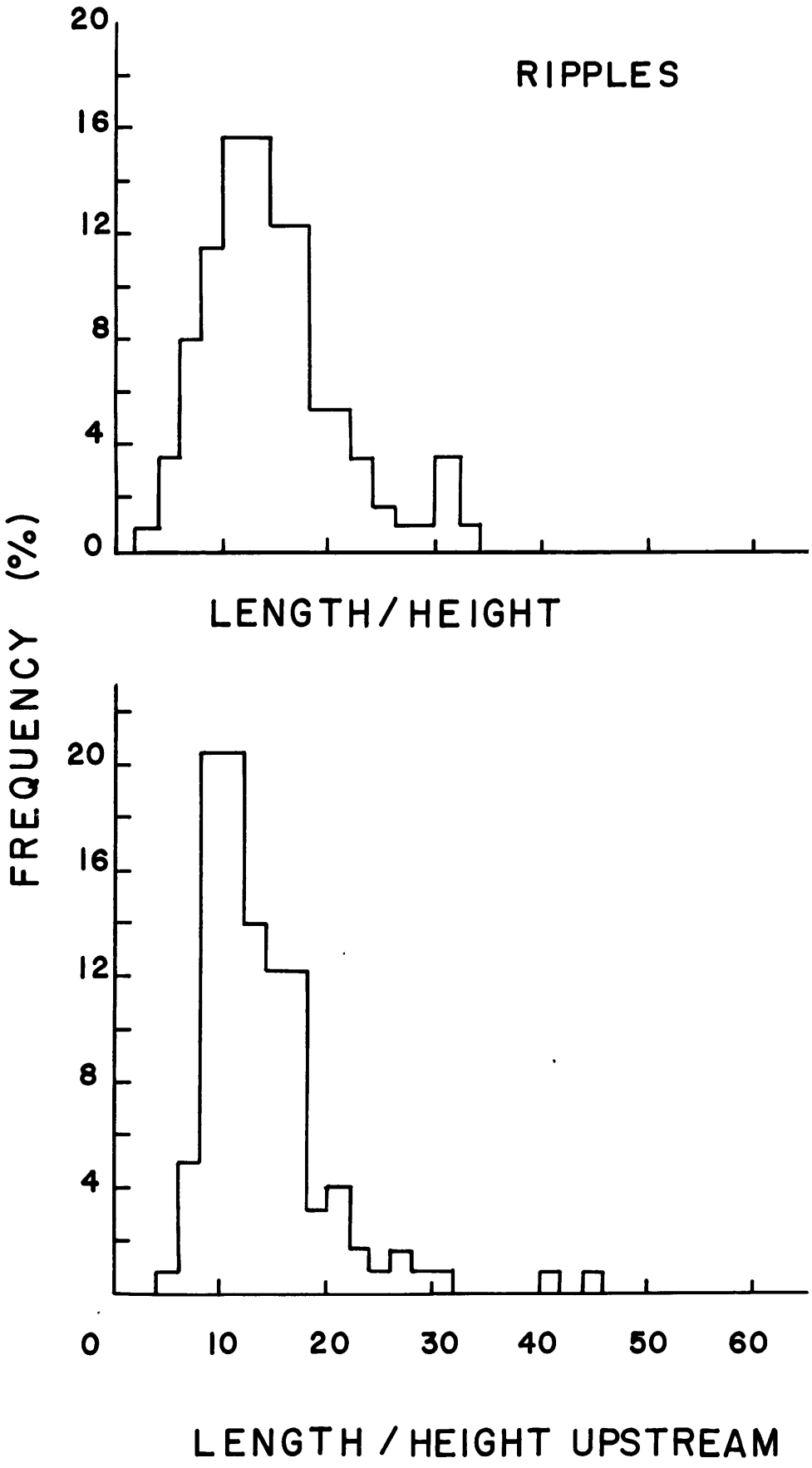

Fig. 4.4. Histograms of ripple length/ripple height and ripple length/upstream ripple height.

is to be expected that a ripple would form some distance downstream of the reattachment point. As shown in Fig. 4.2, reattachment occurs at ℓ/h from 4 to 8. The turbulence intensities should decrease substantially within two or three step heights downstream (Fig. 4.1), so that the extra sediment should be deposited to form a new ripple at ℓ/h_u values of 7 to 11, with a mean of 9. This value is very close to that measured in Fig. 4.4. It is thus clear that flow separation and reattachment control initial ripple spacing.

In summary, many of the characteristics of ripples are well described by theory incorporating flow separation and reattachment. The initial hummocky bed topography needed to start ripple development spontaneously is characteristically produced by the action of a turbulent boundary layer. Ripples are initiated from a perturbation and develop continuously downstream in a train, not instantaneously over the bed as in an instability model (i.e., Bagnold, 1956; Liu, 1957; Yalin, 1972). The spacing of ripples is dependent on the height of the ripple crest upstream, not on any lag distance or other artifice. Ripple development can also be initiated by applying a large flow-separation obstacle to the bed surface, which will cause formation of the metastable

ripple phases observed. The sediment transport maximum from which ripples develop must be progressively overcome as the flow velocity increases, and this is observed in the transition from the flat bed (metastable ripple) phase to the flat-bed phase. Finally, the strong flow separation over large bar and dune slip faces would provide an ideal setting for ripple development, which is always seen to result.

It is concluded that the observed ripple mechanics are the result of the model proposed by Inglis (1949), Raudkivi (1963), and modified by Williams and Kemp (1971), and Southard and Dingler (1971).

BARS

The term bar has often been used to describe a group of large, structural, sedimentary features in rivers which are generally unassociated with bed configurations (i.e., point bars, alternating bars). Here the term bar is applied to a specific bed configuration. Bars have seldom been identified as separate bed configurations, and as a result have not been the subject of direct theoretical consideration to date. As will be seen, theoretical treatment predicting bar formation has been propounded but largely ignored, since it was being applied to another bed form, namely, dunes.

Kinematic Wave Theory

The theoretical treatments described above all belong to a body of wave theory known as kinematic wave theory (Lighthill and Whitham, 1955). A qualitative outline of the theory is presented here to provide an insight into the physical processes taking place.

The starting point of this kinematic wave theory is a one-dimensional mass conservation equation which for bed load sediment transport is

$$\frac{\partial h}{\partial t} + a\frac{\partial q_s}{\partial x} = 0 \qquad (1)$$

where the constant a incorporates the porosity of the sediment mass, whereas q_s and h represent the local sediment transport rate and bed height. This equation states that the rate of erosion or deposition at a point, $\partial h/\partial t$, is the result of the streamwise rate of change of sediment discharge.

As a first approximation, the assumption is made here that for a given mean flow depth and velocity, q_s is a function of h alone, and is independent of x and t:

$$q_s = f(h)$$

Letting

$$c = \frac{dq_s}{dh} \qquad (2)$$

and introducing (2) into (1)

results in $$\frac{\partial h}{\partial t} + ac\frac{\partial h}{\partial x} = 0 \qquad (3)$$

Similarly h could have been eliminated from (1) instead of q_s. This simple partial differential equation describes a wave of constant height moving along the x axis with velocity ac. Solutions to (1) would take the form

$$h = f(x-act) \qquad (4)$$

Since ac is certainly positive (sediment transport rate is greater at high spots on the bed than low), the waves will propagate downstream only.

If the wave velocity ac is a constant, then the solution would describe a linear wave with no change in form. One such solution might be

$$h = A_1 \cos (x-act) \qquad (5)$$

where A_1 is constant amplitude. The wave referred to here may not necessarily have a physical "wave form". It is ideally a point moving at velocity ac, carrying with it the property h or q_s of constant value. The differential equation (3) has a set of characteristic curves in x-t space. The characteristic curves are straight lines with slopes equal to the wave velocity ac. If c is a constant, all the characteristic curves are straight and parallel, and an imposed bed-form wave would not change shape as it migrates.

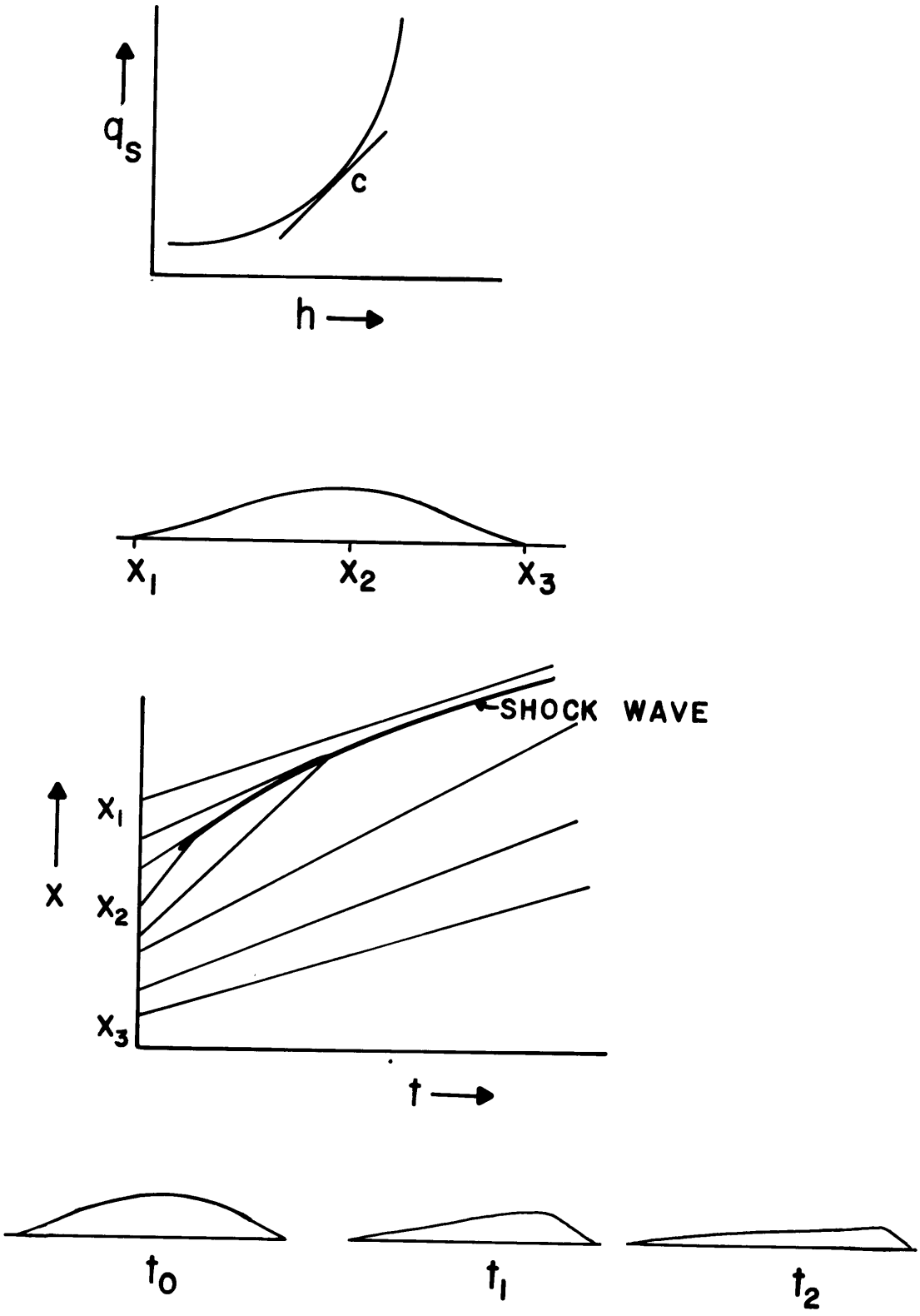

Fig. 4.5. Development of a kinematic shock wave.

In reality the relationship between q_s and h would not be linear, so that c, instead of being constant, would be a function of h, such as is shown in Fig. 4.5. Since velocity depends on height or sediment discharge, waves can change form as they migrate. Higher waves can overtake lower waves, thus leading to existence of two values of height or sediment discharge at a point, so that a discontinuity develops.

The development of a sediment wave can be visualized by plotting the loci of constant bed height in x-t space. These loci must have slopes equal to the wave velocity c. Since c varies with height, different positions on the sediment wave will correspond to lines with different slopes. The slopes depend on the relationship between q_s and h.

Assuming that the curve of q_s versus h is concave upwards, c will increase with height. If an artificial mound is placed on a flat bed, the effects of the q_s-h curve can be observed (Fig. 4.5). On the upstream side of the mound between x_1 and x_2, h increases, as does c. These slopes, plotted as lines on the x-t diagram, diverge between x_1 and x_2. On the downstream side of the mound, between x_2 and x_3, h decreases, and therefore c decreases. These lines converge and eventually cross. At the crossing points there is a discontinuity in bed height, and so a sediment shock wave develops. The discontinuity in

bed height is realized as a slipface at the angle of repose of the sediment, and the sediment shock wave represents a physical bed form. At later times, the characteristic curves meet at smaller and smaller angles, indicating that the bed form is becoming lower and longer.

As will be demonstrated in the next section, this shock wave represents a bar. But it is important to notice that the predicted shock-wave form, a long, low-angle stoss slope and a sharp lee slope, is the form of ripples and dunes also. In fact, ripples and dunes can be viewed as kinematic shock waves. However, in the case of ripples and dunes the effects of flow separation are so dominant as to cause the random kinematic shock waves to be coupled to one another in a definite way which in turn controls the wave lengths. Bars are not coupled by any dynamics, at least to a low degree, but can interact randomly by overtaking one another.

As soon as bed elevations and/or local bed slopes become non-negligable, the original assumption that q_s is a function of h alone breaks down. In this case, q_s becomes a function of h as well as x and the analysis becomes more complex, reflecting the more complex dynamics. The characteristic curves are no longer straight lines, but curves in x-t space. However, the qualitative insight gained from the simplified assumptions examined above is only slightly modified and still very valuable.

The shock waves propagate at different velocities, since they are dependent on the varying velocities of the kinematic waves, which overtake one another. In like manner, a faster-moving shock wave can overtake a slower one. This addition of waves offsets the inherent attenuation of the shock waves as they migrate.

Previous Theory

Exner (1920) seems to have been the first to derive the sediment conservation equation (1). He combined this equation with two assumptions. First, he justifiably assumed that there was constant flow discharge,

$$C_1 = Q = Ub(h_o-h) \tag{6}$$

where Q is flow discharge, U is mean velocity, h_o is water-surface elevation, h is the bed elevation, and b is flow width. Second, he assumed that local sediment transport rate q_s is proportional to the difference between the mean velocity U and some threshold velocity U_o for sediment motion:

$$q_s = C_2(U-U_o) \tag{7}$$

Combining (1), (6) and (7), Exner obtained the equation

$$\frac{\partial h}{\partial t} = -\frac{C_3}{(h_o-h)^2}\frac{\partial h}{\partial x} \tag{8}$$

which has as one solution

$$h = A \cos\frac{2\pi}{L}\left(x - \frac{C_3}{(h_o - h)^2}t\right) \tag{9}$$

This equation predicts than an initial sinusoidal mound on the bed will change with time into a typical ripple or dune shape with a downstream slipface. Note that this solution is identical to that predicted in (5).

By combining (6) and (7), q_s can be expressed as a function of h:

$$q_s = \frac{C_1 C_2}{b(h_o - h)} - C_2 U_o \tag{10}$$

This is a curve of q_s versus h which is concave upward, as assumed. Therefore, Fig. 4.5 provides a view of development of a kinematic shock wave identical (albeit qualitatively) to Exner's initial mathematical model.

Polya (1937) derived (1) through an approach similar to that used to derive Fick's First Law. Both Exner (1925) and Polya (1937) attempted to interject some dynamics into their analysis. Exner combined the one-dimensional momentum equation, along with certain simplifications, with his equations (1), (6) and (7) to derive a second-order partial differential equation with a solution similar to (9) but including an exponential term which resulted in rapid attentuation

of any sinusoidal perturbation applied to the bed. Polya's equation was similar and produced an identical solution. These early mathematical models of Exner (1920, 1925) and Polya (1937) described wave forms that later became known as kinematic waves.

Both Reynolds (1965) and Gradowczyk (1968) attempted a theoretical treatment of wave propagation on an erodible sediment bed. They used conservation equations for sediment and water as well as the one-dimensional shallow-water momentum equation. Gradowczyk's (1968) solution had three sets of characteristics, the first two of which were the solutions for gravity waves in the flow. The other solution was for bed-wave propagation. This wave was identical for the unsteady theory of Gradowczyk (1968) and the quasi-steady theory of Reynolds (1965). Gradowczyk (1968) observed that this bed wave was a surface kinematic wave and was derived, as was Reynolds' solution, from an equation of the same form as (1).

Having obtained these solutions, both Reynolds and Gradowczyk observed that the predicted wave was damped as it traveled downstream, as was the wave predicted in the simplified analyses of Exner and Polya. Since the waves could not grow and propagate quasi-periodically as dunes do, the theory was considered to be incomplete. What was not recognized from these mathematical models was the potential for the attenuating

waves to merge to preserve their form. Gradowczyk (1968) and Reynolds (1965) introduced the artifice of a lag distance or a coupling of the bed and surface waves in order to promote a growth condition for any perturbation to the bed. The kinematic shock waves were then made to grow, and this led to results that were qualitatively the same as those of Kennedy (1963).

Bar Movement

In this section the predictions of the kinematic wave theory are compared to the observed behavior of bars. A main foundation of the kinematic theory is a general relationship between q_s and h, as defined by equation (10) for a given velocity and depth. As has been shown, the simplest assumptions about the sediment transport support such a relationship. More refined assumptions do not alter the basic concave-upward nature of the q_s-h curve.

For a relationship between q_s and h to hold, there should be uniform grain motion on the bed. In the flat-bed phase the grains move intermittently, with grains exposed above the packed bed being most susceptible to movement. Therefore, this small population of exposed grains is responsible for most observations of motion. A larger population of sheltered or well packed grains constitute an armored bed and do not move. A general

q_s-h relationship cannot hold in a situation in which the majority of bed particles are not moving.

The onset of bar formation coincides with the change from intermittent grain motion to general grain motion on a flat bed. If general grain motion results in establishment of a sediment-transport relationship of the form of equation (10), and kinematic waves are spontaneously formed for such a relationship , then the occurrence of kinematic waves is simultaneous with that of bars.

Kinematic waves may or may not constitute a recognizable bed wave. The merging of kinematic waves to produce a shock wave will produce a bed-surface wave with a slipface. Development of a shock wave is dependent on the prior formation of a small bed disturbance or irregularity. Such a disturbance causes a discontinuity in height and/or sediment transport rate. The first recognizable bars that form in an experimental run are only two or three grain diameters high, and the initial bed disturbance giving rise to them must be even smaller. Bed irregularities of this height are observed to form in the flat-bed phase, and by Williams and Kemp (1971) in their experiments with flat-bed transport. Thus, it seems plausible that the interactions of eddies and the bed surface that cause these irregularities in the flat-bed phase would still be effective at the slightly

increased velocities that characterize the bar phase. Therefore, at the onset of general flat-bed grain motion, kinematic waves form and merge to produce kinematic shock waves (Fig. 4.5) whose physical wave form is that of a bar.

Kinematic theory predicts that the shock should attenuate downstream; this is observed for bars as well. Bars that form at the lowest velocities in the bar stability field show a predominance of attenuation over accretion. With increases in velocity, accretion balances attenuation. An increase in velocity also produces bars of greater height and more regular spacing. The initial bars formed at low velocities have a fairly random variation of lengths (Fig. 3.9) whereas those formed at higher velocities have lengths and regularity of spacing similar to dunes, and also have ripples developed on their upstream slopes.

Initial bars formed at low velocities with their attenuating characteristics grow and die randomly in space and time. The randomness of the observed bar lengths reflects this random process. When ripples start to develop on a bar because of flow separation over the bar crest upstream, they have very important effects on bar development. Ripples are small kinematic shock waves that transport sediment to the bar crest. In this way the crest of one bar affects sediment supply to, and

therefore attenuation of, the adjacent bar downstream. The change in attenuation is a consequence of the symbiotic ripple-bar relationship. As accretion predominates over attenuation, fewer of the shock waves developed on the bed will die out, and so the frequency or the density of bars on the bed should increase. This is in fact observed as bars form with shorter lengths similar to those of dunes rather than with a range of extremely long to very short lengths.

A more graphic presentation of bar migration and ripple interaction is shown in Fig. 4.6. A plot of the positions of the bars in space and time was constructed from observation of a series E run. Long continuous lines represent the loci of bar crests. The slope of such a line is inversely proportional to the migration rate of the bar. Shorter lines are the paths of the faster ripples. The slopes of the bar lines vary with position and time, reflecting changes in their heights by downstream attenuation and by ripple capture.

As will be shown in the discussion of dunes, the process that controls dune lengths becomes continuously stronger and more effective as the bar phase changes to the dune phase. This gradational process probably also acts to produce the observed gradational change in the bar lengths from being random to progressively more dunelike in magnitude of spacing and regularity of spacing.

Fig. 4.6. Path lines of bars and ripples in space and time. (Run E-12, D_g= 1.14 mm)

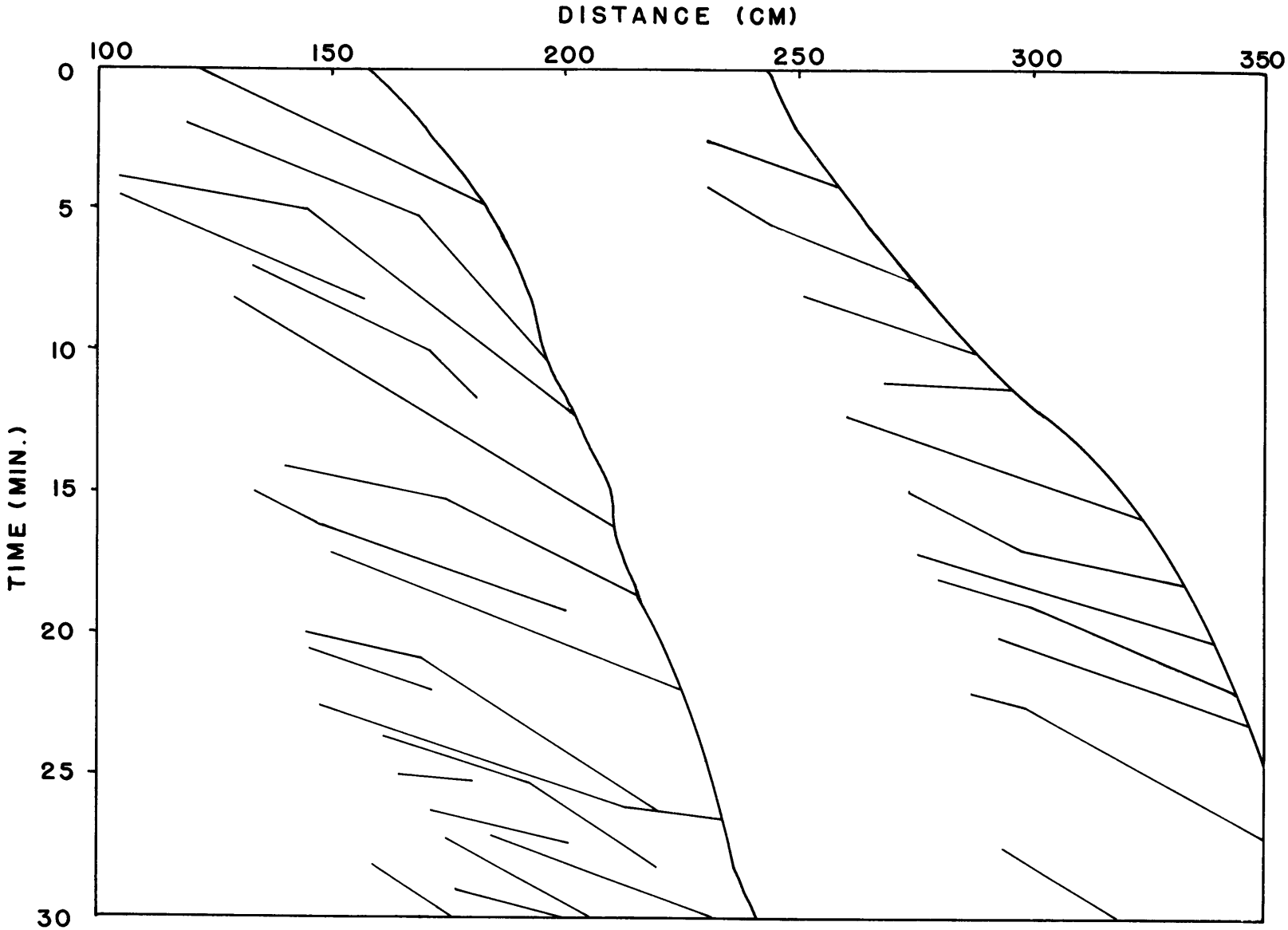
DISTANCE (CM)
100
150
200
250
300
350
0
5
10
15
20
25
30
TIME (MIN.)

The factors which control bar height are much more complex. Both bars and dunes formed in experimental flumes at low flow depths exhibit a depth dependence which is not demonstrated in deep natural flows. Discussion of this depth dependence is deferred until dunes have been described, when the factors will be discussed for both bars and dunes.

In summary, the mechanics of bars are well described by kinematic wave theory. The conditions necessary to initiate kinematic wave relationships match those observed at the onset of bars. The form and attenuating character of kinematic shock waves also matches the bars. Finally, the kinematic theory allows for merging of shock waves to overcome attenuation, and in the same way bars merge with one another, and with ripples, to preserve their form.

DUNES

Unlike ripples, dunes have been the subject of a great deal of analytical theory (Kennedy, 1963; Reynolds, 1965; Gradowczyk, 1968). Dune kinematics have also been treated by Russian scientists (Velikanov and Mikhailova, 1950), and their theories have been incorporated in a new theory by Yalin (1972). In the following sections these established theories will be reviewed and tested. Observations and predictions are not compatible, and so

a new theory for dunes is presented.

Kennedy Model

Kennedy's (1963) analytical theory for bed configurations, incorporating the method first employed by Anderson (1953), uses a potential-flow theory for flow over a wavy bed. Kennedy's theory satisfactorily predicts the onset of antidunes with regard to the Froude number, whereas his theoretical analysis of lower-flow-regime bed configurations does not compare well with observations.

At the time Kennedy constructed his theory, it was not widely accepted that ripples and dunes are two distinct bed forms, and a distinction between them is not made in his analysis. However, the bed forms predicted by Kennedy's theory, being depth-dependent, are assumed to be dunes.

Kennedy's analysis treats both antidunes and dunes with one theory, and yet most observations emphatically point to a great difference in the basic physics between them. Southard (1971) has compiled data on dunes and antidunes and has conclusively demonstrated that they act in physically distinct ways. Antidunes, which are directly coupled to the in-phase surface waves, are well described by potential-flow theory, which has proved to be a valuable tool in surface-wave problems. Dunes,

on the other hand, are largely decoupled from the surface waves and are controlled and modified by flow separation and boundary-layer development. Such real-fluid effects cannot be accounted for in a potential-flow model. To overcome this drawback, Kennedy introduced, as one of his parameters, a quantity j, which is supposed to include all the effects of the real-fluid flow which can not be incorporated in the potential-flow theory.

In Kennedy's theory, different bed forms can be differentiated in a plot of his three important parameters, Fr (Froude number), $2\pi d/\ell$ (dimensionless wave length), and j (real-fluid-effect parameter) (Kennedy, 1963, Fig. 9). The antidunes are well predicted, whereas ripples and dunes are not distinguished and the points are broadly scattered. The degree of scatter is indicative of the inability of the potential-flow theory, even augmented by the real-fluid parameter j, to describe real-fluid effects on sediment transport. The parameter j, on which so much depends, is a function of the lag distance, which has never been proved to exist.

Velikanov-Mikhailova-Yalin Model

Like Kennedy (1963), Velikanov and Mikhailova (1950) suggested a theory to describe both ripples and dunes, making no distinction between them. However, in its revised form, presented independently by Yalin (1972),

this theory is directed at explaining the origin of dunes.

Velikanov and Mikhailova proposed that the wavelength of initial dunes formed on a flat bed is determined by "large-scale structural elements" in the turbulent flow, i.e., large eddies. These large-scale quasi-periodic eddies have sizes comparable with the flow depth, and are associated with variations in turbulence intensity and suspended-sediment concentration. Assuming a downstream correlation in the frequencies of the eddies and in the distributions of the instantaneous velocities, Velikanov (1958) derived a sediment-transport equation that could predict changes in bed profile.

Yalin (1972) accepted the hypothesis that dunes are the result of periodic, large-scale eddies in rivers. He assumes that the maximum velocity U_m is a function of x and t and that U_m can be correlated for changes in x. The eddies are a stochastic process having a frequency described by a spectral density function or its inverse Fourier transform, the autocorrelation function. Yalin assumes an autocorrelation function of the form

$$K(x) = e^{-\alpha x} \cos(x/d)$$

which provides for positive correlations between U_m at distances of $2\pi d$, $4\pi d$, etc. and negative correlations at πd, $3\pi d$, etc. An increment in U_m is then repeated at $2\pi d$ spacing downstream, but the tendency dies out

progressively downstream due to the exponential attenuation term. Yalin argues further that the local velocities at any given level should be correlated in approximately the same way.

Sediment discharge q_s is a function of boundary shear stress τ_o, which is in turn a function of the velocity gradient at the boundary $(dU/dy)_0$. Therefore Yalin argues that if changes in velocity profiles can be correlated downstream, so can changes in q_s. If there is an initial decrease in $(dU/dy)_0$, then q_s should decrease and there should be accretion of the bed at this point and at downstream distances of $x = 2\pi d$. Conversely, an increase in $(dU/dy)_0$ should lead to erosion of the bed at intervals of $x = 2\pi d$. Yalin predicts that if an initial perturbation is applied to the eddies, then a wave-like deformation will occur on the bed surface with a spacing of $\ell = 2\pi d \sim 6d$. He compares this prediction to his empirical suggestion (Yalin, 1964) of $\ell \sim 5d$ and Hino's (1969) prediction of $\ell \sim 7d$.

When comparing Yalin's theory to observations, many discrepancies become apparent. The initial assumption is that the values of U_m generated by eddies could be correlated at set distances downstream. Generalization of this correlation to include not only U_m but also the complete velocity profile is more uncertain. Moreover, correlation of values of τ_o at set distances downstream

requires that the local velocity gradient at the boundary also be correlated with distance.

However, dunes can develop from a rippled bed surface. The ripple profile causes large-scale changes in the turbulent boundary layer because of flow separation and acceleration. These effects must dominate the structure of the turbulent boundary layer and overwhelm any periodicity in the mean flow structure. A very simple flow separation greatly modifies the boundary-layer profile downstream for distances of $x \sim 10d$. Therefore, the flow disturbances initiated by ripples produce effects that are stronger and more lasting than those hypothesized for correlated large eddies.

Mechanics of Dunes

As with ripples, there are two necessary conditions for dune development. The first is the formation of some initial perturbation to the flow-sediment system, like the hummocky, streaky topography formed prior to ripple development. Second, there must be some downstream transmission mechanism to develop a series of quasi-periodic forms, similar to the flow separation and reattachment for ripples.

The first prerequisite is met by the recognition of a separate bar bed form which is inherently constructed from a flat bed. The second prerequisite is harder to

visualize, and has been previously ascribed to the correlation between large-scale eddies (Velikanov-Mikhailova-Yalin), the lag between sediment transport and velocity changes (Kennedy, 1963; Reynolds, 1965), or to coupling between bed and surface waves (Gradowczyk, 1968). None of these processes appears to be physically realistic.

In order for a new sediment mound to form downstream from an existing one, there must be a maximum in q_s downstream so that there will be deposition. The effect of the presence or absence of a maximum in q_s can be visualized in Fig. 4.7 for flow past a negative step. For the case in which there is no maximum, q_s will increase monotonically downstream. Since this means that $\partial q_s/\partial x$ is everywhere positive, Exner's sediment conservation equation (1) states that $\partial h/\partial t$, the rate of change of bed height at a point, must be negative. Therefore there will be net erosion all along the bed, which will tend to zero far downstream (Fig. 4.7). If there is a maximum in q_s, then $\partial q_s/\partial x$ will change from positive to negative at some point downstream of the step. Therefore $\partial h/\partial t$ will be positive past that point, and a sediment mound will tend to develop (Fig. 4.7).

To determine whether the development of a maximum in sediment transport is responsible for the transition from bars to dunes, a series of experiments in the 5.5 m

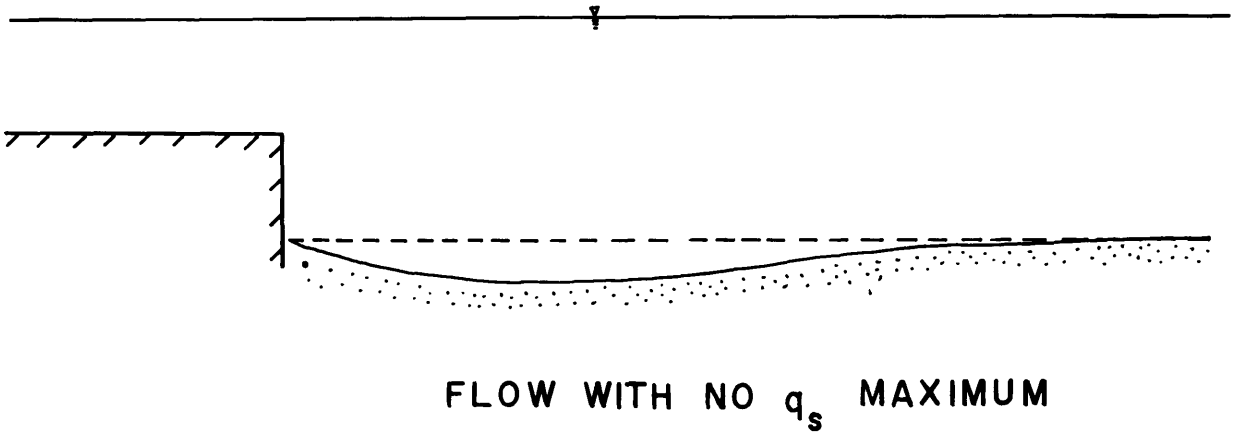

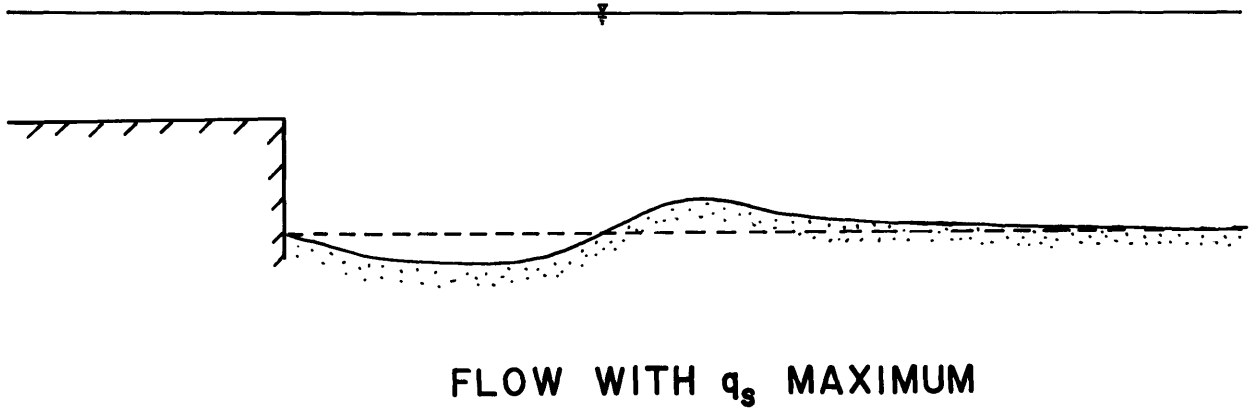

Fig. 4.7. Idealized effect of maximum in q_s.

flume were made over a flat sediment bed (1.14 mm sand) downstream of a small stationary artificial step 0.50 to 1.25 cm high. Prior to an experiment at a given velocity, depth, and step height, the level of the sediment bed was carefully measured every 2 cm with a point gage for one meter downstream of the step. The flow was turned on for one minute and then gently stopped, so as not to disturb the bed. The bed elevation was remeasured and the process repeated. If a sediment-transport maximum was generated, a region of higher elevation would be built up on the bed, and this would deform as a kinematic shock wave.

The results of these experiments are plotted in Fig. 4.8. Also plotted in Fig. 4.8 are the different phase fields for the experimental runs with 1.14 mm sand of series E (Fig. 3.12). The locus of onset of the maximum in q_s lies along the boundary between bars and dunes defined from the flume experiments. The excellent agreement supports the view that development of a maximum in sediment transport is responsible for the transition from bars, which are largely independent of one another, to a quasi-regular train of coupled dunes.

Smith (1969, 1970) and Yalin (1972) have both proposed this criterion of a maximum in sediment transport for development of dunes. Since sediment discharge is

Fig. 4.8. Depth-velocity diagram for measurements of a maximum in sediment transport downstream of a negative step.

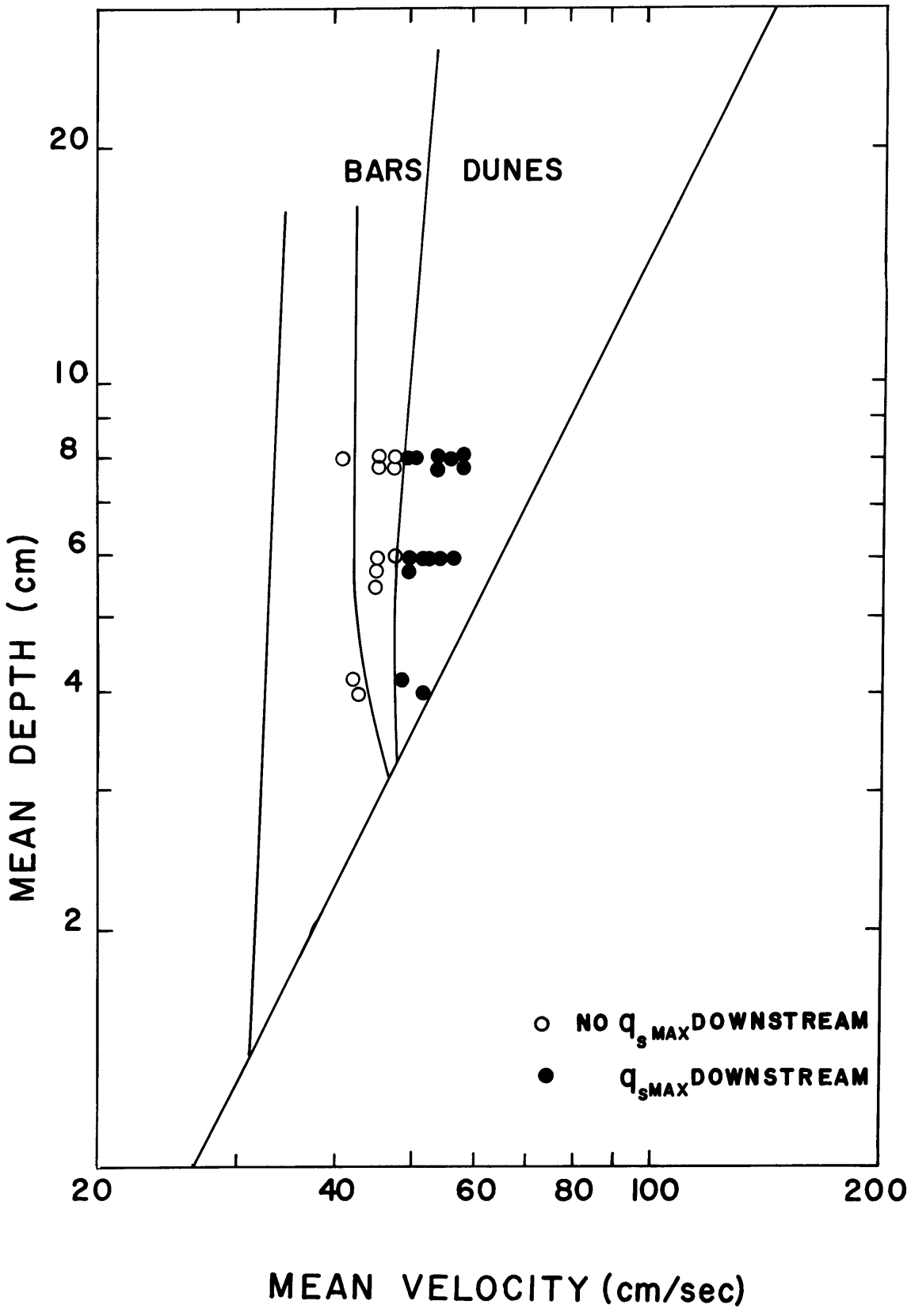

Fig. 4.8. Depth-velocity diagram for measurements of a maximum in sediment transport downstream of a negative step.

a function of bed shear stress, both Smith and Yalin assume that a maximum in q_s is representative of a maximum in bed shear stress. This seems to be a reasonable assumption, and no other processes, exclusive of shear stress, have been presented to explain a maximum in q_s. Furthermore, Smith has demonstrated that for reattaching flow over a negative step a maximum in boundary shear stress is created just downstream in a redeveloping boundary layer. As will be shown in the next section, this maximum in boundary shear stress is common to all strongly accelerated reattaching flows but does not develop for more weakly accelerated flows such as those over ripples.

Flow Separation and Reattachment

The proposed mechanics of dunes are very similar to those described before for ripples. Both bed configurations require a maximum in sediment transport downstream of flow separation. However, the similarities in processes cease at this point.

Ripples are initiated on beds having a relatively weak sediment transport rate in comparison to that for dunes. The maximum in sediment transport lies just downstream of reattachment (Fig. 4.4), where the temporal mean boundary shear stress is zero. However, the reattaching flow interacting with the bed has large values

of turbulence intensity and energy (Tani, 1957; Walker, 1961; Mueller and Robertson, 1962). This turbulence can cause instantaneous velocities and instantaneous shear stresses near the bed which give rise to a small maximum in sediment transport (Raudkivi, 1963; Williams and Kemp, 1971, 1972). The initial bed irregularities which initiate ripples on a flat bed are very small (on the order of a grain diameter) and are caused by interactions of turbulent eddies and the bed. These small irregularities do not give rise to large local flow acceleration.

Dunes form on bed surfaces characterized by high sediment transport rates and having large bars developed. The bars always precede dune development and cause flow separation which initiates ripples on the bars downstream. In this section it will be shown that the maximum in q_s set up by flow separation and reattachment and responsible for initiation of dunes is related to the mean boundary shear stress distribution, not an instantaneous boundary shear stress as for ripples, and the q_s maximum occurs at downstream distances about twice those characteristic of ripples. The two maxima in sediment transport are therefore genetically different and largely independent of one another.

Mechanics of flow separation over a negative step have been described in the last chapter; the focus here

will be on flow reattachment. Most studies of reattaching flow take the simplified view that the reattaching flow can be modeled as a developing turbulent boundary layer with an exterior wakelike flow. Smith (1970) has attempted such an analysis, but recent studies (Tani, 1968) reviewing perturbed turbulent boundary layers show that even the simplest reattaching shear flows are extremely complicated, and do not react like normal turbulent boundary layers for great distances downstream (on the order of one hundred step heights).

The perturbations to the turbulent boundary layer can be weak, as for a change in roughness (Makita, 1968; Antonia and Luxton, 1972), strong, as in the case of flow over a step (Mueller and Robertson, 1962; Bradshaw and Wong, 1971), or overwhelming, as for reattaching jets (Rajaratnam and Subramanja, 1968). Yet all these flows have similar characteristics, one of the most important being the nonequilibrium behavior of wall shear stress soon after reattachment or just past the perturbation. As Tani (1968) concludes, "the wall shear stress overshoots the equilibrium value, and then returns slowly toward equilibrium. The rapid adjustment of the flow near the wall presents itself as the rapid establishment of the law of the wall, but not necessarily results in the immediate attainment to equilibrium of the wall shear stress as frequently mis-

interpreted."

Velocity profiles immediately downstream of reattachment clearly show an increase in velocity gradient close to the wall over that expected of a normally developing turbulent boundary layer (Tani, 1957, Fig. 7,8 and 9; Mueller and Robertson, 1962, Fig. 4; Bradshaw and Wong, 1972, Fig. 8; Rajaratnam and Subramanya, 1968, Fig. 2). This nonequilibrium, internal boundary-layer development is further evidenced by observations of large-scale departures in the turbulent energy budget and in the mixing length close to the boundary just downstream of a change in roughness or reattachment (Antonia and Luxton, 1972; Bradshaw and Wong, 1972).

It seems reasonable to assume that all accelerating flows interacting with a boundary will initially have too high a velocity gradient near the wall and that it will take time and also distance downstream to readjust to equilibrium. The stronger the flow acceleration interacting with the bed, the greater is the possibility of the wall shear stress overshooting its equilibrium value. Qualitatively, then, flows with higher velocity over steps large compared to flow depth will have greater acceleration, a higher wall-shear maximum, and possibly a better defined position of maximum shear stress.

Using data from experiments on reattaching turbulent boundary layers, a qualitative test can be made of this

Fig. 4.9. Shear stress maximum for reattaching flows. (After Antonia and Luxton, 1972; Bradshaw and Wong, 1971; Rajaratnam and Subramanja, 1968; Smith, 1970).

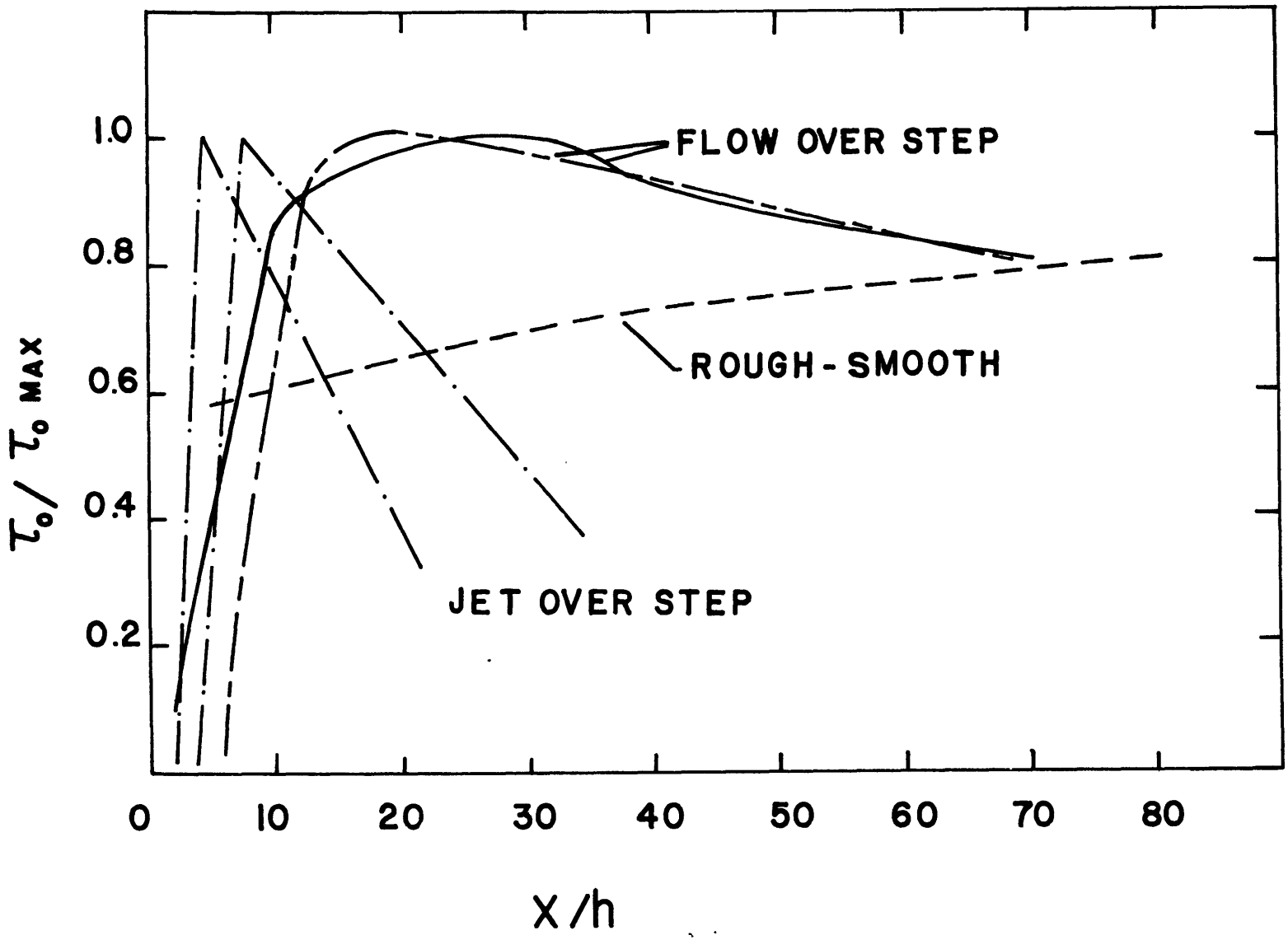

Fig. 4.9. Shear stress maximum for reattaching flows. (After Antonia and Luxton, 1972; Bradshaw and Wong, 1971; Rajaratnam and Subramanja, 1968; Smith, 1970).

hypothesis. In Fig. 4.9, the ratio of boundary shear stress to maximum boundary shear stress is plotted against position downstream from a step. For the case of a change from small-scale roughness (3.2 mm high) to a smooth surface (Antonia and Luxton, 1972), no shear stress maximum develops. For flows over a negative step (Smith, 1970; Bradshaw and Wong, 1972), where the step height was 15 to 20 percent of the flow depth over the step, a weak and relatively widespread (15 to 40 step heights downstream) maximum in boundary shear stress develops. Data for a reattaching jet over a negative step (Rajaratnam and Subramanya, 1968), where the step height is 2 to 3 times the flow depth over the step, show a sharp and very strong maximum in boundary shear stress.

The change in roughness and the reattaching jet are two theoretical end members in the wide range of possible flow conditions over the bed. Small bed irregularities (on the order of the grain size) are qualitatively similar to the case of a change from a rough to a smooth surface. Development of a maximum in mean shear stress should not take place, but the flow separation can still initiate ripples through the action of the instantaneous shear stresses. Dunes, on the other hand, are observed to form only after large bar slipfaces are developed to provide a strong flow separation, as in the case of flow over a negative step. A second very important conclusion from

this qualitative comparison is that the process of setting up a shear stress maximum is gradational. For weak flows over low steps, the magnitude of the τ_o maximum is small and its position downstream varies over a wide range. With increasing flow velocity over a larger step, the amplitude of the τ_o maximum increases and its position becomes better defined. Hence with an increase in velocity (bed height has been shown to increase with velocity), there is more local flow acceleration downstream of a slipface, and the shear stress maximum becomes more efficient in controlling q_s (increased magnitude of the τ_o maximum) and less diffuse in its position. Again, this is seen in the transition from bars to dunes. There is a progressive transition from isolated, randomly spaced bars to quasi-periodic dunes with an increase in velocity.

Dune Model

There are great similarities in form and physics, although not in scale, between ripples and dunes. The process of dune development can be visualized in the same terms as the ripple process.

For high-velocity flow over a crest, there can be two independent sediment-transport maxima set up on the bed. At the reattachment point, the instantaneous shear stress due to eddy impingement can create a finite

sediment transport rate which is not supported by the mean flow at some small distance downstream (Fig. 4.3) (Raudkivi, 1963; Williams and Kemp, 1971, 1972). A maximum in q_s is established and forms a ripple. This process occurs for even the weakest flow separation. For stronger flows, the flow acceleration at separation over a bar is increased to the point where it causes the mean bed shear stress downstream of reattachment to overshoot its equilibrium value (Fig. 4.9). This τ_o maximum creates a q_s maximum which in turn becomes a dune. As is the case for ripples, the flow-separation process should determine the spacing of the dunes.

Histograms of the frequency of ℓ/h and ℓ/h_u for dunes are compared in Fig. 4.10. The crest spacing, nondimensionalized with respect to the step or slip-face upstream, has the stronger mode. This suggests that spacing of dunes, like that of ripples, is controlled by flow separation. Furthermore, the distance from the step to the maximum in τ_o predicted by Smith (1969) and Bradshaw and Wong (1972) is 15 to 40 step heights. Smith's data (solid line in Fig. 4.9) are for flow over a 4 cm step at flow depths and velocities characteristic of the ripple field. Flow velocities would have to be 2.5 to 3 times higher than those Smith used to accurately portray the dune field. As Fig. 4.9 indicates, this would cause a more jetlike flow, and the position of the τ_o

Fig. 4.10. Histograms of dune length/ dune height and dune length/ upstream dune height.

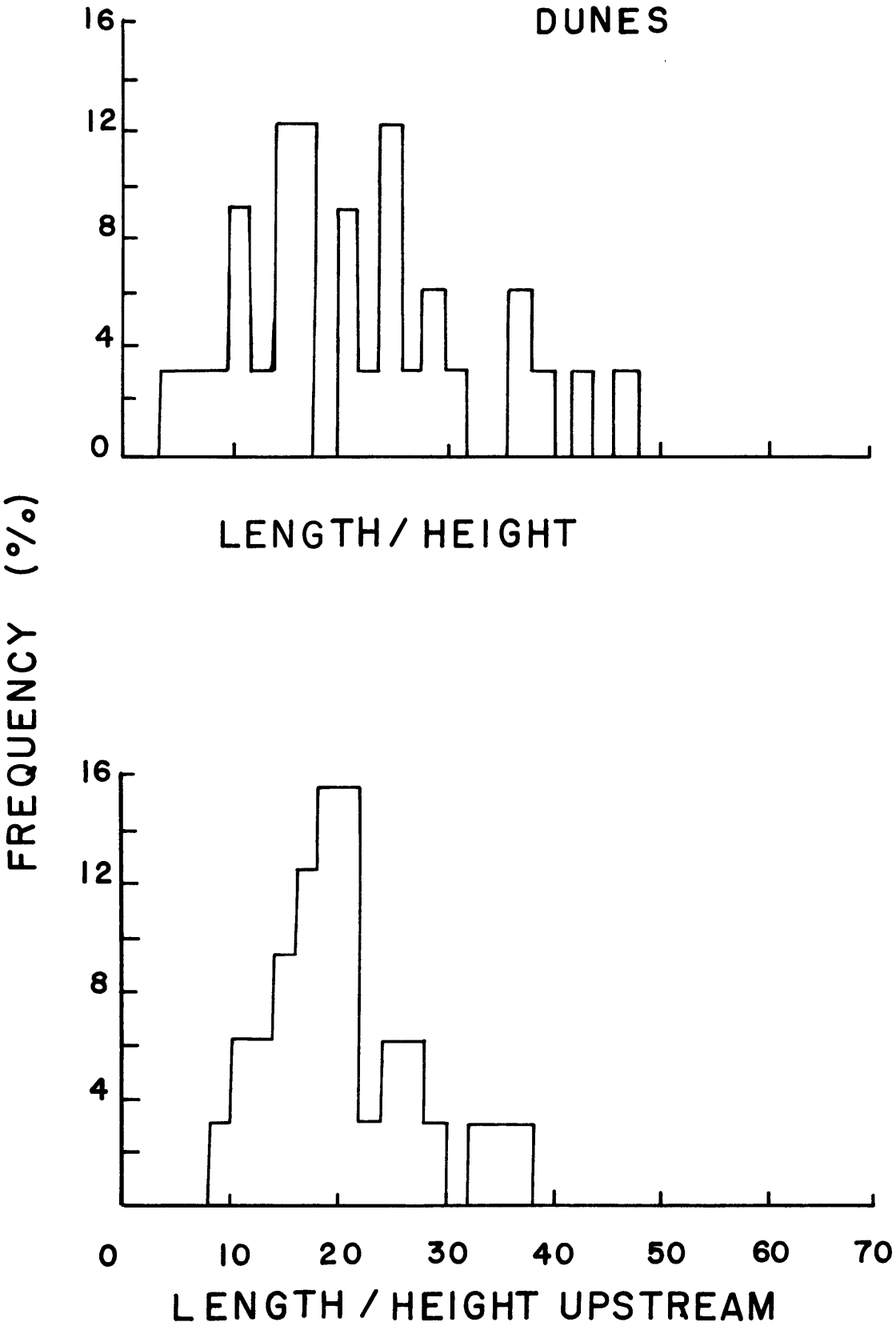

Fig. 4.10. Histograms of dune length/dune height and dune length/upstream dune height.

maximum would probably be in the range x/h = 15 to 25. Since dunes will form just downstream of the q_s maximum, the spacing of dune crests, nondimensionalized with respect to the height of the crest upstream, should be in the range 16 or 17 to 30 x/h. This is in good agreement with observation (Fig. 4.10).

Experiments to measure the mean shear stress distribution downstream of a negative step, for flow velocities and depths characteristic of dunes, are needed to accurately determine the position of a τ_o maximum and to compare with Fig. 4.10. However, the order of magnitude comparison outlined above is good supporting evidence for the hypothesis that dunes are initiated by a mean shear stress overshoot downstream of flow separation.

The strength of the τ_o maximum measured in the step experiments is on the order of 5 to 10 percent greater than the mean shear stress downstream (Fig. 4.9). However, q_s is a function of τ_o raised to some power ($q_s \sim \tau_o^3$ according to the Einstein-Brown theory). Although the τ_o maximum is only 5 to 10 percent greater than the mean value, the resulting q_s maximum can be to the cube of this τ_o maximum. Therefore, a substantial q_s maximum can be produced by a weak τ_o maximum.

As shown, dune lengths correlate very well with distance to a maximum in boundary shear stress downstream from a negative step. The problem of predicting dune

height is much more complex. Yalin (1964) has proposed that dunes grow to be twenty percent of the flow depth. But other observations in experimental flumes (Guy et al., 1966) show that dunes can reach heights of fifteen to thirty percent of the flow depth. On the other hand, in large rivers dunes are found to be independent of depth (Coleman, 1969), with equal heights in varying depths of water. Therefore, heights of dunes and bars are dependent on depth only in the relatively shallow flow depths used in experimental flumes.

Equilibrium dune height is dependent upon a mass balance between rate of erosion at the dune crest and rate of sediment supply to the crest. Rate of erosion at the crest is related to (1) the height to which the dune extends into the flow, (2) the strength of the local flow acceleration up the stoss slope of the dune, (3) the migration rate of the dune, and (4) the depth of scour downstream of the crest. Rate of sediment supply is related to (1) the mean sediment transport rate on the stoss slope of the dune (including sediment transported as ripples), (2) the position of the maximum in sediment transport in relation to the crest, and (3) the strength of the maximum in sediment transport.

These factors are interrelated in a complex fashion which at the present time is not clearly understood. The process of controlling dune height probably involves a

continuous feedback mechanism that makes adjustments among the interrelated variables. It is likely that for experiments in flumes, the dune heights cannot grow too large without extending into regions of the boundary layer which have velocities capable of continuously eroding the dune crest. Also, in flumes with fixed width, dunes locally accelerate the flow over their crests, which causes more erosion.

The presence of ripples on dunes can be understood in light of the proposed model for dunes. Flow separation is inherent in flows with bed forms. The operation of two independent sediment-transport maxima due to flow separation has already been outlined. For strong flow separation, both processes can act simultaneously. Dunes develop downstream from bars because the reattaching flow is still accelerating for a short distance downstream of reattachment. This initiates a maximum in mean boundary shear stress and also in sediment transport rate. Ripples are generated near reattachment because the instantaneous shear stresses set up by turbulence interacting with the bed create a maximum in q_s. Ripples are formed by flow separation at one dune crest and are trapped at the next crest downstream. It would seem much more likely that one process, flow separation and reattachment, is responsible for the coexistence of ripples and dunes, rather than having two instabilities competing to produce

each feature (Kennedy, 1963).

In summary, the predictions of the proposed dune model compare favorably with observations. Dune spacing correlates very well with the predicted values, and the model accounts for no dune development at lower flow velocities with flow separation over small bed irregularities. Dunes are not predicted to arise from some instability and grow because of an artifice, such as a lag distance. Instead, dunes are initiated from bars, which are inherently formed once there is general grain motion on a sediment bed. The mechanism of developing a new dune downstream of a bar has been shown to be due to another inherent characteristic of separated flow, the overshoot in τ_o downstream of reattachment.

CONCLUSION

The differences in form of ripples, bars, and dunes reflect their different mechanics of formation.

Ripples are well described by the model proposed by Inglis (1949), Raudkivi (1963), Williams and Kemp (1971), and Southard and Dingler (1971). Initially the flow constructs a streaky or hummocky bed topography which causes small-scale flow separation. The flow separation arrests grains moving downstream and initiates scour where it reattaches downstream. The scour is the result of turbulence acting on the bed, which entrains sediment

and transports it a short distance downstream, where it is deposited. At the site of deposition a new mound forms (approximately 10 step heights downstream) and becomes a ripple, and the process repeats itself downstream.

Ripples can also be initiated by placing obstacles or irregularities on the bed. This gives rise to the metastable ripple phases and the formation of ripples on dunes.

Bars are formed spontaneously once there is general grain motion uniformly distributed over the bed surface. Bars are kinematic shock waves which overcome attenuation by merging with one another. Bars are randomly generated, and this randomness carries over into their spacing and height. With increases in velocity bar spacing becomes more regular and dunelike.

Dunes develop from bars when the flow velocities and bar heights interact to strongly accelerate the flow over a bar crest. This acceleration persists near the bed even after the flow has reattached. It is hypothesized that the flow acceleration near the bed causes a maximum to develop in the temporal mean boundary shear stress and sediment transport at approximately 15 to 25 step heights downstream of the crest. The maximum in sediment transport forms a mound of sediment, which becomes a dune.

5. FIELD OBSERVATIONS OF BED CONFIGURATIONS

Studies of large rivers and shallow marine currents have identified ripples and dunes similar to those observed in laboratory flumes, as well as larger bed configurations not observed in flumes. Echo soundings indicate that these larger forms are up to several hundred meters long and ten meters high. These features have been classed either as large-scale dunes or as larger-scale features completely distinct in origin from bed configurations observed in laboratory flumes. In rivers they have been called linguoid bars (Allen, 1968; Collinson, 1969) or transverse bars (Smith, 1971); in marine environments they have been called sand waves.

MARINE SAND WAVES

Van Veen (1935) was one of the first to give a detailed description of sand-wave geometries. He noted their asymmetrical form, with downstream slipface, and the crest-line pattern perpendicular to the tidal current direction, and so deduced that the sand migrated in response to tidal currents. Van Veen also demonstrated that when the tidal currents reversed directions over a tidal cycle, the asymmetry and therefore the direction of migration of sand waves could reverse. He concluded that asymmetrical sand waves are representative of flow conditions for which there is inequal-

ity of flood and ebb tidal strengths. Separate localities for flood-dominated and ebb-dominated currents are a common observation in tidal areas (Van Veen, 1935; Klein, 1970). In areas of equal flood and ebb tidal currents, sand waves with symmetrical profiles are observed (Jones et al.,1965; Knight, 1972). Symmetrical sand waves usually have both slopes considerably less than the angle of repose of the sediment.

Sand waves with varying degrees of profile asymmetry, forming in trains or as solitary features, have been extensively studied around the British Isles (Cartwright and Stride, 1958; Stride and Tucker, 1960; Stride, 1963; Belderson and Stride, 1966; Kenyon and Stride, 1968, 1970). Dyer (1971) has described sand waves 16 m long and 1 to 2 m high forming in gravels and coarse sands near the Isle of Wight. Sand waves longer than 30 m and over 2 m high composed of fine sands have been observed by McCave (1971) in the North Sea.

Sand waves form in deep water on the continental shelf, with lengths ranging from 20 to 1000 m and heights of 1 to 2 m (Stride, 1963; Jordan, 1962). In shallower bays and estuaries, sand waves with lengths of 10 to 50 m and heights of 0.5 to 3 m are common (Salsman et al., 1966; Boothroyd and Hubbard, 1972). Besides having large size variations in areas of different depths, sand waves can show very large variations in length and height in a single area with uniform depth (Stride, 1970). Jordan (1962) points out that sand waves of

equal heights are found in deep and shallow water, suggesting that, in flow depths greater than those attainable in the laboratory, height of dunes and sand waves is independent of depth.

Sand waves formed in areas of strong current reversal show substantial modifications in their forms. These modifications are especially predominent in shallow esturaries (Klein,1970; Knight, 1972) and result in sand waves of either simple or complex form. Simple sand waves have large tabular foresets and have no dunes superimposed on them, whereas complex sand waves are composed of accreted sets of dunes. Complex sand waves are produced by interacting dunes which reverse direction with changes in the tidal cycle. These complex sand waves display internal laminations with the characteristic herringbone structure (Klein, 1970).

Dunes have been observed to change direction of migration over a tidal cycle (Knight, 1972), but larger sand waves do not completely change direction. A current reversal sometimes causes the sand-wave profile to become flat-topped or humpbacked (Van Veen, 1935; McCave, 1972). This occurs because sand transport reverses direction and starts to initiate a small slipface in the direction of the reversed current.

Sand waves can themselves be superimposed on large-scale features, such as linear sand ridges (Off, 1962), but usually they are the largest bed configuration present and have smaller bed configurations superimposed on them. Super-

position has been the basis for differentiating among the various bed configurations (ripples, dunes, and sand waves), since the differences in lengths are readily apparent and superimposed forms are thought to reflect different processes of formation. Besides this superposition, the three bed configurations represent three diferent geometrical size populations. McCave (1971), in observations of bed configurations in the North Sea, found that ripples have lengths less than 60 cm, whereas dunes have lengths between 60 cm and 30 m and sand waves have lengths greater than 30 m. In the Minas Basin of the Bay of Fundy, Klein (1970) found that ripples have lengths up to 50 cm, whereas dunes have lengths from 0.8 to 11.0 m and sand waves have lengths from 8 to 200 m. Boothroyd and Hubbard (1972) found different length characteristics for each bed configuration they described from the Parker River Estuary of Massachusetts, and these characteristic lengths are different from those described by McCave and Klein. It is thus apparent that, although lengths and heights can be used to distinguish different bed configurations within one geographic area, the variations in bed geometries with changing flow conditions make it impossible to transfer criteria from one area to another.

Dunes superimposed on sand waves are a common occurance in deep flows (McCave, 1971; Langhorne, 1973). Dunes are easily distinguished by their smaller size and three-dimensional geometry in comparison to the larger and long-

crested sand waves. Superimposed dunes exhibit two very different relationships to the sand waves.

First, dunes can be continuous across sand-wave crests and show a migration direction oblique to that of the sand waves (Langhorne, 1973). This implies that the association of dunes and sand waves is not an equilibrium association, with dunes being the active form on inactive sand waves. Superimposed dunes can mantle the slipface to produce a slope much smaller than the angle of repose. However, sand waves can still show movement, as dunes supply sediment to build the sand-wave slipfaces forward. The reason for the continued existence of the sand waves might be that there is a lag between change in bed configuration and change in flow conditions (Allen, 1973). In this case the dunes are the equilibrium form, but the pre-existing sand waves are effaced very slowly because of their enormous size. In marine environments flow conditions change fairly rapidly such as over a lunar tidal cycle, and there is not enough time for a current to wipe out the sand waves before flow conditions favorable to their formation occur again.

A second pattern of dune development occurs when dunes form just downstream of sand-wave slipfaces. The dunes become progressively larger up to the crest of the next sand wave downstream (McCave, 1971), where sediment is deposited to build the sand wave forward. McCave (1971) found dunes only on sand waves with crest heights greater than 5 m.

These observations indicate that dunes develop because of flow separation over the sand-wave crests, and that strong flow separation is required since only the highest sand waves can initiate dunes downstream. McCave (1971) suggested that the coexistence of the two configurations was due to perturbations in the bed-load transport (dunes) and the suspended-load transport (sand waves); this seems not to be of general applicability, however, because sand waves very commonly develop where there is only bed-load transport (Boothroyd and Hubbard, 1972).

In this second mode of development, dunes and sand waves are both active, as opposed to the first example, in which sand waves are the nonequilibrium, inactive bed configuration. Crests of large sand waves appear to be perturbing the flow so that dunes develop at velocities lower than those at which they normally form. This metastable development of dunes locally on the backs of sand waves is very similar to the excitation of ripples on a bed with zero sediment transport by the introduction of a large bed irregularity that produces flow separation. That dunes can be locally excited at velocities lower than those which characterize the dune phase is proved by the observation by Knight (1972). Ebb-oriented dunes form at the crest of a flood-oriented sand wave (Fig. 5.1). Accelerated flow over the sand-wave crest initiates dunes, but as the dunes migrate away from the crest their amplitude and length decrease

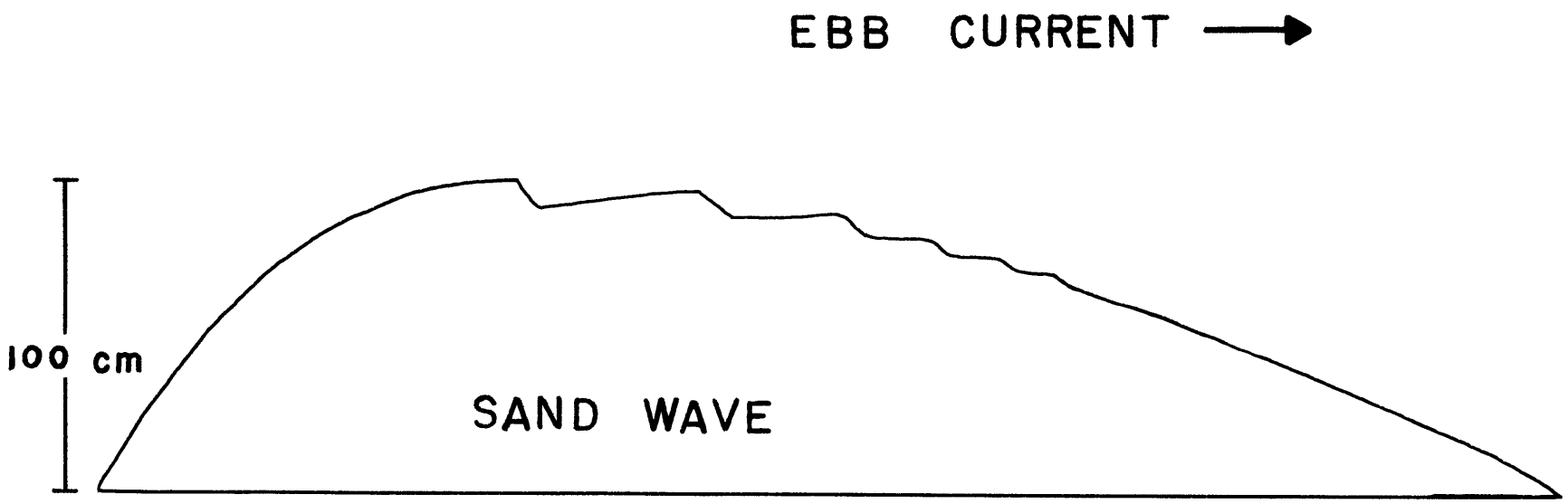

Fig. 5.1. Ebb-oriented dunes on a complex, flood-oriented sand wave from the Minas Basin (after Knight, 1972).

until they die out altogether. Therefore the presence of dunes on sand waves indicates either a nonequilibrium condition in which sand waves are being altered to dunes, or an equilibrium sand-wave state with dunes being a minor bed configuration that is developed only locally.

Comparison of Flume Experiments and Field Observations

Very few field studies have accurately measured flow characteristics, such as mean velocity and mean depth, in conjunction with observations of the bed configurations. One such study (Boothroyd and Hubbard, 1972) was conducted in the Parker River Estuary, Massachusetts. Three stations were manned through tidal cycles, and detailed measurements of velocity and depth were made at 15-minute intervals as divers observed changes in the geometry and migration of bed configurations. Boothroyd and Hubbard (1972) outlined a sequence of bed configurations which develop as mean velocity increases. The generalized sequence is:

RIPPLES → LINEAR DUNES → CUSPATE DUNES → PLANED-OFF DUNES
→ SAND WAVES

Boothroyd and Hubbard (1972) thought that dunes and sand waves developed from a similar straight-crested form with a length close to that of the dunes. They named the straight-crested forms linear dunes. They were inclined to accept sand waves as a completely different bed configuration that has no relation to the ripple and dune sequence. There-

fore sand waves were placed on a separate branch in the sequence. Nonetheless they recognized linear dunes to be very much like " dwarfed sand waves." Linear dunes seem in fact to be sand waves, and linear dunes are the initial form in regions where dunes develop. Where large sand waves form, they grow from these initial small sand waves (linear dunes). It is suggested that the actual sequence is:

RIPPLES → SAND WAVES → CUSPATE DUNES → PLANED-OFF DUNES

The sequence is then very similar to the sequence ripples→ bars → dunes observed in flume experiments.

Pratt (1971) conducted flume experiments on 0.49 mm sand with flow depths up to 46 cm. His data are plotted in a depth-velocity diagram in Fig. 5.2. The bar phase (his intermediate flattened dunes) is the stable phase over an increasingly greater range of velocities as depth increases. Since the range of velocities commonly observed in tidal environments is between 20 and 100 cm/sec, it would seem likely that bars should develop rather than dunes in deep flows.

To test the hypothesis that the experimental bars represent the same phase as the sand waves, the data of Boothroyd and Hubbard (1972) for sand sizes of 0.35 to 0.40 mm are also plotted in a depth-velocity diagram (Fig. 5.3.). The boundaries between ripples and bars and between bars and dunes extrapolated from Fig. 5.2 are drawn on Fig. 5.3. Points representative of no sediment movement plot in the

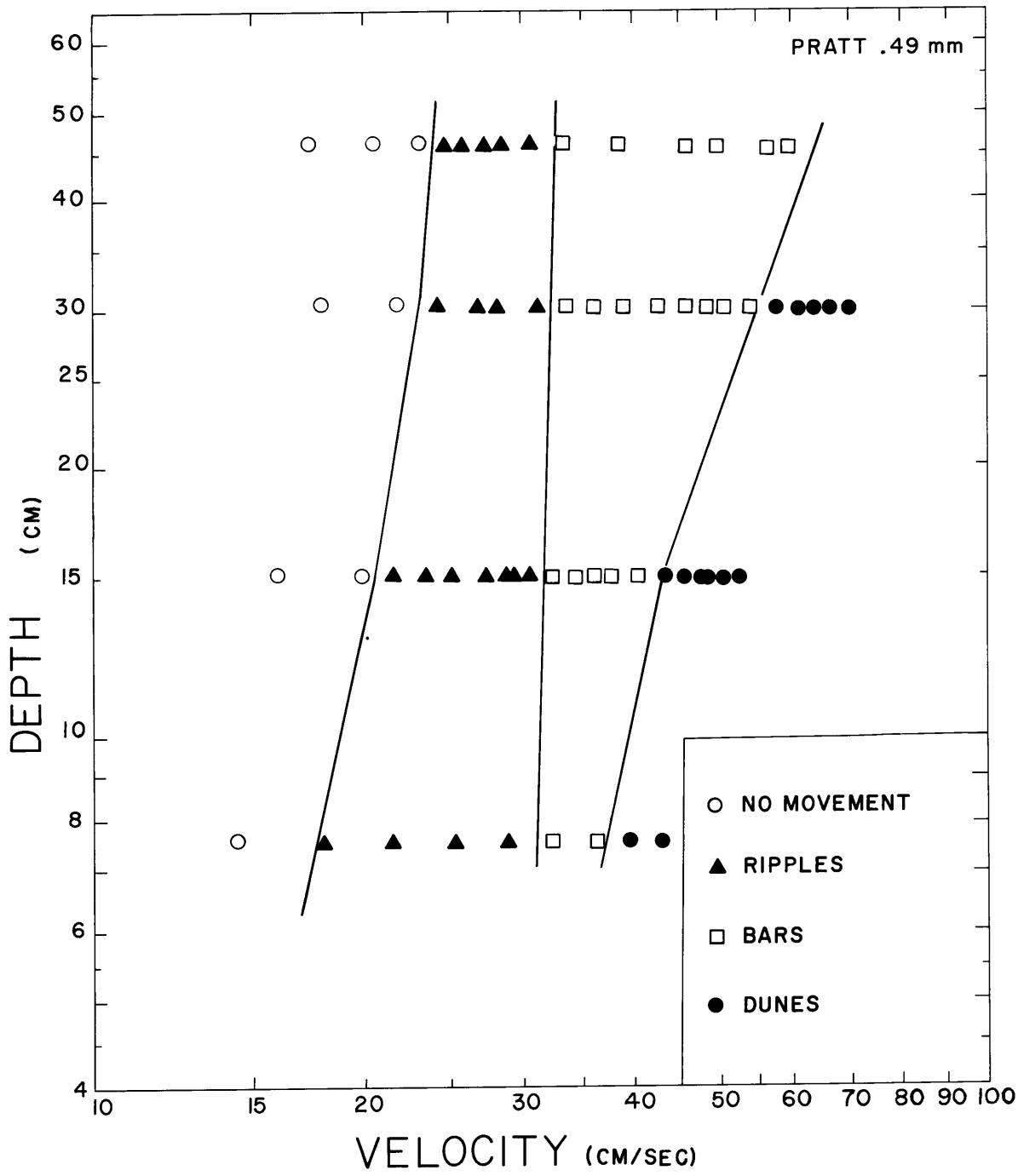

Fig. 5.2. Depth-velocity diagram for 0.49 mm sand.

Fig. 5.3. Depth-velocity diagram for the bed configurations in the Parker River Estuary (after Boothroyd and Hubbard, 1972).

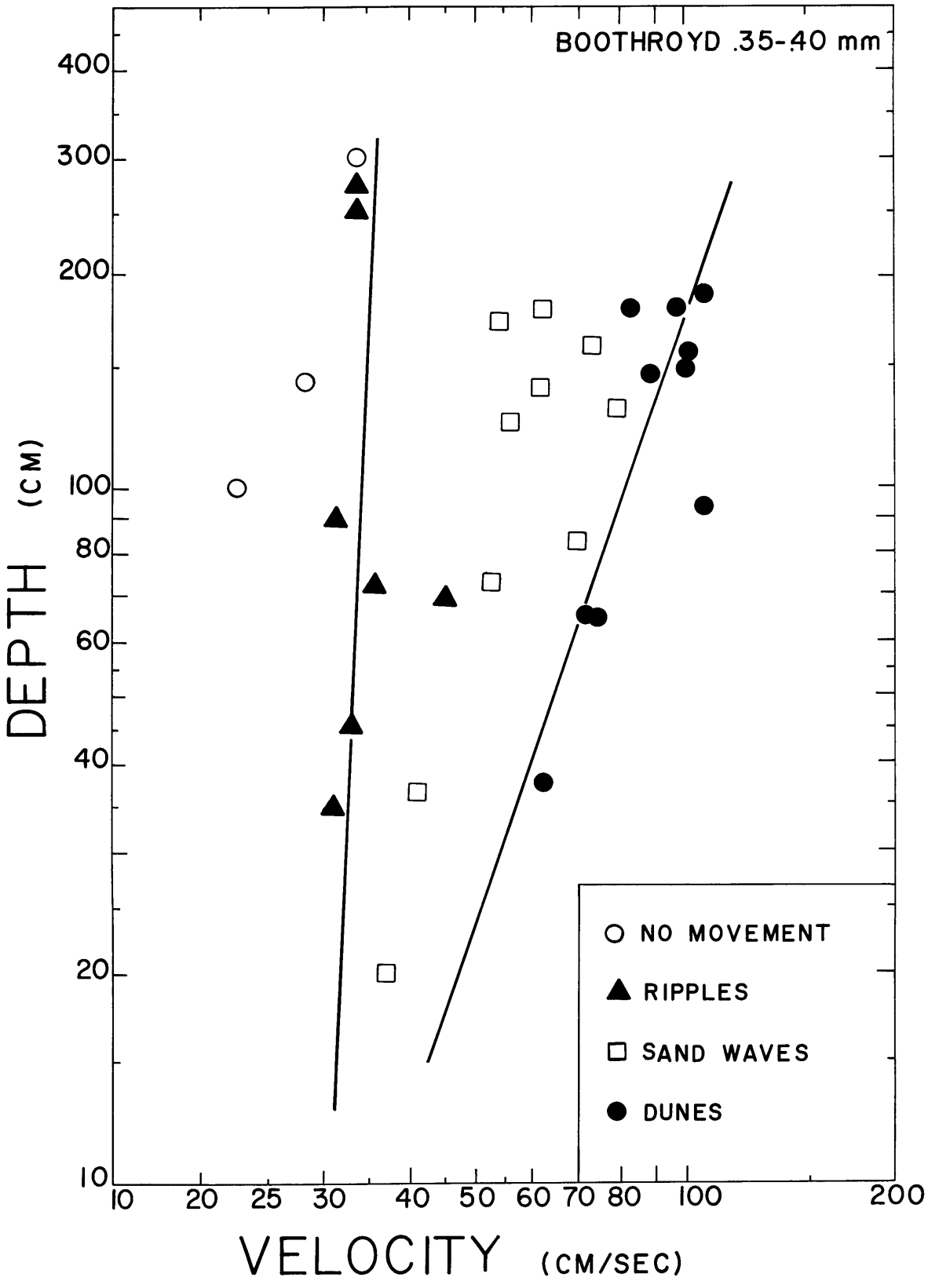

Fig. 5.3. Depth-velocity diagram for the bed configurations in the Parker River Estuary (after Boothroyd and Hubbard, 1972).

ripple field, but this is probably a consequence of the divers' inability to make detailed observations very close to the bed and to be able to see sediment grains moving. The observed ripples were superimposed on sand waves, and as a consequence they are seen to plot in the bar field as well as in the ripple field. Sand waves plot in the middle of the bar field, suggesting that sand waves are indeed large bars. The position of dunes in the graph also agrees fairly well with the predicted phase field.

Considering the slightly different sand size and the substantially different sorting of the estuarine sands, agreement between field and flume data is very good.

Discussion

The flow system studied by Boothroyd and Hubbard (1972) is a simple one compared to other estuaries such as that studied by Klein (1970). Flow in the Parker River Estuary is marked by strong asymmetries in flow: some areas are ebb-dominated, others are flood-dominated. These strong ebb or flood flows are unsteady but almost unidirectional, and therefore to a great extent compareable to unidirectional flume experiments. However, flume runs are steady flows and so it is important to gauge the effect of the time variation in tidal flows.

Changes in depth and velocity with time can be recorded as a continuous curve on a depth-velocity diagram. For a flood

tidal cycle, the initial depth would be small and the velocity zero. As the flood tide proceeds velocity and depth increase until by the end of the flood cycle the velocity is again zero but the depth is large. Such a curve of velocity and depth is plotted in Fig. 5.4 for a generalized,typical tidal cycle. It is apparent that velocity increases rapidly at first and then remains fairly uniform for most of the tidal cycle. Also indicated in Fig. 5.4 are the bed phase fields which are related primarily to flow velocity. Therefore, although depth varies, velocity remains within one phase field for the greater part of the tidal cycle. This rapid change followed by leveling off of velocity indicates that at the peak flow of the tidal cycle, when bed configurations are initiated, the flow can be described as quasi-steady. Changes in flow velocity should not then alter the initiation of bed configurations.

In flows characterized by strong reversals of current, there can be substantial modifications of the bed configurations. The resulting complexity of form can confuse the interpretation. There are almost no hydraulic data on areas with complex, modified bed configurations. A small number of data in the region of a complex sand wave in the Minas Basin have been obtained (Knight, personal communication). Velocity profiles and depths were recorded at fifteen-minute intervals over a large flood-oriented sand wave through flood and ebb tidal cycles. These data are

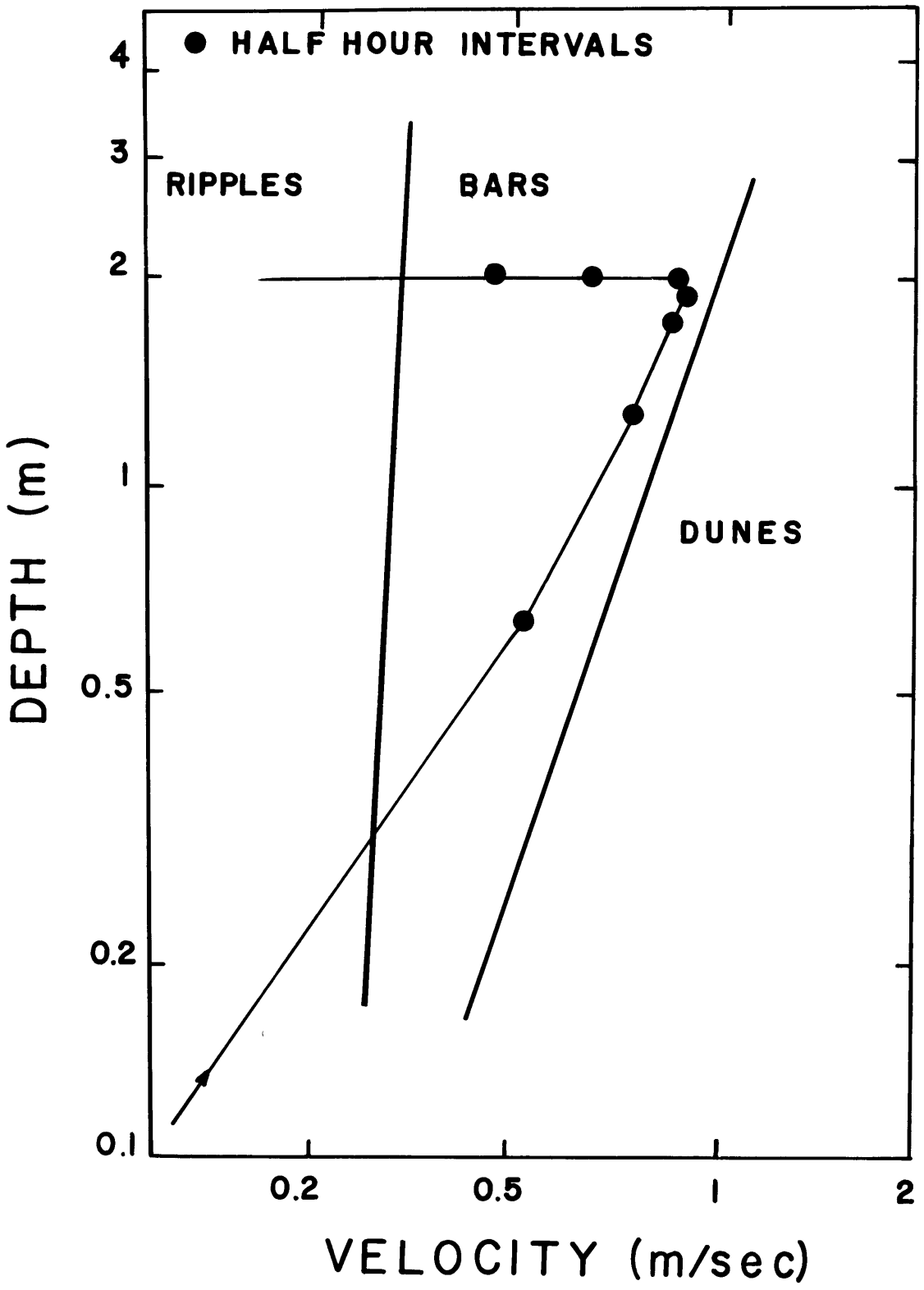

Fig. 5.4. Hypothetical time pathline of depth and velocity through a flood tide.

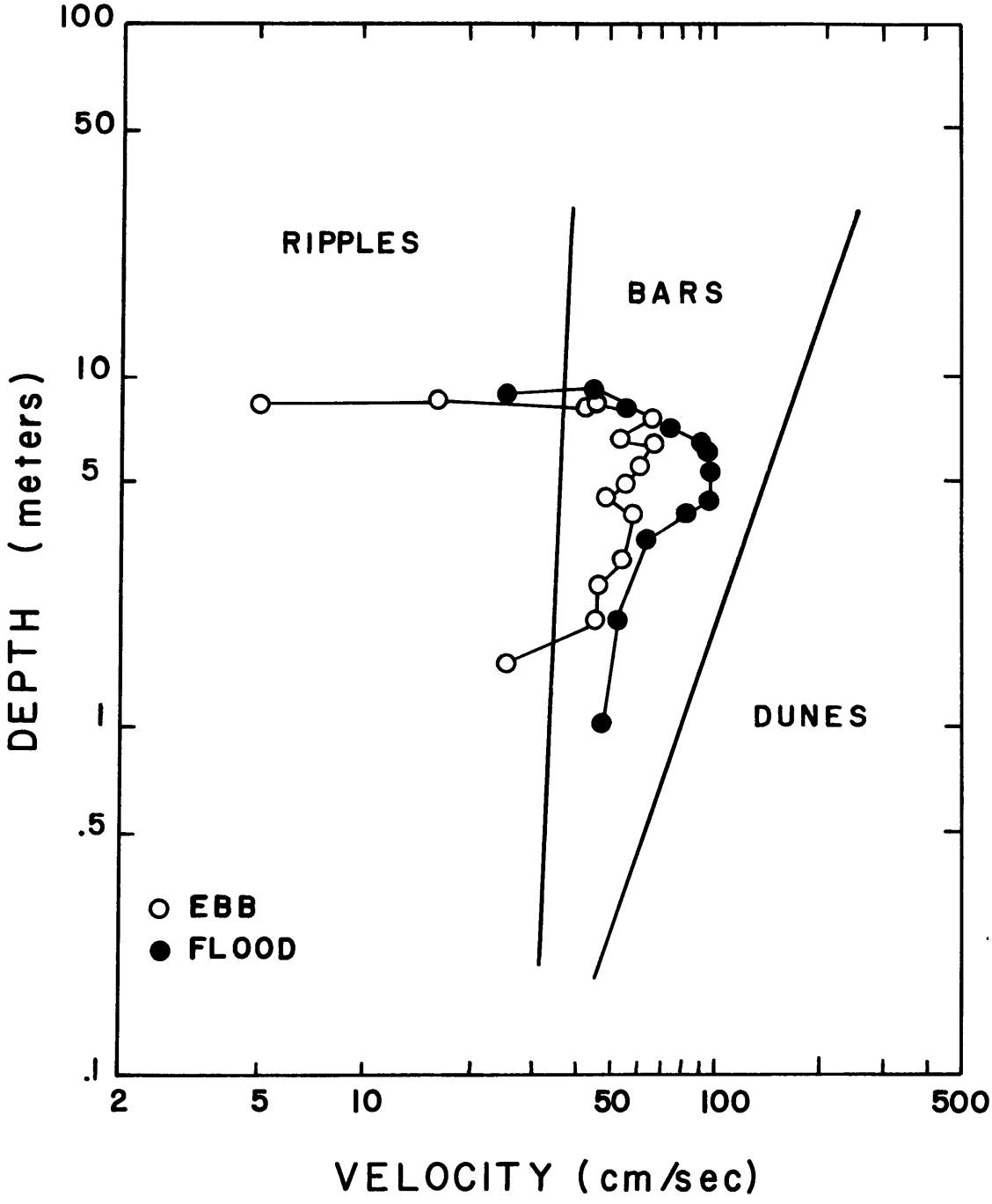

Fig. 5.5. Time history of depth and velocity over ebb and flood tides in the Minas Basin.

presented in Fig. 5.5. Sand size in the sand wave was slightly finer than 0.40 mm. Again the time history of the velocity indicates that for a major part of the time, through the ebb and flood cycle, the velocities remain characteristic of the bar phase. The flood and ebb velocities are not symmetrical; flood velocities are up to thirty percent higher. This flood dominance results in the observed flood orientation of the sand wave.

Dunes form on the sand wave during both ebb and flood currents, and the internal structure of the sand wave displays complex interfingering of dune-produced cross-stratification. The velocities remain characteristic of the bar phase throughout the ebb and flood tides, and therefore the dune phase should not be the equilibrium phase. However, it is in this area that Knight (1972) described ebb-oriented dunes that are formed just downstream of the large crests of the flood-oriented sand waves. It would then seem highly likely that the dunes are a metastable, secondary form superimposed on, and initiated by, the large sand waves.

Fig. 5.3 suggests once more that experimental bars and sand waves are the same bed phase. In physical characteristics, bars and sand waves are very similar. Both have straight crests, and both can have quite variable heights and lengths or quite regular heights and lengths. Also, sand waves overtake one another, as bars do. The

main difference between the two bed configurations is size. In experimental flumes the shallow depths do not allow bars or dunes to become very large. Once they start to grow in height, the flow is contracted and accelerated over them, resulting in high shear at their crests. A balance between erosion at the crest and resupply of sediment to the crest seems to determine bar or dune height.

In very deep flows a bar must grow to become a substantial percentage of the depth before the flow is accelerated over it to produce high shear at the crest. If a small bar is initiated in a deep flow, it grows by merging with other faster bars and ripples that overtake it, as kinematic wave theory predicts. This growth process is independent of flow depth and depends on the frequency of merging events, and perhaps also the angle of the stoss slope, since too high a local flow acceleration up the stoss slope will cause erosion at the crest. Therefore a small bar should be able to grow continuously in size up to the size of sand waves.

TRANSVERSE BARS IN RIVERS

Flow in rivers is unidirectional, as in flume experiments, and the ripples and dunes that form in flumes are commonly observed in rivers. However, river flow is subject to very large changes in discharge throughout the year.

The changes can represent a month-long flood or a spring runoff lasting several months.

Transverse bars have been described in both large rivers, such as the Mississippi (Carey and Keller, 1957) and the Bramaputra (Coleman, 1969), and in small rivers, such as the Klarälven (Sundborg, 1956). Lengths of transverse bars are typically 200 m, and heights are 2 to 6 m. However, Coleman (1969) described very large transverse bars in the Bramaputra with lengths of 1000 m and heights of 17 m. The grain size of the sediment composing transverse bars can range from fine sand (0.17 mm) in the Bramaputra to coarse sand (1.0 mm) in the Red Deer River (Neill, 1969).

Crests of transverse bars are long and straight, usually extending across most of the width of the river (Jordan, 1962; Coleman, 1969). At low flow stages, transverse bars can have a lobed shape, with the lobe extending downstream in regions of greatest depth (Collinson, 1970; Smith, 1971). At this low stage, transverse bars are observed as large solitary features (Collinson, 1970), but at higher stages they can be present as trains or fields (Jordan, 1962; Coleman, 1969).

Coleman (1969) measured transverse bars with the same heights in depths of 3 m and 14 m. This again indicates that bed configurations formed in natural deep flows seem not to have the depth dependence shown by bed configurations

formed in small depths.

As was the case for marine sand waves, smaller bed configurations such as ripples and dunes are superimposed on fluvial transverse bars. Ripples are ubiquitous on larger dunes and transverse bars. Collinson (1970) and Smith (1971) also observed dunes on transverse bars but suggested that this was a nonequilibrium occurrence, with dunes modifying the large transverse bars at a low flow stage. Coleman (1969) recognized four separate bed configurations in the Bramaputra, the two smallest being ripples and dunes as described here. The two larger bed configurations were straight-crested transverse bars, probably occurring in two different sizes. These transverse bars usually had no smaller features superimposed on them except at low flow stages, when dunes formed on the transverse bars in shallow water.

The characteristics of fluvial transverse bars are identical to those of the marine sand waves. Both form in deep flows and are very long and high in comparison to ripples and dunes. Also, both features have very long, straight crests, and where they occur in trains or fields their spacing can be irregular. Transverse bars and sand waves represent the same process actually operating in rivers and in the ocean.

Comparison of Experimental Bars and Transverse Bars

There is very little detailed information on velocity, depth, and grain size associated with development of transverse bars. However, most descriptions of bars in natural environments are in agreement on a number of important points. Transverse bars form at high discharges in rivers, usually during floods or spring runoff (Pretious and Blench, 1951; Whetten and Fullam, 1967; Neil, 1969; Coleman, 1969; U.S. Army Corps of Engineers, 1969; Collinson, 1970; Smith, 1971). In these periods of high discharge the percentage increases in depth are greater than those in velocity. Neill (1969) reports that velocities double, whereas the depths triple in magnitude. This greater percentage increase in depth than velocity is a general observation and is reflected in the Manning equation.

Pretious and Blench (1951) recorded the change in size of bed configurations through a month-long flood cycle in which the discharge first increased and then subsided. Allen (1973) has plotted bed-form length versus discharge from the data of Pretious and Blench. As discharge and depth increase, the initial dunes (up to 7 m long) start to coalesce to form progressively larger forms, so that at peak discharges transverse bars up to 20 or 30 m long form. As discharge and depth decrease, dunes form on top of the transverse bars. As Allen (1973)

points out, these data clearly show a hysteresis effect, in that changes in size of bed forms lag behind changes in discharge. Thus, although the flow conditions favor dune development it takes some time for the dunes to erode the transverse bars and become the only bed configuration. Neill (1969) observed the change from smaller dunes to large transverse bars with increases in discharge. He also observed the coalescing of dunes to form bars, as did Smith (1971).

Changes from dunes to transverse bars can be visualized qualitatively in a depth-velocity diagram (Fig. 5.6). Depths and velocities at low discharges are characteristic of the dune phase. As the discharge increases, velocity and depth increase. However, velocity does not increase as fast as depth, and so the flow conditions become those characteristic of the bar phase, and dunes start to slow down and coalesce to form bars. As the discharge decreases, velocity and depth decrease, but the bars are slow in reverting to dunes because there is a lag in modification of the bed configuration. This qualitative hypothesis cannot presently be tested against actual field data. Data on bed configurations in rivers are available only for those rivers with fine sand beds. But the bed phase diagrams with which to compare the river data are worked out only for coarse sands. However, it seems most likely that the depth-velocity diagrams for fine sands will be similar to

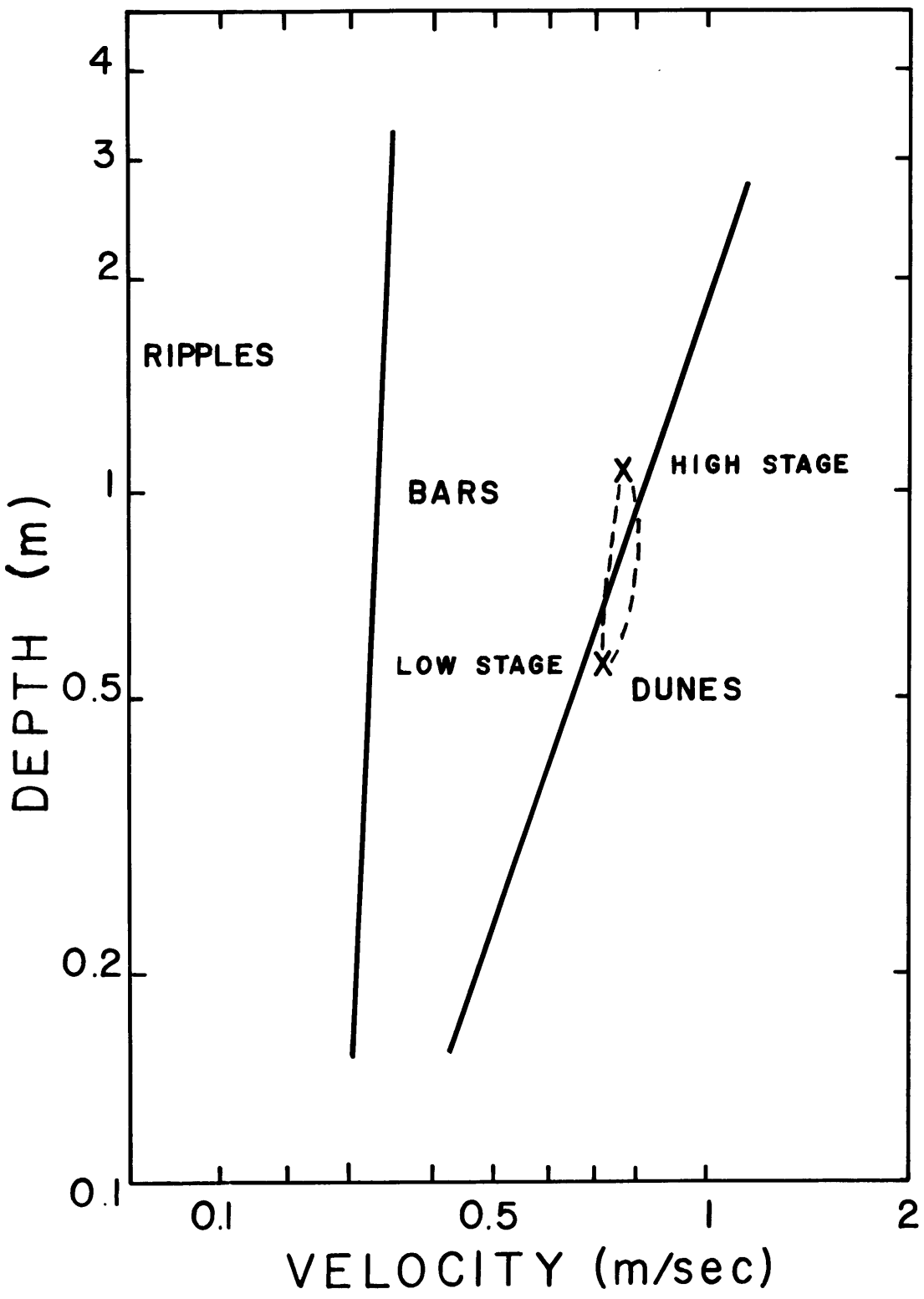

Fig. 5.6. Idealized time history of depth and velocity through a river flood cycle.

that for the 0.49 mm sand (Fig. 5.2), and so the qualitative hypothesis outlined above should prove correct.

CONCLUSIONS

In rivers and oceans, ripples and dunes are observed along with large-scale bars. The large bars are straight crested, two-dimensional forms with very little scour downstream of their slipfaces. The large bars migrate in trains that do not always display regular spacing and are observed to overtake one another. Bars even within one train can have a very wide range of heights as well as lengths. These geometrical properties are the same as are observed for the smaller experimental bars. The small flow depths at which the experimental bars are formed constrain the bars to be very low.

Measurements of the flow parameters characteristic of large bars in an estuary suggest that natural bars occupy the same phase stability field as do experimental bars. No such comparative data exist for the large bars developed in rivers, but general observations suggest that these bars form at high discharges and depths, for which the bar phase field is predominant. Ripples and dunes observed in rivers and the ocean are geometrically similar to those found in flumes, and the flow conditions match those of the ripple and dune phases.

The similarities in form and behavior and the matching

flow conditions strongly suggest that sand waves and transverse bars are identical features and are genetically the same as the experimentally produced bars. Sand waves and transverse bars are therefore large-scale members of the bar phase.

6. SUMMARY OF CONCLUSIONS

Seven different bed phases have been delineated in this study on the basis of the effect the bed configurations have on the flow (changes in bed friction factor and energy slope), and the geometries and kinematics of the bed configurations. In addition to bed phases that have been previously described, a new bar bed phase is defined and three separate ripple phases are described (Southard and Boguchwal, 1973).

The no-movement, bar and dune bed phases have continuous stability fields throughout the range of grain sizes studied (0.51 to 1.14 mm),whereas the ripple phases and the flat-bed phase interfinger and die out. The flat-bed phase dies out for sand sizes finer than 0.55 mm. The ripple phase ceases to exist at sand sizes coarser than 0.60 mm,while the metastable ripple phases, no movement (metastable ripples) and flat bed (metastable ripples), exist up to sizes of 0.70 mm. However, ripples exist as minor forms on the upstream slopes of bars and dunes for sand sizes coarser than 1.0 mm.

Ripples develop from small pilings of grains on a sediment bed that are constructed by the interaction of eddies in the turbulent boundary layer, and the bed surface. The eddies impinge on the bed and erode a linear patch of sediment. The eroded sediment is constructed into a

small ridge one to two grain diameters high. The flow separates over the small ridges in a hummocky bed topography and causes grains to be trapped at the ridges and build them up so that eventually small slipfaces form. The reattaching flow striking the bed downstream has a high turbulence intensity which sets up a weak average sediment transport rate. Eroded grains are transported a short distance downstream until the turbulence dies out and they can no longer be supported by the flow (q_s has a maximum). Grains are then deposited to form a new mound which in turn becomes a ripple and the process starts over once again.

Ripples can develop on a bed where there are no flow-constructed bed irregularities that can cause separation. If an irregularity is imposed on the bed by chance, ripples develop downstream of the imposed irregularity. Therefore, ripples can be excited in flow conditions that would not normally initiate them. This is observed for the no movement (metastable ripple) phase, the flat bed (metastable ripple) phase and for ripples developed on bars and dunes.

Dunes are also initiated by development of a maximum in q_s downstream from flow separation over an obstacle. However,in this case a large bar crest is needed to provide strong flow acceleration prior to separation. The accelerated flow that reattaches to the bed surface

causes the boundary shear stress to overshoot its equilibrium value and so a maximum in shear stress is developed. It is hypothesized that this shear-stress maximum gives rise to a maximum in q_s which in turn causes a mound of sediment to form at approximately 15 to 25 step heights downstream of the upstream bar crest. The initiation of a shear stress maximum only happens in strongly accelerated, separated flows over bed irregularities large in comparison to flow depth. This process does not take place for the flow separation over small bed irregularities that cause ripples to develop.

Bars form once there is general grain motion uniformly distributed over the bed surface. Bars form spontaneously and randomly in a manner predicted by the conservation-of-sediment equation, and they represent kinematic shock waves which initially attenuate as they migrate downstream. Attenuation is balanced by the merging of bars of different sizes and migration rates. When the bars become well developed, ripples form on their stoss slopes and transport sediment to the bar crests to balance attenuation. Bars do not have their lengths controlled as do ripples and dunes, which can be considered as coupled kinematic shock waves.

The sequence ripples → bars → dunes described from flume observations is found in natural environments.

Ripples and dunes formed in rivers and in the ocean are very similar to those developed in the flumes. The experimental bars have their analog in the very large transverse bars found in rivers and sand waves found in the ocean. Transverse bars and sand waves are identical bed configurations that can be substantially modified by unsteady and reversing flows. These large natural bars have many of the geometrical properties and movement characteristics demonstrated by the experimental bars. The sizes of the two features are very different, but this is due to the depth dependence of the bars in shallow flume experiments. Experimental bars have the freedom to grow in size in deeper flows. Lastly, the large natural bars occupy the bar phase stability field. Experimental bars and the natural bars are therefore the same type of bed configuration.

The identification of the separate bar phase is important for two reasons. First, the recognition of the bars and their mechanics has provided the initial bed perturbation from which dunes grow. Second, the new bar phase explains the presence of the well known but little understood transverse bars and sand waves observed with ripples and dunes. Therefore, bars are the missing step needed to explain dunes and to complete the sequence of observed bed configurations.

REFERENCES

Abbott, D.E., and Kline, S.J., 1962, Experimental investigation of subsonic turbulent flow over single and double backward facing steps: J. Basic Eng. Trans. A.S.M.E., 84, 317-325.

Albertson, M.L., Simons, D.B., and Richardson, E.V., 1958, Discussion of "Mechanics of sediment-ripple formation" by H.K. Liu: Am. Soc. Civil Engineers Proc., J. Hydraulics Div., 84, 1558-23-1558-32.

Allen, J.R.L., 1968, Current ripples; their relation to patterns of water and sediment motion: North Holland Publ. Co., Amsterdam.

Allen, J.R.L., 1973, Phase differences between bed configuration and flow in natural environments, and their geological relevance: Sedimentology, 20, 323-329.

American Society of Civil Engineers, Task Force on Bed Forms in Alluvial Channels, 1966b, Nomenclature for bed forms in alluvial channels: Am. Soc. Civil Engineers Proc., J. Hydraulics Div., 92, 51-64.

Anderson, A.G., 1953, The characteristics of sediment waves formed by flow in open channels: Proc. Third Mid-Western Conf. on Fluid Mech., Univ. of Minnesota, 379-395.

Antonia, R.A., and Luxton, R.E., 1972, The response of a turbulent boundary layer to a step change in surface roughness. Part 2. Rough-to-smooth: J. Fluid Mech., 53, 737-757.

Ashida, K., and Tanaka, Y., 1967, A statistical study of sand waves: Proc. 12th Congress I.A.H.R., 2, 103-110.

Bagnold, R.A., 1956, The flow of cohesionless grains in fluids: Trans. Royal Soc., London, 249, 235-297.

Belderson, R.H., and Stride, A.H., 1966, Tidal current fashioning of a basal bed: Mar. Geol., 4, 237-257.

Blench, T., 1969, Coordination in mobile-bed hydraulics: Am. Soc. Civil Engineers Proc., J. Hydraulics Div., 95, 1871-1898.

Bogardi, J., 1959, Hydraulic similarity of river models with moveable bed: Acad. Sci. Hung. Acta Tech., 24, 417-445.

Bonnefille, R., 1965, Etude d'un critere de debut d'apparition des dunes et des rides fluviales: Bull. Cent. Rech. Ess. Chatou, 11, 17-22.

Boothroyd, J.C., and Hubbard, K.D., 1972, Bed form development and distribution pattern, Parker and Essex Estuaries, Mass.: Final Rept. DACW-72-70-C-0029, C.E.R.C.

Bradshaw, P., and Wong, F.Y.F., 1972, The reattachment and relaxation of a turbulent shear layer: J. Fluid Mech., 52, 113-135.

Brooks, N.H., 1958, Mechanics of streams with moveable beds of fine sand: Am. Soc. Civil Engineers Trans., 123, 526-549.

Carey, W.C., and Keller, M.D., 1957, Systematic changes in the beds of alluvial rivers: Am. Soc. Civil Engineers Proc., J. Hydraulics Div., 83, 1331-1-1331-24.

Cartwright, D.E., and Stride, A.H., 1958, Large sand waves near the edge of the continental shelf: Nature, 181, 41.

Chabert, J., and Chauvin, J.L., 1963, Formation des dunes et des rides dans les modeles fluviaux: Bull. Cent. Rech. Ess. Chatou, 4, 31-51.

Coleman, J.M., 1969, Brahmaputra River; Channel processes and sedimentation: Sed. Geology, 3, 129-239.

Collinson, J.D., 1970, Bedforms of the Tana River, Norway: Geograf. Ann., 52A, 31-56.

Corino, E.R., and Brodkey, R.S., 1969, A visual investigation of the wall region in turbulent flow: J. Fluid Mech., 37, 1-30.

Costello, W.R., and Southard, J.B., 1971, Development of a bed of coarse sand under unidirectional flow: Abstract: Annual Meeting Geol. Soc. Am., Washington, D.C., Nov. 1-3.

Deacon, G.F., 1892, Proc. Inst. Civil Engineering, 118, 93.

Dyer, K.R., 1971, The distribution and movement of sediment in the Solent, Southern England: Marine Geology, 11, 175-187.

Engelund, F., and Hansen, E., 1966, Investigations of flow in alluvial streams: Acta Polytech. Scand., Civil Eng. Bldg. Constr. Ser., 35.

Exner, F.M., 1920, Zur Physik der dünen: Akad. Wiss. Wien, Sitzungsber., Mathem.-Naturw. Kl., Abt. IIa, Bd. 129, H. 1, 929-952.

Exner, F.M., 1925, Uber die Wechselwirkung zwischen Wasser und Greschieke in Flüssen: Akad. Wiss. Wien, Sitzungsker., Mathem.-Naturw. Kl., Abt. IIa, Bd. 134, H-3-4, 166-204.

Garde, R.J., and Albertson, M.L., 1961, Bed load transport in alluvial channels: La Houille Blanche, 16, 274-281.

Garde, R.J., and Ranga Ruju, K.G., 1963, Regime criteria for alluvial streams: Am. Soc. Civil Engineers Proc., J. Hydraulics Div., 89, 153-164.

Gilbert, G.K., 1914, Transportation of debris by running water: U.S. Geol. Surv. Prof. Paper 86.

Gradowczyk, M.H. 1968, Wave propagation and boundary instability in erodible-bed channels: J. Fluid Mech., 33, 93-112.

Grass, A.J., 1971, Structural features of turbulent flow over smooth and rough boundaries: J. Fluid Mech. 50, 233-255.

Guy, H.P., Simons, D.B., and Richardson, E.V., 1966, Summary of alluvial channel data from flume experiments, 1956-61: U.S. Geol. Surv. Prof. Paper 462-I.

Harms, J.C., 1969, Hydraulic significance of some sand ripples: Geol. Soc. Am. Bull., 80, 363-390.

Hayashi, T., 1970, Formation of dunes and antidunes in open channels: Am. Soc. Civil Engineers Proc., J. Hydraulics Div., 96, 357-366.

Hino, M., 1968, Equilibrium-range spectra of sand waves formed by flowing water: J. Fluid Mech. 34, 565-573.

Inglis, C.C., 1949, The behaviour and controls of rivers and canals: Res. Publ. 13, Part II, Central Water Power, Irrigation and Navigation Research Station, Poona, India.

Johnson, J.W., 1942, The importance of side-wall friction in bed-load investigations: Civil Eng. 12, 329-331.

Jones, N.C., Kain, J.M., and Stride, A.H., 1963, The movement of sand waves on Warts Bank, Isle of Man: Marine Geol. 3, 329-336.

Jordan, G.F., 1962, Large submarine sand waves: Science, 136, 839-843.

Kennedy, J.F., 1963, The mechanics of dunes and antidunes in erodible-bed channels: J. Fluid Mech., 16, 521-544.

Kenyon, N.H., and Stride, A.H., 1968, The crest length and sinuosity of some marine sand waves: J. Sed. Petrology, 38, 255-259.

Kenyon, N.H., and Stride, A.H., 1970, The tide-swept continental shelf sediments between the Shetland Isles and France: Sedimentology, 14, 159-173.

Kim, H.T., Kline, S.J., and Reynolds, W.C., 1971, The production of turbulence near a smooth wall in a turbulent boundary layer: J. Fluid Mech. 50, 133-160.

Klein, G.D., 1970, Depositional and dispersal dynamics of intertidal sand bars: J. Sed. Petrology, 40, 1095-1127.

Kline, S.J., Reynolds, W.C., Shraub, F.A., and Runstadler, P.W., 1967, The structure of turbulent boundary layers: J. Fluid Mech., 30,

Knight, R.J., 1972, Cobequid Bay Sedimentology Project: A progress report: Maritime Sed. 8, 45-60.

Langhorne, D.N., 1973, A sandwave field in the Outer Thames Estuary, Great Britain: Marine Geol., 14, 129-144.

Larras, J., 1963, Passage des rides aux dunes dans les ecoulements uniformes sur fond mobiles: Acad. Sci. (Paris), Comptes Rendus, 257, 3818-3820.

Lighthill, M.J., and Whitham, G.B., 1955, On kinematic waves. I. Flood movement in long rivers: Proc. Royal Soc., A229, 281-316.

Liu, H.K., 1957, Mechanics of sediment-ripple formation: Am. Soc. Civil Engineers Proc., J. Hydraulic Div., 83,

Makita, H., 1968, M. Eng. Thesis, University of Tokyo, Japan.

McCave, I.N., 1971, Sand waves in the North Sea off the coast of Holland: Marine Geol., 10, 199-225.

Menard, H.W., 1950, Sediment movement in relation to current velocity: J. Sed. Petrology, 20, 148-160.

Mueller, T.J., and Robertson, J.M., 1962, A Study of the mean motion and turbulence downstream of a roughness element: Proc. of the First Southeastern Conference on Theoretical and Applied Mathematics, Gatlinburg, Tenn., May 3-4.

Neill, C.R., 1969, Bed forms in the Lower Red Deer River, Alberta: J. Hydrology, 7, 58-85.

Nordin, C.F., and Algert, J.H., 1966, Spectral analysis of sand waves: Am Soc. Civil Engineers Proc., J. Hydraulics Div., 92, 95-114.

Off, T., 1963, Rhythmic linear sand bodies caused by tidal currents: Bull. Amer. Assoc. Petroleum Geol., 47, 324-341.

Polya, G., 1937, Concerning the kinematics of bed load transport - Zur kinematik der Geschiebebewegung: Verlag Rascher and Co., Zurich.

Pratt, C.J., 1971, An experimental investigation into the flow of water and the movement of bed material in alluvial channels: Unpublished Ph.D. Thesis, Univ. of Southampton, England.

Pretious, E.S., and Blench, T., 1951, Final report on special observations of bed movement in Lower Fraser River at Badner Reach during 1950 Freshet: Nat. Res. Council Canada, Fraser River Model, Vancouver, Canada.

Rajaratnam, N., and Subramanya, K., 1968, Plane turbulent reattached wall jets: Am. Soc. Civil Engineers Proc., J. Hydraulics Div., 94, 95-111.

Rathbun, R.E., and Guy, H.P., 1967, Measurement of hydraulic and sediment transport variables in a small recirculating flume: Water Resources Research, 3, 107-122.

Raudkivi, A.J., 1963, Study of sediment ripple formation: Am. Soc. Civil Engineers Proc., J. Hydraulics Div., 89, 15-

Reynolds, A.J., 1965, Waves on the erodible bed of an open channel: J. Fluid Mech., 22, 112-

Salsman, G.G., Tolbert, W.H., and Villars, R.G., 1966, Sand ridge migration in St. Andrew Bay, Florida: Marine Geol., 4, 11-19.

Simons, D.B., and Richardson, E.V., 1962, Resistance to flow in alluvial channels: Am. Soc. Civil Engineers Trans., 127, Part I, 927-954.

Simons, D.B., and Richardson, E.V., 1963, Forms of bed roughness in alluvial channels: Am. Soc. Civil Engineers Trans., 128, Part I, 284-302.

Smith, J.D., 1969, Investigations of turbulent boundary layer and sediment transport phenomena as related to shallow marine environments: Report No. A69:7, Dept. Oceanography, Univ. of Washington.

Smith, J.D., 1970, Stability of a sand bed subjected to a shear flow of low Froude Number: J. Geophys. Research, 75, 5928-5939.

Smith, N.D., 1971, Transverse bars and braiding in the Lower Platte River, Nebraska: Geol. Soc. Amer. Bull., 82, 3407-3420.

Sorby, H.C., 1853, On the oscillation of the current drifting sandstone beds of the southeast of Northumberland, and on their general direction in the coal field in the neighborhood of Edinburgh: Repts. Proc. Geol. Polytechnic Soc. of the West Riding of Yorkshire, 225-231.

Sorby, H.C., 1859, On the structures produced by the currents present during the deposition of stratified rocks: Geologist, 2, 137-147.

Southard, J.B., 1970, Grain movement and bed form on flat sand beds near threshold of transport: Annual Meeting, Amer. Geophys. Union, Washington, D.C., April 20-24.

Southard, J.B., 1971, Representation of bed configurations in depth-velocity-size diagrams: J. Sed. Petrology, 41, 903-915.

Southard, J.B., and Dingler, J.R., 1971, Flume study of ripple propagation behind mounds on flat sand beds: Sedimentology, 16, 257-263.

Southard, J.B., and Boguchwal, L.A., 1973, Flume experiments on the transition from ripples to lower flat bed with increasing grain size: J. Sed. Petrology, (in press, 43).

Squarer, D., 1970, Friction factors and bed form in fluvial channels: Am. Soc. Civil Engineers Proc., J. Hydraulics Div., 88, 77-107.

Stride, A.H., and Tucker, M.J., 1960, Internal waves and waves of sand: Nature, 188, 933.

Stride, A.H., 1963, Current swept sea floors near the southern half of the British Isles: Quart. J. Geol. Soc. London, 119, 175-199.

Stride, A.H., 1970, Shape and size trands for sand waves in a depositional zone of the North Sea: Geol. Mag., 469-477.

Sundborg, A., 1956, The River Klarälven: A study in fluvial processes: Geograf. Ann. 38, 127-316.

Sutherland, A.J., 1967, Proposed mechanism for sediment entrainment by turbulent flows: J. Geophys. Research, 72, 6183-6194.

Swift, D.J.P., Cook, A.E., and Lyall, A.K., 1966, A sub-tidal sandbody in the Minas Channel, Eastern Bay of Fundy: Maritime Sed., 2, 175-179.

Tani, I., 1957, Experimental investigation of flow separation over a step: I.U.T.A.M. Proc., Bound. Layer Research Sympos., Freiburg, 377-386.

Tani, I., 1968, Proc. Computation of Turbulent Boundary Layers, AFOSR-IFP-Stanford University.

U.S. Army Corps of Engineers, 1969, Missouri River Channel Regime Studies: U.S. Army Corps Eng., Missouri River Div., Sediment Ser. No. 13B.

Vanoni, V.A., and Brooks, N.H., 1957, Laboratory studies of the roughness and suspended load of alluvial streams: California Inst. Technol., Sedimentation Lab., M.R.D. Sediment Ser. No. 11.

Vanoni, V.A., 1964, Measurements of critical shear stress for entraining fine sediments in a boundary layer: California Inst. Technol., W.M. Keck Lab. Hydraulics and Water Resources, Rept. KH-R-7.

Van Straaten, L.M.J.U., 1953, Megaripples in the Dutch Wadden Sea and in the basin of Arcachon (France): Geol. en Mijnb, 15, 1-11.

Van Veen, J., 1935, Sand waves in the North Sea: Int. Hydrographic Rev., 12, 21-29.

Velikanov, M.A., and Mikhailova, N.A., 1950, The effect of large-scale turbulence on pulsations of suspended sediment concentration: Izvestiya, Akad. Nauk. SSSR, seriya geograficheskaya i geofizicheskaya, 4, 421-424.

Velikanov, M.A., 1958, Alluvial process (fundamental principles): State Publ. House for Physical and Math. Literature, Moscow.

Walker, G.R., 1961, A study of the two-dimensional flow of turbulent fluid past a step: Unpublished M.Eng. Thesis, U. of Auckland, Auckland, New Zealand.

Wallace, J.M., Eckelmann, H., and Brodkey, R.S., 1972, The wall region in turbulent shear flow: J. Fluid Mech. 54, 39-48.

Whetten, J.T., and Fullam, T.J., 1967, Columbia River Bed Forms: Inter. Assoc. Hydraul. Research, Proc. Twelth Congress, 1, 107-114.

Williams, G.P., 1967, Flume experiments on the transport of a coarse sand: U.S. Geol. Surv. Prof. Paper 562-B.

Williams, G.P., 1970, Flume width and water depth effects in sediment-transport experiments: U.S. Geol. Surv. Prof. Paper 562-H.

Williams, P.B., and Kemp, P.H., 1971, Initiation of ripples on flat sediment beds: Am. Soc. Civil Engineers Proc., J. Hydraulics Div., 97, 505-522.

Williams, P.B., and Kemp, P.H., 1972, Initiation of ripples by artificial disturbances: Am. Soc. Civil Engineers Proc., J. Hydraulics Div., 98, 1057-1070.

Willmarth, W.W., and Lu, S.S., 1972, Structure of the Reynolds stress near the wall: J. Fluid Mech., 55, 65-92.

Yalin, M.S., 1964, Geometrical properties of sand waves: Am. Soc. Civil Engineers Proc., J. Hydraulics Div., 90, 105-119.

Yalin, M.S., 1972, Mechanics of sediment transport: Pergamon Press, Oxford.

APPENDIX A

SIDEWALL CORRECTION

The detailed outline for the sidewall correction is provided by Vanoni and Brooks (1957, p. 100-106). A sample calculation for Run A-2 is presented below.

The measured quantities of Run A-2 are:

$Q = 0.0390\ m^3/sec$

$d = 14.80\ cm$

$b = 91.5\ cm$

$S = 0.00047$

$T = 31.0°C$

The derived quantities are:

area of cross section $A = bd = (91.5)(14.80) = 1354.2\ cm^2$

mean velocity $U = Q/A = 39000/1354.2 = 28.80\ cm/sec.$

wetted perimeter $P = b+2d = 91.5 + 2(14.8) = 121.1\ cm.$

hydraulic radius $r = A/P = 1354.2/121.1 = 11.18\ cm.$

shear velocity $V_* = (grS)^{1/2} = [(980)(11.18)(.00047)]^{1/2}$

$= 2.27\ cm/sec.$

friction factor $f = 8\left(\frac{V_*}{U}\right)^2 = 8\left(\frac{2.27}{28.80}\right)^2 = 0.050$

kinematic viscosity $\nu = 0.803 \times 10^{-2}\ cm^2/sec$

Reynolds number $R = 4Ur/\nu = 160{,}390$

Reynolds number for the channel walls

$Rw = 4U_w r_w/\nu = 4Ur_w/\nu$

hydraulic radius of the walls

$$r_w = rf_w/f$$

therefore

$$R_w/f_w = R/f = 3{,}207{,}800$$

From Fig. 39 of Vanoni and Brooks (1957) at R_w/f_w = 3,207,800, $f_w = 0.0196$

bed friction factor

$$f_b = f + \frac{2d}{b}(f-f_w)$$

$$= 0.05 + \frac{2(14.2)}{91.5}(0.05 - 0.0196) = 0.06$$

bed hydraulic radius

$$r_b = r\frac{f_b}{f} = (11.18)\ (0.06)/(0.05) = 13.37$$

bed shear velocity

$$V_{*_b} = (gr_b s)^{1/2} = [(980)(13.37)(0.00047)]^{1/2} = 2.48$$

BIOGRAPHICAL SKETCH

The author was born October 5, 1945 in Cheltenham, England,where he and his family resided until 1953, when they moved to Toronto, Ontario, Canada. After receiving a B.Sc. from McMaster University, Hamilton, Ontario, he entered graduate school,also at McMaster University, graduating with an M.Sc. in 1970. He entered graduate school at M.I.T. in September 1969.

The author is a member of the International Association of Sedimentologists and the Society of Economic Paleontologists and Mineralogists.